STATISTICAL QOS ASSURANCES FOR WIRELESS PACKET DATA and INTEGRATION METHODOLOGIES FOR 3G/WLAN

by

Ferit Ozan Akgül

A Thesis Submitted to the
Graduate School of Engineering
in Partial Fulfillment of the Requirements for
the Degree of

Master of Science

in

Electrical & Computer Engineering

Koç University

December, 2004

Koç University

Graduate School of Sciences and Engineering

This is to certify that I have examined this copy of a master's thesis by

Ferit Ozan Akgül

and have found that it is complete and satisfactory in all respects,
and that any and all revisions required by the final
examining committee have been made.

Committee Members:

_____

Asst. Prof. Oğuz Sunay

_____

Prof. Murat Tekalp

_____

Prof. Reha Civanlar

_____

Asst. Prof. Özgür Gürbüz

Date: _____

The discovery of electrical waves has not merely scientific interest though it was this alone which inspired it. Like Faraday's discovery of electromagnetic induction, it has had a profound influence on civilization; it has been instrumental in providing methods which may bring all the inhabitants of the world within hearing distance of each other and has potentialities social, educational and political which we are only beginning to realize.

Sir J.J. Thomson, 1931

To my family

ABSTRACT

Rapid developments in the wireless technologies require the networks of tomorrow be more versatile and able to handle different types of load with adaptive approaches. The future wireless systems will employ all-IP architectures to provide seamless interconnection with the global data network, the Internet. The type of content that will be carried over the wireless networks is also changing towards rich multimedia and interactivity via the use of packet switching. Hence the design of these wireless systems requires the consideration of many aspects of content transport from physical layer issues to application layer requirements. At this point a cross-layer design is essential for future wireless systems. Since all types of content, whether they be background data, interactive web services or streaming audio/video, are becoming more packet oriented, efficient resource management methodologies should be developed to satisfy user requirements as well as increase overall system performance. QoS is thus an important issue in the design of data networks, whether wireless or wireline.

The study involved in this thesis focuses on the QoS aware resource management algorithms for the recently standardized IS-856 data only cellular system. QoS aware algorithms are proposed and numerous system evaluations are performed with respect to the algorithms already present in the literature. A wideband study is also conducted by utilizing 3x MC option for the IS-856 system. Besides 3G system evaluations, 3G/WLAN integration methodologies are also investigated. System performance of an integrated scheduling/routing algorithm is studied.

ÖZETÇE

Kablosuz teknolojilerdeki hızlı gelişmeler, yarının ağlarının çok yönlü ve farklı nitelikteki sistem yüklerini uyarlamalı yaklaşımlarla desteklemesini gerektirir. Geleceğin kablosuz sistemleri, küresel veri ağı Internet'le muntazam bağlantıyı sağlamak amacıyla tamamıyla IP mimarisini destekleyecektir. Kablosuz ağlar üzerinden taşınacak veri tipi de zengin çokluortam ve etkileşimli içeriğe dönük olarak paket anahtarlamalı yapıya dönüşmektedir. Bu yüzden kablosuz ağların tasarımı fiziksel katmandan uygulama katmanına kadar içerik aktarımının pek çok yönünü ele almalıdır. Bu noktada çapraşık-katman tasarımı geleceğin kablosuz sistemleri için çok önemlidir. Arka-plan verisi, etkileşimli web servisleri veya duraksız ses/görüntü gibi veriler artık daha fazla paket verisine yöneldiği için, hem kullanıcı isteklerini karşılamak hem de genel sistem başarımını artırmak için verimli kaynak yönetim mekanizmaları geliştirilmelidir. Hizmet niteliği bu yönden hem kablolu hem de kablosuz sistemler için önemli bir unsurdur.

Tezde yer alan bu çalışma, yeni standart haline gelen IS-856 sistemi için hizmet kalitesine vakıf kaynak yönetimi algoritmaları üzerinde yoğunlaşmıştır. Hizmet kalitesine vakıf algoritmalar önerilmiş olup literatürde bulunan algoritmalara göre çeşitli sistem başarım değerlendirmeleri yapılmıştır. Ayrıca geniş bantlı bir sistem analizi de 3x çoklu taşıyıcı kullanan IS-856 sistemi için yapılmıştır. 3. nesil sistem değerlendirmelerinin yanı sıra, 3. nesil ve kablosuz yerel ağların bütünleştirme mekanizmaları da incelenmiştir. Bütünleşik kaynak yönetimi/rota tespiti algoritma başarımı da ayrıca çalışılmıştır.

ACKNOWLEDGMENTS

I would like thank my advisor Dr. Oğuz Sunay for his guidance, patience and belief in me, for the valuable discussions we have had and the support as well as the professional advices he has given me for my future career.

I would also like to thank Ali Ekşim and Serkan Dost for their valuable suggestions and for the helpful discussions.

I sincerely acknowledge the environment and the opportunity given by the Faculty of Engineering and the Department of Electrical Engineering at Koç University. This study would not be possible without their generous support and motivation.

I would like to thank Dr. Murat Tekalp, Dr. Reha Civanlar and Dr. Özgür Gürbüz for serving on my advisory committee.

For the wonderful friendships and the moral support of my friends here at Koç University, I would like to thank Umut Küçükkabak, Ali Selim Aytuna, Tanır Özçelebi, Müge Pirtini, Kıvılcım Büyükhatipoğlu, Işıl Yıldırım, Can James Wetherilt, Mustafa Can Filibeli, Can Kızılkale and many others. A sincere gratitude also goes to Umut for his hospitality and generosity and to Selim for his long-lived friendship starting from middle school years.

Finally, for all the patience and the physical and moral support they have provided, I am indebted to my family. I would like to thank my mother, Hatice, my father, Azat and my brother, Onur, and other family members for their encouragement and support.

TABLE OF CONTENTS

LIST OF TABLES

LIST OF FIGURES

NOMENCLATURE

BPSK	Binary Phase Shift Keying
QPSK	Quadrature Phase Shift Keying
QAM	Quadrature Amplitude Modulation
16-QAM	16-Quadrature Amplitude Modulation
64-QAM	64-Quadrature Amplitude Modulation
GMSK	Gaussian Minimum Shift Keying
Hz	Hertz
kHz	kilohertz
MHz	Megahertz
GHz	Gigahertz
CDMA	Code Division Multiple Access
WCDMA	Wideband Code Division Multiple Access
TDMA	Time Division Multiple Access
FDMA	Frequency Division Multiple Access
OFDM	Orthogonal Frequency Division Multiplexing
OFDMA	Orthogonal Frequency Division Multiple Access
GSM	Groupe Spécial Mobile
UMTS	Universal Mobile Telecommunications System
HSDPA	High Speed Downlink Packet Access
1xEV-DO	1xEvolution Data Optimized
1xEV-DV	1xEvolution Data and Voice
FM	Frequency Modulation
bps	bits per second
kbps	kilobits per second
Mbps	Megabits per second

ICI	Inter Carrier Interference
ISI	Inter Symbol Interference
SINR	Signal to Interference plus Noise Ratio
SNR	Signal to Noise Ratio
FFT	Fast Fourier Transform
IFFT	Inverse Fast Fourier Transform
dB	decibel
AMPS	Advanced Mobile Phone Service
BS	Base Station
MS	Mobile Station
SC	Single Carrier
MC	Multi-Carrier
WLAN	Wireless Local Area Network
HS	Hot Spot
QoS	Quality-of-Service

Chapter 1

INTRODUCTION

1.1 Background

The discovery of electromagnetic waves in the late 19th century following the studies of James C. Maxwell and Heinrich R. Hertz has opened a new era in the world of communications. Hertz was the first to send and receive radio waves. He investigated the characteristics of electromagnetic waves via several experiments and he published his findings in one of the most renowned books in the history of science [1]. With his practical studies on electromagnetic waves, it became possible to convey signals from one point to another without the need for wires.

The foundations of wireless communications rely on electromagnetic theory [2, 3]. The first means of wireless communications were analog signals and these signals formed the basis of our communication dependent society today. The first radios, the TVs were all based on analog signal transmissions. With the rapid developments in the field of microelectronics and digital computers, it became possible to transmit signals in digital format. Today's modern communication systems all employ state-of-the-art digital technologies that provide us with seamless interconnectivity between various networks.

The communication networks all around the world, whether wireline or wireless, rely upon the very fundamentals of information theory introduced by the phenomenal paper of Claude Shannon [4]. By defining a single information bit as the basic unit of data transmission, Shannon formulated and showed the upper limits that can be reached theoretically in communication systems.

Under the light of Shannon's work, communication engineers have been developing systems that are pushing the limits of technology in terms of coverage, data rate and spectral efficiency.

The most influential impact of wireless systems has been through the deployment of cellular systems. The concept of cellular systems for mobile communications has been first introduced by D. H. Ring in an unpublished paper [5] and later the first cellular system, AMPS, had been deployed [6, 7].

The deployment of the AMPS has opened a new era in the way point-to-point communications are realized. By dividing the geographical area into virtual cells and by utilizing frequency reuse it became possible to cover large areas via wireless systems.

Together with the advances in digital signal processing, the wireless networks including stations and terminals have evolved into today's modern systems. Starting from the 1^{st} generation analog systems (AMPS) to 3^{rd} generation cdma2000 IS-856 (1xEV-DO), 1xEV-DV and WCDMA, cellular wireless technologies have come a long way. Table 1.1 summarizes the specifications of the cellular wireless technologies and Figure 1.1 shows the transition path from the 2G systems to 3G and beyond.

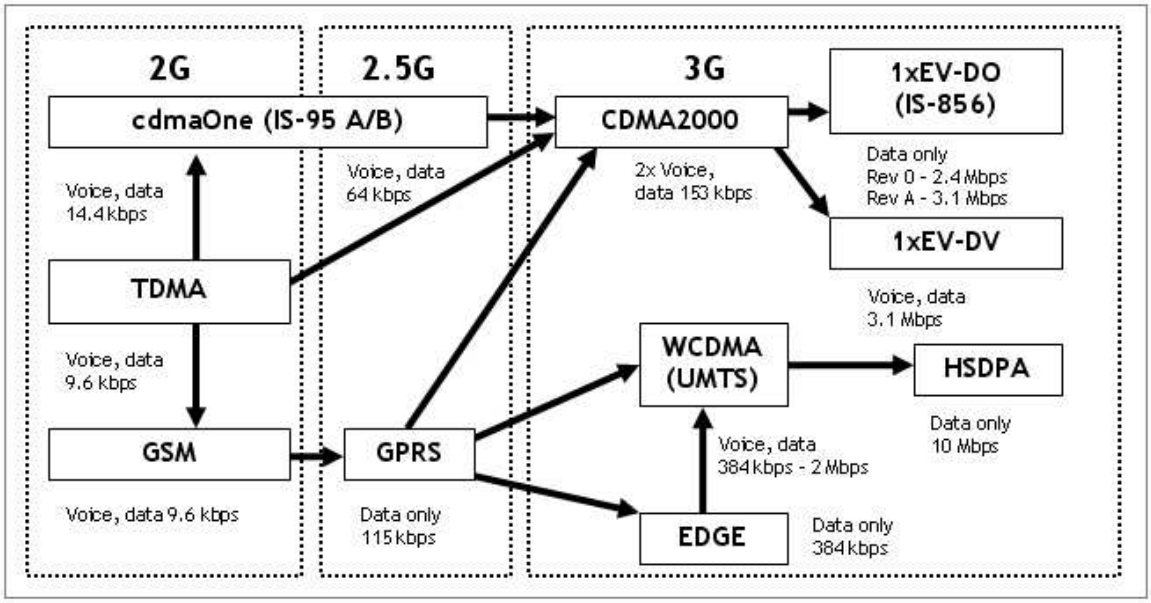

Figure 1.1: Path to 3G

Table 1.1: Wireless Standards

Technologies	**Generation**	**Multiple Access Scheme**	**Carrier Bandwidth**	**Peak Data Rate**	**Modulation Scheme**	**Data / Voice Support**
GPRS	2.5G	TDMA	0.2 MHz	115 kbps	GMSK	data
	Designed as overlay on GSM/TDMA networks					
EDGE	2.5G	TDMA	2.4 MHz	384 kbps	8PSK/GMSK	data
	Designed as overlay on GSM/TDMA networks					
cdma2000 1x	3G	CDMA	1.25 MHz	625 kbps	BPSK/QPSK	data + voice
cdma2000 1xEV-DO (HDR / IS-856)	3G+	CDMA / TDMA	1.25 MHz	2.457 Mbps	QPSK/8PSK/ 16QAM	data
	Designed as high data rate extension to cdma2000 1x					
cdma2000 1xEV-DV Rev. D (as of 2004/03)	3G+	CDMA / TDMA	1.25 MHz	3.09 Mbps	QPSK/8PSK/ 16QAM	data + voice
	Designed as high data rate extension to cdma2000 1x with voice support					
WCDMA	3G	CDMA	3.84 MHz	2 Mbps	BPSK/QPSK	data + voice
HSDPA	3G+	CDMA	3.84 MHz	8-10 Mbps	16QAM/ 64QAM	data
	Designed as high throughput, high peak data rate extension to WCDMA					

1.2 Motivation

The primary goal of the wireless systems at the time of first deployments was to provide the users with "connection" regardless of the geographical location. The term "connection" was first interpreted as being able to transmit voice signals, since it was the revolutionary land phone services that brought people within hearing distance of each other. Thus it was the primary reason to transmit voice via wireless medium in transferring the technology from wired to wireless. Hence early wireless systems have all been designed with the unique thought in mind: to transmit voice signals as efficiently as possible.

As it became more practical to process all sorts of signals (voice, image, video) in the digital format, much research has been carried out to establish large scale data distribution systems like global data networks. As a result of the DARPA project initiated by the Department of Defense (DoD), the fundamentals of the Internet have been established under the name ARPANET [8].

The next target for the wireless systems engineers has thus been the global exchange of information anywhere, anytime. Transfer of technology from the wired to wireless for the

digital forms of data have brought unique challenges. The proper modeling of the wireless channel, the constraints on system parameters subject to the type of data (non-realtime, audio, video), expected system load necessitate some form of service quality without sacrificing overall system performance at a considerable level. The QoS is thus an important issue in today's wired/wireless data networks. Depending on the service type intended to be served, certain service guarantees need to be satisfied.

Current algorithms employed in 3G wireless systems do not handle applications requiring QoS well enough. There is thus room for further research in the investigation of systems that are able to deliver layer specific outputs. Hence, a cross-layer design perspective is needed to achieve the desired performance levels. Varying QoS levels of the users should be satisfied in the coming wireless systems so system design should be implemented as to optimize constraints in a joint manner across layers starting from the physical layer up to the application layer.

The motivation of this thesis is to develop schemes and methodologies to provide wireless packet data users with predefined service guarantees for streaming type of data and at the same time exploit multi-user diversity to enhance overall system performance.

1.3 Contributions

During the course of the studies leading up to this thesis, the main research work has been on the development of scheduling algorithms that incorporate QoS parameters in a cross-layer framework. Furthermore, 3G/WLAN integration methodologies have been studied in this thesis by integrating scheduling and routing algorithms for a WLAN embedded 3G cell. Another study focus has been the performance of the multiple carrier 3G system. Since future wireless applications will require more data rates, wireless systems with higher bandwidths where multiple carrier approaches are applied, will be in use.

To summarize, the contributions may be listed as:

- A comprehensive simulation platform for the IS-856 system has been developed. The platform includes system level, link level and physical layer simulations complete with channel modeling and system parameter choice in accordance with the standard supporting 4-slot interlaced packet scheduling.

- Several QoS aware scheduling algorithms for the IS-856 system have been developed
- A 3G/WLAN scheduling/routing methodology has been developed for both enhanced 3G system performance and fair battery usage among WLAN terminals.
- Investigated 3x multiple carrier version of IS-856 and corresponding scheduling algorithms have been developed
- Applied QoS aware algorithms for both single and multiple carrier IS-856 and compared system performance against common algorithms in literature with respect to data rate, latency, statistical QoS assurance, number of supported users for given statistical guarantee.

1.4 Outline

The thesis has been organized as follows: Chapter 2 introduces the IS-856 system forward channel structure. Chapter 3 forms the basis of the thesis and discusses the QoS and the service levels in wireless systems. Proposed IS-856 scheduling algorithms incorporating the QoS awareness and the other common algorithms are presented here. Chapter 4 explains in detail the simulation platform and the channel models that have been used. In chapter 5, a brief introduction to WLANs is given. WLAN standards are summarized along with key technologies. Chapter 6 elaborates on the research that has been carried out for the integration of 3G/WLAN systems. In this chapter, a number of combined scheduling/routing algorithms are developed and these are compared to the common routing methodologies from the literature. Finally chapter 7 concludes the thesis pointing out the achievements obtained in the thesis and discusses some application areas together with possible future directions.

Chapter 2

IS-856 FORWARD LINK

In this chapter, the forward link structure of the IS-856 [9] system is briefly described. Throughout the thesis the terms IS-856, High Data Rate (HDR) and 1xEV-DO will be used interchangeably.

IS-856 system has been specifically designed to provide high speed data access for mobile users. From an information theoretic point of view serving one user at a time with adaptive modulation and coding is optimal. The optimality of the so-called "water-pouring" in time is shown in [10, 11]. Following the optimality of serving one user at-a-time, IS-856 forward link allocates the resources to only one user at a given time. That user employs adaptive coding and modulation to maximize its data rate within the allowance limits of its channel conditions. The asymmetric character of the IP traffic puts special importance on the forward link as opposed to reverse link. The forward link waveform is structured in a time-division-multiplexed (TDM) manner in order to eliminate the unused power margin which is the case in IS-95 [12] forward link. Figure 2.1 shows the power level distribution for both IS-95 and IS-856 systems. The sync and paging channels in IS-95 are used for the synchronization of the mobile terminals to the network time and for the transmission of messages specific to the mobiles such as call requests respectively. These channels are replaced with MAC and control channels in the IS-856 system. The channels are transmitted via code (power) sharing in IS-95 whereas the channels are transmitted in fractions of time and at the full BS transmit power in IS-856. This increases the SINR values of the mobiles as well as increasing the cell coverage.

Very recently, the release A of the IS-856 has been announced and standardized with further improvements to the system [13]. The forward link data rate has been increased from 2.4 Mbps to 3.1 Mbps and reverse link from 153.6 kbps to 1.8 Mbps. The new standard defines subtype 0, 1 and 2 packets [13]. The information given in this chapter refers to subtype 0 and 1 physical layer packets as defined in the new IS-856-A standard.

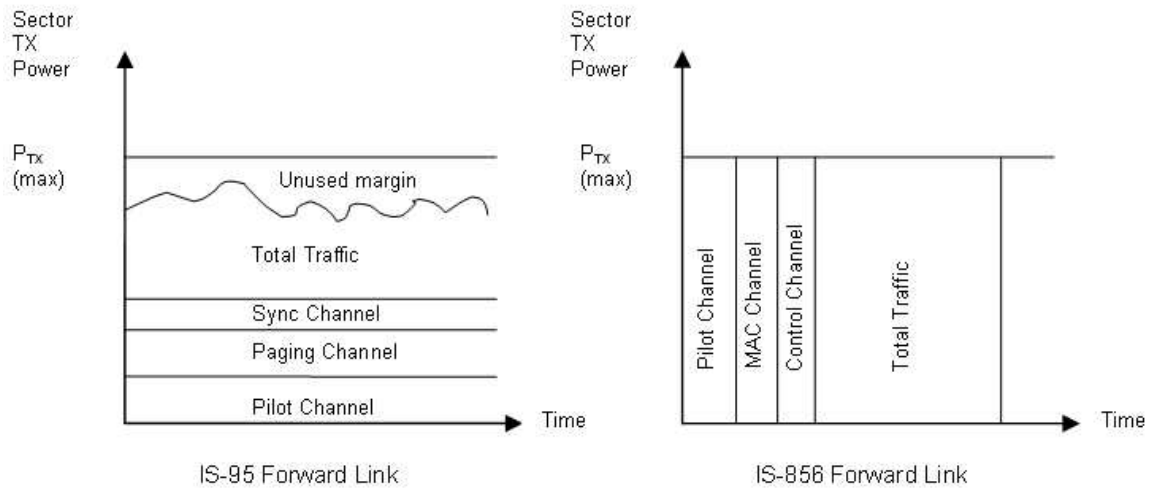

Figure 2.1: Forward Link Power Distribution for IS-95 and IS-856 [14]

2.1 Forward Link

The forward link of IS-856 is a shared link over which all the users may receive information. Power control is not applicable hence the channels are transmitted at full BS power. The forward link consists of the following TDM channels:

1. The Pilot Channel
2. The MAC Channel
3. The Forward Traffic Channel
4. The Control Channel

Furthermore the MAC channel consists of three subchannels:

1. The Reverse Activity (RA) Channel
2. The DRCLock Channel
3. The Reverse Power Control (RPC) Channel

Figure 2.2 shows the hierarchical structure of the channels in the forward link.

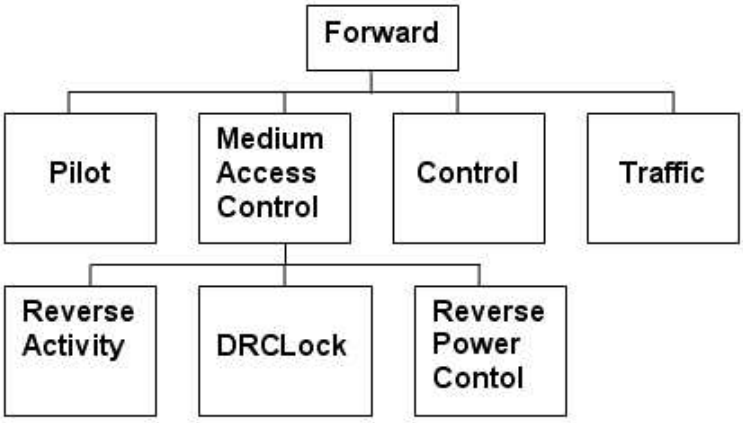

Figure 2.2: Forward Link Channel Hierarchies [14]

2.1.1 Forward Link Waveform

The forward link carrier is allocated a bandwidth of 1.25 MHz that is direct-sequence spread at the rate of 1.2288 Mcps [14]. The smallest unit of transmission is a time-slot which consists of 2048 chips thus making the duration of a time-slot approximately 1.667 ms. Within a time-slot, the Pilot, the MAC, and the Traffic or Control Channels are time-division multiplexed (TDM) and all are transmitted at the same maximum power level. When there is no control or traffic data to transmit, an idle slot is transmitted. An idle slot consists of only the pilot and MAC channels. Figure 2.3 shows the slot structure of the forward link.

The forward link spreading and channel structure is given in Figure 2.4 [9].

2.1.2 The Pilot Channel

In the pilot channel [9], unmodulated signal is transmitted with full sector power. The pilot signal is composed of all 0's. As it can be seen in Figure 2.3, the Pilot is transmitted twice in a slot. The sectors are differentiated by the PN offsets. The Pilot signal is used for initial acquisition, phase and timing recovery and symbol combining. Another important function of the pilot signal is to provide a channel estimate for rate adaptation.

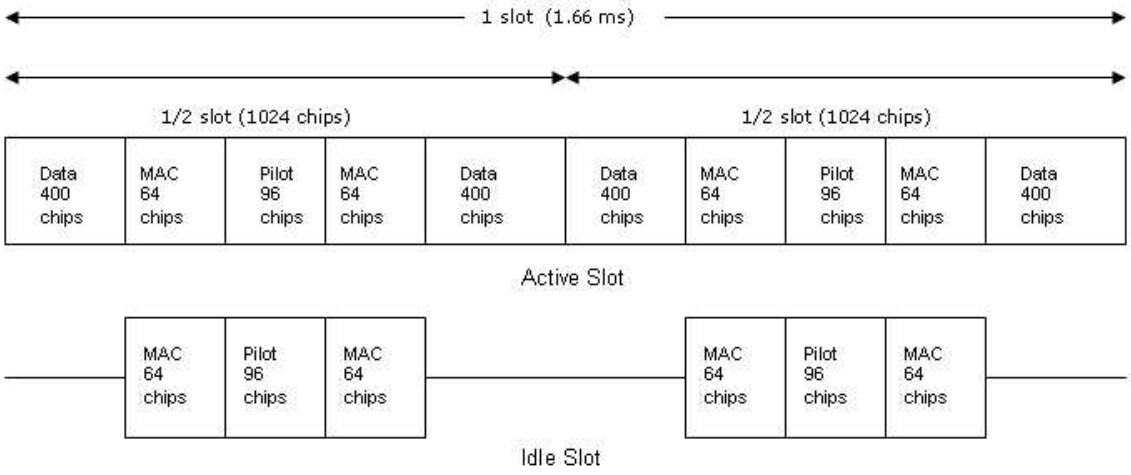

Figure 2.3: Forward Link Slot Structure [14]

2.1.3 The Forward MAC Channel

The Forward MAC channel [9] is used for the scheduling of the users on the forward link. It also informs the users of the reverse link capabilities of the system. The MAC channel is transmitted twice in a slot in 256 chips surrounding the two pilot bursts (Figure 2.3). MAC channels consists of Walsh channels that are orthogonally covered and BPSK modulated. Each of the Walsh channels are assigned MACIndex values for identification and each active user is assigned a distinct MACIndex. Depending on the MACIndex value, a Walsh channel is modulated on either in-phase or quadrature phase of the carrier.

The Walsh functions [15] that are assigned for a channel depending on MACIndex i are given as:

$$W_{i/2}^{64} \text{ for } i = 0, 2, ..., 62$$
$$W_{(i-1)/2+32}^{64} \text{ for } i = 1, 3, ..., 63$$

where W_i^N is the i^{th} row of a N by N Walsh-Hadamard matrix [16]. Walsh codes with even numbered MACIndex values are transmitted over the in-phase carrier and the odd numbered codes are transmitted over quadrature phase carrier.

The RA channel [9] is used by the reverse MAC algorithm to control the level of interference received by a particular sector. On the RA channel the RA bit (RAB) is transmitted in order to provide information about the loading of the reverse link and whether the users

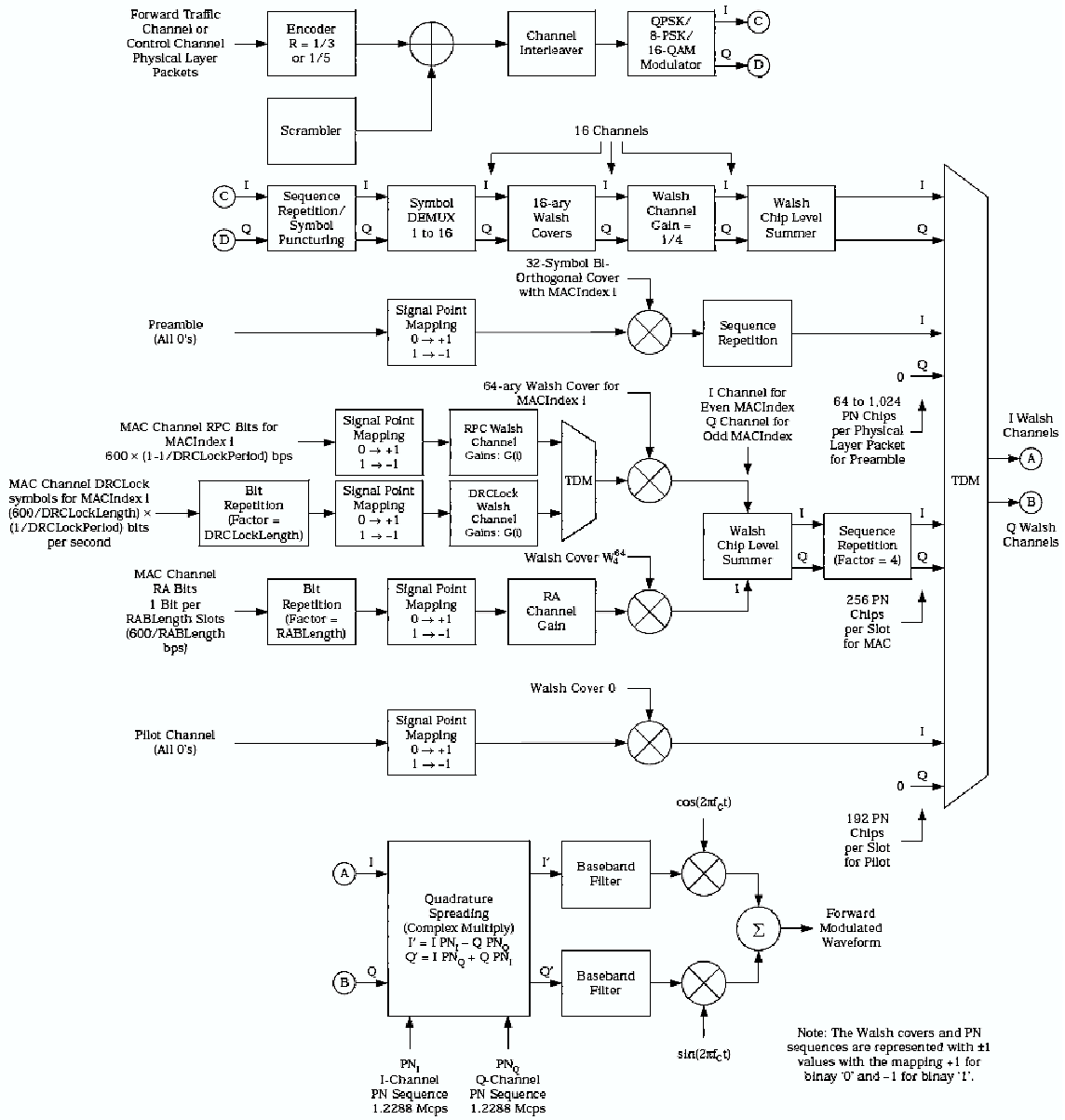

Figure 2.4: Forward Link Channel Structure (taken from [9])

should increase or decrease their data rates.

The DRCLock channel [9] is used to inform the terminals whether or not the sector can reliably decode the DRC sent by the terminal. The DRCLock channel is assigned a 64-ary Walsh code between indices 5 and 63.

The RPC channel [9] is used to transmit RPC bit stream that is destined for a specific terminal for the purpose of reverse link power control.

Table 2.1 shows the MAC channel use versus MACIndex

Table 2.1: MAC Channel Use versus MACIndex

Walsh Code Index i	**MAC Channel Use**
0 and 1	Not used
2	Not used
3	Not used
4	RA Channel
5-63	RPC and DRCLock Channel

2.1.4 The Forward Traffic Channel

The forward traffic channel is a shared medium that carries user physical layer packets. Since only one user is served at a time, a preamble sequence is transmitted to indicate the start of a physical layer packet as well as the intended receiving terminal. The preamble uses bi-orthogonal modulation. A bi-orthogonal set of M signals can be constructed from a set of $M/2$ orthogonal signals [17]. The negatives of these $M/2$ signals are also used to form the bi-orthogonal set thus reducing the complexity of the demodulator.

The preamble sequence consists of all 0 symbols on the I channel. The covering of the preamble is determined by the MACIndex of the desired terminal as follows:

$$W_{i/2}^{32} \text{ for } i = 0, 2, ..., 62$$
$$\overline{W_{(i-1)/2}^{32}} \text{ for } i = 1, 3, ..., 63$$

where $\overline{W_i^{32}}$ is the bit-by-bit complement of the 32 chip Walsh function of order i. Table 2.2 shows the preamble use versus MACIndex values.

Table 2.2: Preamble Use versus MACIndex

Walsh Code Index i	**Preamble Use**
0 and 1	Not used
2	76.8 kbps Control Channel
3	38.4 kbps Control Channel
4	Not Used
5-63	Forward Traffic Channels

2.1.5 Packet Types

Closed-loop rate control is supported by the use of different packet types for the forward traffic channel physical layer. Each packet has a specific nominal data rate and a nominal packet length. With Hybrid-ARQ [18] multi-slot packets can be terminated early and this leads to truncated packet types. The coding scheme of the packets allows the receiving terminal to decode the packet before it is received in nominal length. Table 2.3 shows the packet types used in the HDR forward traffic link with the corresponding parameters.

Table 2.3: Available Data Rates in HDR

Rate (kbps)	**Slots**	**Bits**	**Code Rate**	**Modulation**	**TDM Chips (Preamble, Pilot, MAC, Data)**
38.4	16	1,024	1/5	QPSK	1024, 3072 4096, 24576
76.8	8	1,024	1/5	QPSK	512, 1536 2048, 12288
153.6	4	1,024	1/5	QPSK	256, 768 1024, 6144
307.2	2	1,024	1/5	QPSK	128, 384 512, 3072
614.4	1	1,024	1/3	QPSK	64, 192 256, 1536
307.2	4	2,048	1/3	QPSK	128, 768 1024, 6272
614.4	2	2,048	1/3	QPSK	64, 384 512, 3136
1,228.8	1	2,048	1/3	QPSK	64, 192 256, 1536
921.6	2	3,072	1/3	8-PSK	64, 384 512, 3136
1,843.2	1	3,072	1/3	8-PSK	64, 192 256, 1536
1,228.8	2	4,096	1/3	16-QAM	64, 384 512, 3136
2,457.6	1	4,096	1/3	16-QAM	64, 192 256, 1536

2.1.6 Encoding

The highly destructive nature of the wireless transmission medium necessitates the use of special coding techniques to recover data packets by adding redundancy information. The purpose of encoding the physical layer packets is to provide the data packets with robustness against channel impairments. The coding scheme employed in IS-856 is the Turbo encoding [19].

The coding rates of 1/3 and 1/5 are used in IS-856. The tailing bits (6 bits) of the physical layer forward traffic or control channel packets are discarded before the encoder input.

Turbo Encoding

The turbo encoder utilized in IS-856 is composed of two systematic, recursive, identical parallel convolutional encoders with the second encoder preceded by the turbo interleaver [20]. Turbo interleavers are important components of the turbo encoding scheme in randomizing and spreading the burst errors thus making it easier for the decoder to decode the stream. Another purpose of interleavers is that they make turbo codes look like random but within a certain structure so that decoding is possible. Shannon showed that random coding is optimal in achieving the channel capacity [4].

Table 2.4 gives the encoding parameters used in the encoding process.

The convolutional codes of the encoders are called the constituent codes of the turbo code and the output of the convolutional encoders are punctured and repeated [9] to give desired number of turbo encoder output symbols.

The transfer function for the constituent code is given by:

$$G(D) = [1 \;\; G_1(D) \;\; G_2(D)] \tag{2.1}$$

where

$G_1(D) = \frac{1+D+D^3}{1+D^2+D^3}$

$G_2(D) = \frac{1+D+D^2+D^3}{1+D^2+D^3}$

Table 2.4: Forward Link Encoder Parameters

Data Rate (kbps)	**Values per Physical Layer Packet**				
	Slots	**Bits**	**Turbo Encoder Input Bits**	**Code Rate**	**Turbo Encoder Output Symbols**
38.4	16	1,024	1,018	1/5	5,120
76.8	8	1,024	1,018	1/5	5,120
153.6	4	1,024	1,018	1/5	5,120
307.2	2	1,024	1,018	1/5	5,120
614.4	1	1,024	1,018	1/3	3,072
307.2	4	2,048	2,042	1/3	6,144
614.4	2	2,048	2.042	1/3	6,144
1,228.8	1	2,048	2,042	1/3	6,144
921.6	2	3,072	3,066	1/3	9,216
1,843.2	1	3,072	3,066	1/3	9,216
1,228.8	2	4,096	4,090	1/3	12,288
2,457.6	1	4,096	4,090	1/3	12,288

2.1.7 Scrambling

Prior to modulation the data at the output of the turbo encoder is randomized via scrambling. The scrambling sequence is obtained with the 17-tap linear feedback shift register (LFSR). The generator sequence is given by $h(D) = D^{17} + D^{14} + 1$.

The initial state of the LFSR is determined uniquely by the 6-bit preamble MACIndex values and the transmitted packet data rates.

2.1.8 Channel Interleaving

Following the scrambler, the symbols are input to the channel interleaver for *symbol reordering* and *symbol permuting*. The primary purpose of using channel interleaving is to randomize symbol errors since decoders perform better when dealing with random errors rather than burst errors. The secondary purpose is to assist the HARQ scheme when the packets are terminated early.

2.1.9 Modulation

IS-856 system employs three different modulation schemes depending on the data rate. The output of the channel interleaver is applied to the modulator which outputs an in-phase and a quadrature stream by modulating the input with QPSK, 8-PSK or 16-QAM.

2.1.9.1 QPSK

Physical layer packets of sizes 1024 and 2048 bits are modulated using QPSK. Two consecutive symbols, $x(2i)$ and $x(2i+1)$, $i = 0, 1, ..., M-1$ are mapped to the complex modulation symbols $(m_I(i), m_Q(i))$ as shown in Table 2.5. Figure 2.5 shows the signal constellation corresponding to QPSK [9].

Table 2.5: QPSK Mapping

Interleaved Symbols		**Modulation Symbols**	
s_1 $x(2i+1)$	s_0 $x(2i)$	$m_I(i)$	$m_Q(i)$
0	0	D	D
0	1	-D	D
1	0	D	-D
1	1	-D	-D
Note: D=$1/\sqrt{2}$			

2.1.9.2 8-PSK

Physical layer packets of size 3072 bits are modulated using 8-PSK. Three consecutive symbols, $x(3i)$, $x(3i+1)$ and $x(3i+2)$, $i = 0, 1, ..., M-1$ are mapped to the complex modulation symbols $(m_I(i), m_Q(i))$ as shown in Table 2.6. Figure 2.6 shows the signal constellation corresponding to 8-PSK [9].

2.1.9.3 16-QAM

Physical layer packets of size 4096 bits are modulated using 16-QAM. Four consecutive symbols, $x(4i)$, $x(4i+1)$, $x(4i+2)$ and $x(4i+3)$, $i = 0, 1, ..., M-1$ are mapped to the complex modulation symbols $(m_I(i), m_Q(i))$ as shown in Table 2.7. Figure 2.7 shows the signal constellation corresponding to 16-QAM [9].

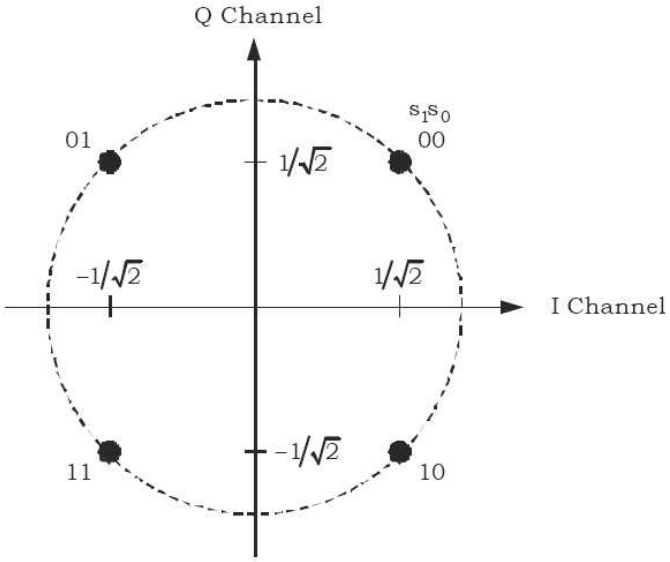

Figure 2.5: QPSK Signal Constellation (taken from [9])

Table 2.6: 8-PSK Mapping

Interleaved Symbols			**Modulation Symbols**	
s_2 $x(3i+2)$	s_1 $x(3i+1)$	s_0 $x(3i)$	$m_I(i)$	$m_Q(i)$
0	0	0	C	S
0	0	1	S	C
0	1	1	-S	C
0	1	0	-C	S
1	1	0	-C	-S
1	1	1	-S	-C
1	0	1	S	-C
1	0	0	C	-S
Note: C=$cos(\pi/8)$ **and S=**$sin(\pi/8)$				

2.1.10 Sequence Repetition and Symbol Puncturing

The modulator may output more or less modulation symbols than needed for the data part of the allocated slots. In this case *symbol repetition* or *symbol puncturing* is applied. If the number of required modulation symbols is more than the number of output symbols then the symbols are repeated as many full-sequence times, followed by a partial transmission to provide the required number of symbols. If the number of required symbols is less than the

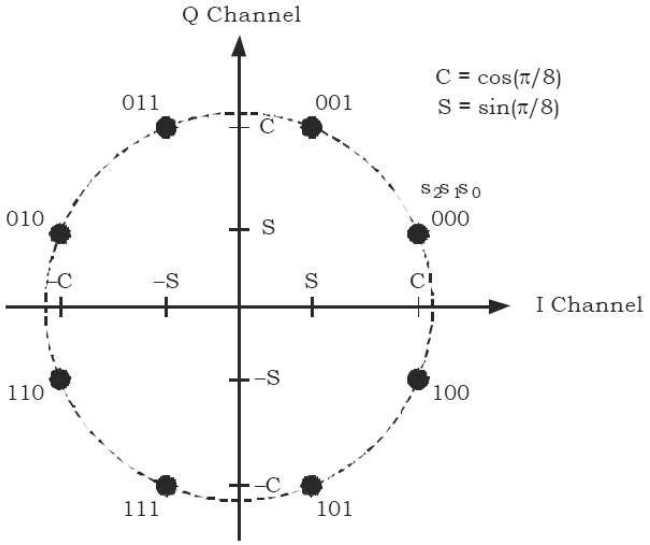

Figure 2.6: 8-PSK Signal Constellation (taken from [9])

Table 2.7: 16-QAM Mapping

Interleaved Symbols				**Modulation Symbols**	
s_3 $x(4i+3)$	s_2 $x(4i+2)$	s_1 $x(4i+1)$	s_0 $x(4i)$	$m_I(i)$	$m_Q(i)$
0	0	0	0	3A	3A
0	0	0	1	3A	A
0	0	1	1	3A	-A
0	0	1	0	3A	-3A
0	1	0	0	A	3A
0	1	0	1	A	A
0	1	1	1	A	-A
0	1	1	0	A	-3A
1	1	0	0	-A	3A
1	1	0	1	-A	A
1	1	1	1	-A	-A
1	1	1	0	-A	-3A
1	0	0	0	-3A	3A
1	0	0	1	-3A	A
1	0	1	1	-3A	-A
1	0	1	0	-3A	-3A
Note: A=$1/\sqrt{10}$					

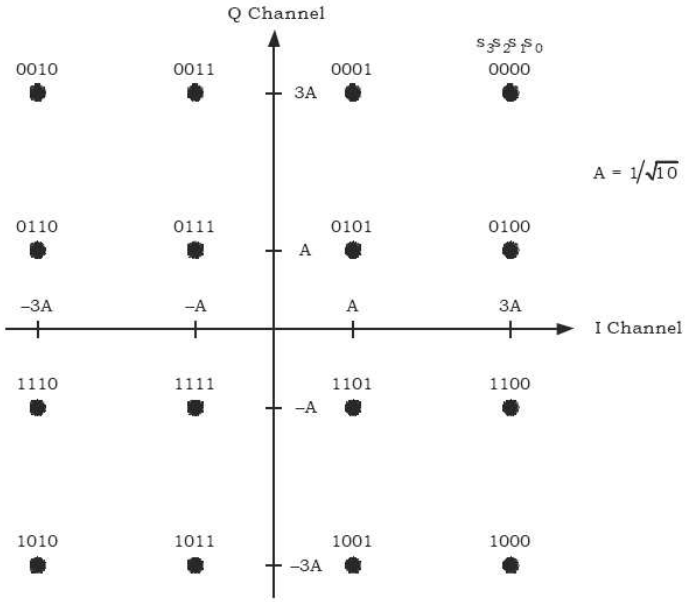

Figure 2.7: 16-QAM Signal Constellation (taken from [9])

number of output symbols then the first portion of the modulation symbols is used. Table 2.8 gives the required number of modulation symbols and the modulation symbols output from the modulator.

Table 2.8: Sequence Repetition and Symbol Puncturing Parameters

Data Rate (kbps)	Values per Physical Layer Packet						Approximate Coding	
	Number of Slots	Number of Bits	Number of Modulation Symbols Provided	Number of Modulation Symbols Needed	Number of Full Sequence Transmissions	Number of Modulation Symbols in Last Partial Transmission	Code Rate	Repetition Factor
38.4	16	1,024	2,560	24,576	9	1,536	1/5	9.6
76.8	8	1,024	2,560	12,288	4	2,048	1/5	4.8
153.6	4	1,024	2,560	6,144	2	1,024	1/5	2.4
307.2	2	1,024	2,560	3,072	1	512	1/5	1.2
614.4	1	1,024	2,560	1,536	1	0	1/3	1
307.2	4	2,048	1,536	6,272	2	128	1/3	2.04
614.4	2	2,048	3,072	3,136	1	64	1/3	1.02
1,228.8	1	2,048	3,072	1,536	0	1,536	1/3	1
921.6	2	3,072	3,072	3,136	1	64	1/3	1.02
1,843.2	1	3,072	3,072	1,536	0	1,536	1/3	1
1,228.8	2	4,096	3,072	3,136	1	64	1/3	1.02
2,457.6	1	4,096	3,072	1,536	0	1,536	1/3	1

2.1.11 Symbol Demultiplexing

The in-phase and the quadrature streams are demultiplexed into 16 streams each at the output of the sequence repetition block. The demultiplexed streams, I_k and Q_k, $k = 0, 1, ..., 15$, carry symbols such that I_k carries $m_I(k)$, $m_I(16 + k)$, $m_I(32 + k)$, ... and Q_k carries $m_Q(k)$, $m_Q(16 + k)$, $m_Q(32 + k)$,... [9]

Each demultiplexed stream has a data rate of 76.8 ksps. The overall system rate is thus 76.8 ksps $\cdot$ 32 streams = 2,457.6 ksps.

2.1.12 Walsh Channel Assignment

The demultiplexed streams I_k and Q_k are assigned to the in-phase and quadrature phases, respectively, of the k^{th} Walsh Channel W_k^{16} [9].

2.1.13 Time-Division Multiplexing

The Forward traffic channel or control channel data chips are time-division multiplexed with the preamble, the pilot channel and MAC channel depending on the data rates.

2.1.14 Quadrature (PN) Spreading

After TDM, the modulation sequence is quadrature spread [9], i.e, multiplied with the PN sequence of length 2^{15} (32768 chips) expressed by the following characteristic polynomials:

For the in-phase sequence (I):

$$P_I(x) = x^{15} + x^{10} + x^8 + x^7 + x^6 + x^2 + 1 \tag{2.2}$$

For the quadrature phase sequence (Q):

$$P_I(x) = x^{15} + x^{12} + x^{11} + x^{10} + x^9 + x^5 + x^4 + x^3 + 1 \tag{2.3}$$

The chip rate of the PN sequence is 1.2288 Mcps so the sequence period is 32768/1228800 = 26.66 ms.

The BSs are differentiated by the PN offsets of their pilot channels. The offset indices take values from the set [0 511] and each index value represents an offset in units of 64 chips, e.g 5 means 5 $\cdot$ 64=320 chips offset from the zero-offset pilot PN sequence. The zero-offset

PN sequence is transmitted every even second in time and this timing is referenced to the access network time.

2.2 Physical Layer Packet Interlacing

The forward traffic and control channel packets are transmitted with 4-slot interlacing for the multiple-slot transmissions, i.e, there are 3 slots in between the slots of the same physical layer packet [14]. This timing mechanism supports the early termination via HARQ. It gives sufficient time for the receiving terminal to decode the received portion of the packet. If the receiving terminal successfully decodes the packet it sends an ACK on the reverse channel hence the packet is terminated early. This effectively increases data rate of the forward traffic channel.

2.3 MC Approach in HDR

The physical layer of the HDR system has been structured to use only 1.25 MHz of spectrum. It has the same RF characteristics as the cdma2000 1x (IS-95) hence HDR is backward compatible with the existing cdmaOne system. Thus it is easier to deploy HDR as an overlay system in comparison with the deployment of other 3G systems.

Future wireless data applications, e.g. streaming audio and video, will undoubtedly require more data rates so it is essential to provide end users with sufficient data rates in order to benefit high data rate content on their MSs. The use of multiple HDR carriers at the same BS opens up the possibility to offer much higher data rates to end users. In such a system the MSs need to be configured to access multiple 1.25 MHz carriers. The major advantage of the MC system is that one MS can access up to k carriers simultaneously (i.e. in the same time slot) thus increasing the effective user throughput greatly. Another important aspect of MC approach is the reduction of total system latency. Since multiple users (up to n different users) can be served within the same time slot overall system latency is reduced. The relationship between the maximum number of users (n) that can be served with k carriers is $n = k$.

In this thesis, the performance of 3x HDR system ($k = 3$ HDR carriers, which will be denoted as 3xHDR) with a total assigned bandwidth of 5 MHz has been investigated. Considering the 5 MHz spectrum of WCDMA (3G technology for UMTS) with a peak data

rate of 2 Mbps, 3xHDR offers a maximum of 7.2 Mbps in the same bandwidth. The data rate extension system of HSDPA offers 8-10 Mbps also in the same bandwidth but deploying a 3x MC system instead of WCDMA may be more feasible for certain applications.

For the 3xHDR system the center frequency is operated at 2000 MHz and side carriers at 1998.75 MHz and 2001.25 MHz respectively.

2.4 Conclusion

In this chapter the forward link of the recently standardized IS-856 system has been explained. The blocks involved in transmitting user data have been outlined in accordance with the standard given in [9]. Since the studies have focused on the downlink of the IS-856 system, the reverse link has not been taken into consideration. The feedback paths for closed-loop rate control mechanisms have been assumed to be error-free.

Chapter 3

EFFICIENT RESOURCE ALLOCATION FOR STATISTICAL QOS ASSURANCES

The rapid growth and deployment of next generation wireless cellular systems have been the driving force for seamless connectivity of mobile users. The advances at the physical layer structures of wireless systems have made it possible to achieve data rates beyond 2 Mbps [21, 22] for the next generation cellular systems. These enabling technologies for such high speed wireless data have also brought up the possibility for high quality multimedia content (audio, video) transmission over wireless networks. Since next generation wireless networks will undoubtedly converge towards one global data network, the Internet, it will be the next logical step to implement all-IP architectures in these wireless systems.

In order to comply with the specific needs of the upper layer applications, certain service guarantees need to be satisfied. These applications may include highly delay intolerant services such as IP telephony, medium delay tolerant services like streaming video or delay tolerant interactive services like web browsing. The classification of these services can be made under the general umbrella of QoS.

The term QoS refers to a broad range of technologies and methods employed in a network to provide guarantees for transmission of various types of data. The internet itself is designed to provide "best effort" service between nodes meaning the transmission may take place at the risk of data (packet) and/or throughput loss. Service guarantees may be provided for:

- Throughput
- Latency
- Packet Loss etc.

values in a network.

Next generation communication systems will be required to provide certain levels of assurances for the traffic they will carry. QoS, in that sense, plays a vital role in the

development of future wireless broadband systems. The so-called killer applications for the next generation wireless systems will most likely feature streaming audio and video. Both audio and video data have strict requirements in terms of their fundamental characteristics. IEEE 802.16 Broadband Wireless Access (BWA) Working Group has defined QoS Classes that are also in accordance with ITU-R for IMT-2000 [23]. The BWA classes are presented in Table 3.1. In the table RT refers to real-time and NRT refers to non-real-time traffic.

Table 3.1: BWA Traffic Classes

Traffic Class	**Conversational Class**	**Streaming Class**	**Interactive Class**	**Background**
	Conversational *RT*	Streaming *RT*	Interactive Best Effort *NRT*	Background Best Effort *NRT*
Fundamental Characteristics	• Preserve time relation (variation) between entities of the stream	• Preserve time relation between information entities of the stream	• Request response pattern	• Destination is not expecting the data within a certain time
	• Conversational pattern (stringent and low delay)		• Preserve payload content	• Preserve payload content
Example of the application	Voice	Streaming video	Web browsing	Background download of e-mails

The QoS mechanism is being implemented in the form of Differentiated Services (DiffServ) [24] for the ultimate wired/wireless data network, the Internet. Marking of packets in the buffers of routers for diffserv applications is the Per-Hop-Behaviors (PHBs) and represents the forwarding behavior of the nodes. The nodes allocate resources for the PHB aggregates (the collection of packets flowing on a certain link) and this resource allocation mechanism is governed by the PHBs. The simplest example of a PHB is the one which guarantees a minimal data rate allocation of X % of a link over some reasonable time interval. IETF DiffServ Working Group proposes to offer QoS in terms of assured forwarding [25] and expedited forwarding [26].

Expedited Forwarding corresponds to a low loss, low latency, low jitter, assured bandwidth service whereas *Assured Forwarding* further classifies services into 4 classes (in terms

of buffer space and bandwidth) and 3 degrees of drop precedence (high, medium, low).

PHBs are implemented at the nodes in terms of buffer management and packet scheduling mechanisms. The realization of these mechanisms takes place with respect to certain service provisioning policies. From this point of view, the scheduling algorithms for managing the network traffic (wireline or wireless) play a vital role.

The service levels for the end users can be assigned at the start of each user session and certain guarantees need to be satisfied for the entire session. Classification of these guarantees defines various service levels. The service types can be broadly listed as:

- Assured Service
- Statistically Assured Service
- Best Effort Service

Assured service (may also be regarded as guaranteed bitrate) is the type of service in which each user participating in a session is guaranteed a pre-defined data rate. This service level is required for constant bit rate (CBR) applications like real-time voice transport.

Best effort service is the current service structure of the Internet in which data packets are sent without any data rate or delay requirements. This type of service is best suited for background non-real time applications like e-mail transport mechanism.

Statistically assured service [27] is a mid-level guaranteed service. It may not provide 100% guarantee on the bandwidth availability of a certain link. When investigated on a statistical basis, the guarantee is the percent of time a specified data rate is provided. Since strictly guaranteed services require dedication of resources to individual users, the overall system performance may degrade at a considerable level and also has major disadvantages in terms of pricing. End users may not want to invest in this type service when an alternative whose performance approaches to that of the guaranteed service exists at lower costs. The basis of our framework for wireless resource management in this thesis is a statistically assured type of service and our performance metric will be the percentage of time (PoT) QoS requirements of the users are satisfied. The related performance metric will be the percentage of time QoS requirements of (in terms of data rates) the users are satisfied and will be denoted as percentage of time performance (PoTP).

This chapter will investigate the QoS performances of various scheduling algorithms for

the HDR system and will propose QoS aware scheduling algorithms in order to provide "statistically assured services".

3.1 Service Levels

The first generation of wireless systems (AMPS [6]) utilized analog methods in conveying audio information and relied on FM and circuit switching. There were no data services available. 2G wireless systems, on the other hand, have been designed as fully digital systems and the majority of wireless systems around the world still are 2G systems. 2G systems employ different multiple access methods dubbed as TDMA, FDMA and CDMA. The Current GSM system uses a combination of TDMA and FDMA whereas the American IS-95 system utilizes CDMA as the multiple access method.

2G systems mainly focused on voice transmission over wireless networks so these systems were optimized for constant bit rate (CBR) voice data. The main principle of maintaining the minimum bit rate on the wireless link to transmit voice signals is to virtually establish a circuit connection between the end points. This circuit connection is a dedicated link on which only one call/traffic can be supported at a time. Dedicating system resources to end nodes greatly limits total system capacity. Both GSM and IS-95 systems rely on circuit switching to realize voice communication between end nodes. Allocating all system resources to these CBR applications is not a feasible solution for the upcoming packet oriented wireless systems. Future generation systems will be seamlessly connected to the Internet and will benefit from the All-IP architecture. In order to support both high speed data and CBR, data next generation wireless systems must utilize a combination of power and rate control mechanisms as in cdma2000 1xEV-DV revision D [28].

Current GSM system uses a hybrid of TDMA and FDMA to assign incoming connections to fixed time-slots on 124 different channels each with 200 kHz bandwidth [29]. The accepted users are served in a round-robin fashion for the duration of their calls. The system can assign at most 8 users on a channel. The total transmission rate of the frame is 270.83 kbps and is divided among 8 connections thus granting 33.85 kbps for each individual connection for user data plus overhead information. Since GSM is specifically designed for circuit switched voice transmission, it does not exploit the channel conditions of MSs and hence is not well suited for bursty traffic like packet data transmissions. In fact, Figure 3.1 shows

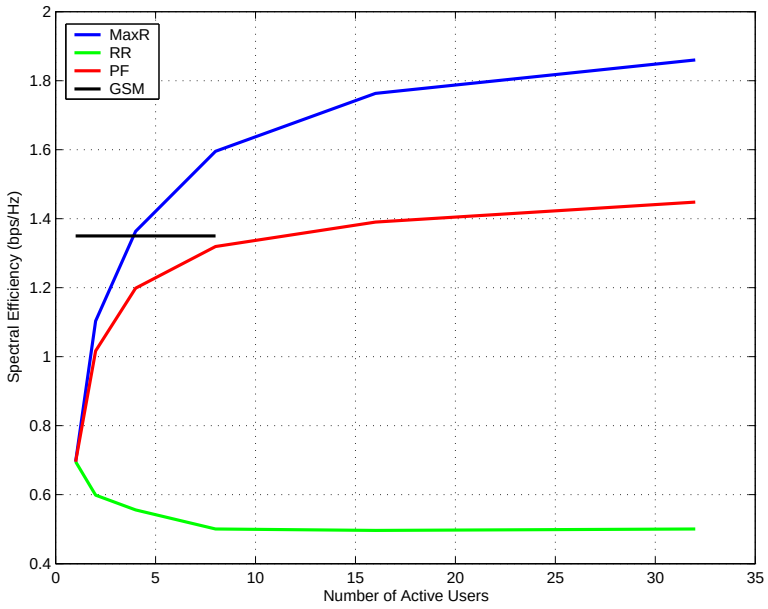

Figure 3.1: Spectral Efficiency Comparison of HDR and GSM

the system performance of HDR in terms of spectral efficiency versus the number of active users in the system. Spectral efficiency (SE) is the measure of the overall system capacity in terms of the amount of information that can be carried within an allotted radio spectrum and is defined by

$$SE = \frac{R(bps)}{BW(Hz)} \tag{3.1}$$

where R is the total system throughput in bps and BW is the total system bandwidth in Hz. The unit for spectral efficiency is bps/Hz.

The spectral efficiency values have been evaluated for the most common scheduling algorithms for HDR, namely Maximum Rate (MaxR), Round Robin (RR) and Proportional Fairness (PF). These algorithms will be discussed in detail in section 3.2.

As can clearly be seen from Figure 3.1, GSM has a fixed spectral efficiency of 1.35 bps/Hz, which is calculated from the frame data rate (270.833 bps) and the allocated bandwidth (200 kHz), whereas HDR has different spectral efficiencies for different number of active users as well as different scheduling algorithms. This is an expected result since HDR is a data optimized system with adaptive coding and modulation and it greatly benefits from

multiuser diversity. HDR also has the ability to allocate resources to users in a soft manner (soft capacity as opposed to hard capacity in GSM) thus the maximum number of users that can be allocated resources is only limited with the Walsh code space. When only 8 active users are considered and RR scheduling is assumed for the HDR, GSM has a better spectral efficiency. The voice oriented system design and the use of fixed type 0.3 GMSK modulation in GSM gives an advantage over HDR using RR when guaranteed bitrate services are of concern (like CBR voice traffic).

IS-95 is a CDMA system [12] in which the users are assigned codes to access the BS. Power control is essential in CDMA based systems since users near the BS shadow users that are relatively distant from the BS. This is known as the near-far problem and is taken care of by utilizing proper power control methodologies. Users closer to the BS transmit at lower power levels and distant ones at higher levels to maintain a constant SNR of the received waveforms at the BS so as to provide fixed data rates for circuit switched voice transmission. A certain guaranteed grade of service is thus provided for such voice oriented systems. However for time varying forward link and packet oriented systems, it is essentially better to employ rate control than power control for a specified average data rate. The gain of rate adaptation over power adaptation subject to average data rate is shown to be equal or greater than 1 as shown in Appendix C.

3.2 Overview of the Scheduling Algorithms

Wireless medium is a shared and a scarce resource due to bandwidth limitations, hence wireless systems should be designed to maximize system performance under the constraint of a given allocated bandwidth. Thus resource management (user scheduling) is a crucial issue in wireless systems engineering. Proper design and implementation of resource management methodologies will lead to higher performance wireless systems.

There are many scheduling algorithms that have been developed and proposed for the HDR, since the IS-856 standard does not specify a certain algorithm. This section briefly explains the most common algorithms.

3.2.1 Round Robin Rule

One well-known scheduling scheme is the round robin (RR) rule [30]. In this type of scheduling the users are served in cyclic order without regard to their channel conditions unless they are in outage. This scheduling has the highest level of fairness among users but the system performance suffers from low average throughput since channel conditions are not exploited.

3.2.2 Maximum Rate Rule

The maximum rate (MaxR) rule is a straightforward implementation of the one user-at-a-time system to maximize the overall system throughput without any delay or fairness constraints. This algorithm is theoretically the best algorithm to maximize total system capacity [10] however it cannot be directly implemented due to fairness considerations. The rule is given by:

$$s = \arg\,\max_i \left(R_i(t)\right) \tag{3.2}$$

where $R_i(t)$ is the maximum supportable data rate requested by the user i at time t and s is the selected user. The information regarding data rate request is sent via the reverse link in the Data Rate Request Channel (DRC) in the IS-856 standard and hence $R_i(t)$ will hereafter be denoted as the DRC request of user i at time t.

3.2.3 The Proportional Fairness Rule

The proportional fairness (PF) rule as described by [31] tries to serve a user when its current channel condition is much better than its average condition calculated over a certain window. This results in achieving a good overall system throughput as well as providing some degree of fairness among users. The rule is given by:

$$s = \arg\,\max_i \left(\frac{R_i(t)}{\overline{R_i(t)}}\right) \tag{3.3}$$

where $R_i(t)$ is the DRC request of the user i at time t, $\overline{R_i(t)}$ is the average rate actually awarded to user i over a certain window of size $Ws = 1000$. The update of the average rate is made at each slot according to:

$$\overline{R_i(t+1)} = \left(1 - \frac{1}{Ws}\right)\overline{R_i(t)} + \frac{1}{Ws}R_i(t) \tag{3.4}$$

The average data rate of each user is updated by using (3.4). If a user is scheduled its current DRC request is used as $R_i(t)$ otherwise $R_i(t) = 0$.

3.2.4 The Exponential Rule

The authors in [32] describe an exponential algorithm that takes into account the delays of the Head of Line (HOL) packets in the user queues as well as the current channel conditions of the users to handle the overall latency and the system throughput in a joint manner. For $a_i > 0, i = 1, 2, ..., N$ the rule is given by

$$s = \arg\max_i \left[\left(\frac{R_i(t)}{\overline{R_i(t)}}\right)\exp\left(\frac{a_i L_i(t) - \overline{aL}}{1 + \sqrt{\overline{aL}}}\right)\right] \tag{3.5}$$

where $L_i(t)$ is the delay of the HOL packet at time t, $R_i(t)$ is the DRC request of the user i at time t, $\overline{R_i(t)}$ is the average rate actually awarded to user i over a window of size $Ws = 1000$ and

$$\overline{aL} = \frac{1}{N}\sum_i a_i L_i(t) \tag{3.6}$$

where N is total number of users and a_i's are the service specific user weights. a_i's have been assumed to be equal to 1 throughout this thesis. This algorithm tries to equalize the weighted delays of the user queues. If the weighted delay of a certain queue is larger than the weighted delays of the others by more than a certain amount then the exponent term overrides the channel considerations and the scheduler gives priority to this queue. If the weighted delay differences among users are small the algorithm behaves like the PF algorithm. The factor 1 in the denominator of the rule is present simply to prevent the exponent from blowing up when the weighted delays are small.

3.2.5 Opportunistic Transmission with Resource Sharing Constraints

The scheduling algorithm presented in [33] takes into account the channel variations in the wireless medium in order to obtain optimality of the overall system throughput under the constraint of time sharing. Time sharing imposes a fairness criterion among the active users

in the system. This algorithm assigns a weight U_i to a potential packet transmission to user i in a given slot.

The rule tries to find a feasible policy $Q \in \Theta$ that maximizes the average system performance. Θ denotes the set of all feasible policies. The problem may be stated as:

$$\max_{Q \in \Theta} E(\sum_{i=1}^{N} U_i 1_{\{Q(\overline{U})=i\}}) \tag{3.7}$$

where

$$1_A = \begin{cases} 1, & \text{if A occurs,} \\ 0, & \text{otherwise} \end{cases}$$

Following the derivations stated in [33] the rule becomes:

$$s = \arg\max_i (U_i + v_i) \tag{3.8}$$

where v_i is a real-valued parameter used to satisfy time-fraction assignment constraint.

The practical implementation of the opportunistic transmission with resource sharing constraints rule is given in [34]. The name slot-fair (SF) will be used for this rule hereafter. When adapted for use in IS-856, U_i becomes the user requested rates normalized to the lowest possible rate of 38.4 kbps. Table 3.2 gives the values for U_i, for the corresponding data rates in HDR.

Table 3.2: U_i Values

Data Rate	U_i
38.4	1
76.8	2
153.6	4
307.2	8
614.4	16
921.6	24
1228.8	32
2457.6	64

The parameter v_i is updated in each slot according to the following equation:

$$v_i(k+1) = v_i(k) - a[1_i(k) - r_i] \tag{3.9}$$

where

$$1_i(k) = \begin{cases} 1, & \text{if user } i \text{ is selected in slot } k, \\ 0, & \text{otherwise} \end{cases}$$

and a is a constant to track the variations in the system. Its value is set such that the allocation of time-slots among users is approximately equal.

The initial parameter values for all users are zero. r_i is the proportion of time-slots user i should receive in the long run. Although this proportion can be set differently for individual users, each user will be treated equally for our simulations. This implies

$$r_i = \frac{1}{N} \tag{3.10}$$

where N is the total number of active users in the system.

3.2.6 Minimum Performance Rule

The authors in [35] describe a scheduling algorithm in which users are guaranteed a certain minimum throughput. This algorithm will be denoted as MinPerf. The minimum throughput can be chosen differently for each user. The algorithm selects the user according to:

$$s = \arg\max_i \left(\alpha_i(t) U_i(t)\right) \tag{3.11}$$

where $\alpha_i(t)$ is a parameter with a minimum value of 1 (also the initial value for each user) that is updated every slot and $U_i(t)$ is the performance value of user i in time slot t. The performance value we are going to assume in this paper will be the throughput of a user normalized to the lowest throughput available in the system. For HDR the lowest throughput is 38.4 kbps so a user with a scheduled transmission rate of 614.4 kbps would, as the performance value, have 16.

The update of the parameter $\alpha_i(t)$ is made using stochastic approximation [36] and includes the minimum performance guarantee as throughput. The update is as follows:

$$\alpha_i(t) = max\left[(\alpha_i(t-1) - a(\overline{R_i(t)} - C_i)), 1\right] \tag{3.12}$$

where $\overline{R_i(t)}$ is the average user data rate that is updated as in PF and C_k is the minimum performance value specified as throughput. In the simulations C_k will be the QoS param-

eter to compare the performance of this algorithm to the proposed algorithm in terms of statistical assurance.

3.3 QoS Aware Scheduling Algorithms for HDR

3.3.1 The RExpQoS Rule with Threshold Extension

The PF and the Exponential rules in their originally proposed forms do not have satisfactory QoS performances in terms of the PoTP. I will propose and present two rules that incorporate the QoS parameter to improve the PoTP. Both of these rules use a modified version of the exponential rule. My motivation for using the exponential rule is that instead of equalizing weighted delays of the queues, I try to equalize the average data rates of all the users with respect to the QoS requirements. In this thesis, I assume the QoS requirements for all of the users are the same, i.e. all users are to be given the same average data rate as specified by QoS. However, the proposed scheduling algorithms can also be used in a wireless system that provides a multitude of services, each requiring different QoS values. The first rule can be explained as follows:

STEP 1: Select the user with the highest argument according to:

$$s = \arg\ \max_i \left[R_i(t) \exp\left(\frac{QoS - \overline{R_i(t)}}{1 + \sqrt{QoS}} \right) \right] \tag{3.13}$$

STEP 2: Check the current requested data rate of user s.

STEP 3: If the current requested data rate for user s is equal to or greater than a certain threshold (optimized via simulation) service this user.

STEP 4: Otherwise select the user with the next highest argument and proceed with step 2 until all the users are scanned in the array to satisfy the condition.

STEP 5: If none of the users satisfy the threshold requirement, select the user with the highest argument regardless of its requested data rate.

If the average data rate of a user falls below the QoS requirement by more than order $\sqrt{QoS}$ the exponential term dominates, overriding the $R_i(t)$ term thus favoring this user. When the average data rate is close to QoS the exponential term is close to 1 and the algorithm behaves like MaxR. The threshold extension to the algorithm is needed to provide higher throughputs to the users to maintain high average data rates over the window size.

As the QoS requirements increase, thresholds increase to maintain higher average data rates over the window so as to get closer to QoS levels. This can be seen in Figures 3.3 and 3.4 for both SC and MC systems. During the simulations, the calculation of the thresholds have been made by employing a simple optimization method. In obtaining the PoT results, all possible threshold values (ranging from 38.4 kbps to 2.457 Mbps) have been considered by running the same simulation setup (fixed number of users and fixed QoS parameter) once with each threshold. The threshold giving the minimum PoT value has been chosen as the optimum threshold corresponding to a certain fixed number of users and fixed QoS case. For proper assessment, the thresholds from 38.4 kbps to 2.457 Mbps have been assigned values from 1 to 9 respectively. Figure 3.2 shows an example on the determination of the threshold for an example case with 24 users and with QoS requirement 64 kbps. The minimum PoT value (30%) is obtained for the threshold index 7 which corresponds to 1228.8 kbps. The thresholds for any number of users and any given QoS requirement can be calculated at the BS by using a function incorporating the number of active users and QoS parameter as the two input variables and the threshold as the output variable. For this purpose, based on the simulation data, surface fitting method may be applied to determine the function that calculates the threshold corresponding to a certain number of users and a certain QoS requirement. By using this function, real-time computation of the thresholds may be achieved. This, however, necessitates additional computation power at the BS.

The QoS set I have used in the simulations is 16 kbps 32 kbps 64 kbps 128 kbps for SC and 64 kbps 128 kbps 256 kbps 512 kbps for MC which have been chosen to cover the typical range of streaming audio or video encoded at one of these rates. The simulation results for this algorithm show that there is a considerable improvement over PF and Exp rules in terms of the PoT the users are granted their QoS requests. For the SC case, as the QoS requirement increases from 16 kbps to 128 kbps the PoT these rates are granted to the users falls as expected. Large differences are observed for the low QoS requirements, 16 kbps and 32 kbps. The algorithm still has slightly higher performance than the PF and the Exp rules for the 64 and 128 kbps QoS requirements.

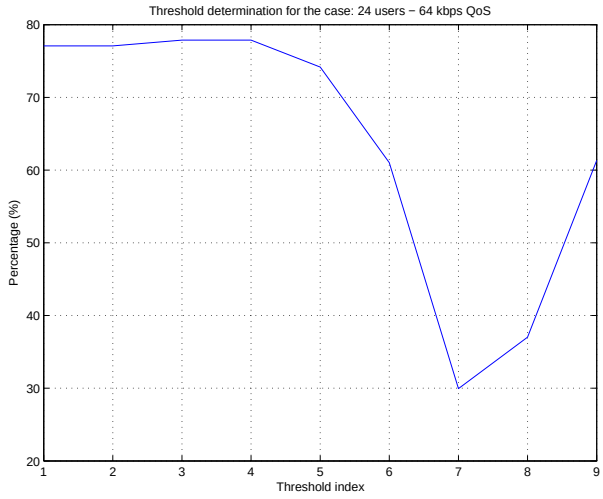

Figure 3.2: Threshold determination for an example case with 24 users and 64 kbps QoS requirement

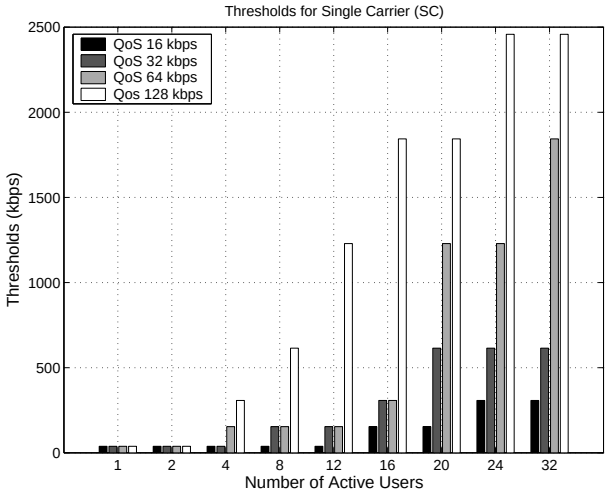

Figure 3.3: Optimized threshold values for SC

3.3.2 The $R^2ExpQoS$ Rule

The second proposed rule places more importance on the current data request of the users than the exponential part. These rates, as I have mentioned before, play an important role to increase the average data rate of the users over the window thus helping users get closer data rates to their QoS requirements.

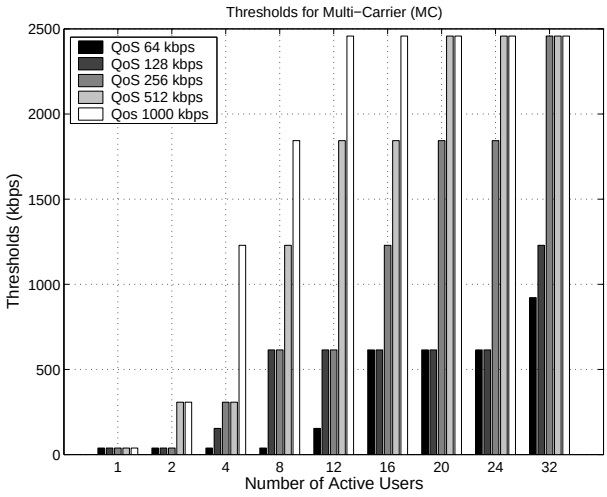

Figure 3.4: Optimized threshold values for MC

The second rule is:

$$s = \arg\max_i [R_i(t)]^2 \exp\left(\frac{QoS - \overline{R_i(t)}}{1 + \sqrt{QoS}}\right) \tag{3.14}$$

The difference of this rule from the first rule is that the current data rate request term is squared and there is no threshold requirement. From the simulation results we see that this rule still outperforms the PF and the Exp rules in terms of the PoT QoS is guaranteed. For higher QoS and higher number of active users, the rule results in 0 % satisfaction to the PoTP requirement meaning the system cannot support this many users at the corresponding QoS (i.e. 64 and 128 kbps) values. In the SC case, for 16 and 32 kbps the rule performs fairly well, for 64 kbps, the rule starts to reject users beyond a capacity of 16 and finally for 128 kbps the system can only support 8 users with QoS. For 16 and 32 active users the rule cannot provide an acceptable PoTP to the users. The implementation complexity for this rule is less than the first rule since there is no threshold adjustment.

3.4 Conclusion

In this chapter, the service levels and the packet scheduling algorithms in wireless systems have been introduced along with the proposed QoS aware scheduling algorithms. The performance evaluations of these algorithms are presented in chapter 4.

Chapter 4

WIRELESS CHANNEL MODELING AND SIMULATIONS

4.1 Wireless Channel Modeling

One of the most important challenges in the field of wireless communications is the proper modeling of the wireless channels. The performance of the wireless communication systems rely heavily upon the models that are developed in accordance with the specific requirements of the wireless systems.

In order to develop the most suitable wireless channel model for the system being considered, it is almost imperative to clearly identify the limits (or required specifications) of the wireless system taking into account the geographical factors which directly affect the system performance. These factors may include:

- Mobility of the users
- Land structure
- Population density etc.

Geographical factors impose specific design methodologies for the wireless system so the choice of system parameters and the attainable performance metrics are defined according to these factors. Important system parameters can be listed as:

- Typical operation range
- Typical system coverage
- System capacity
- Services to be offered etc.

Today's wireless networks operate on a cellular structure to extend the range and the capabilities of wireless services. A typical cellular radio system is comprised of a collection of fixed BSs and MSs scattered randomly within the coverage range of the cell. Figure 4.1

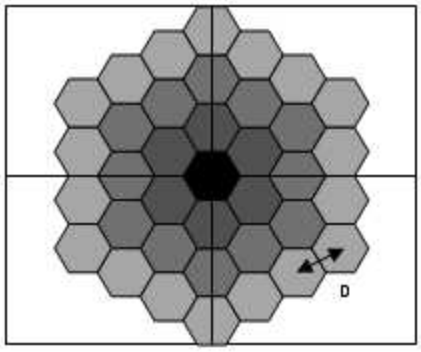

Figure 4.1: A typical cellular structure

shows a typical cellular structure with emphasis on the middle black cell. Channel and system modeling is generally done in a single cell while taking into account the interference effects of the neighboring cells.

In the mobile radio environment there are natural and man-made objects between the BS and the MS. These objects reflect and scatter the radio waves so the signals sent from the BS arrive at the MS from different directions with different delays. This effect is the multipath propagation (Rayleigh Fading) and is an important characteristic of the mobile radio channel. As a result of multipath propagation the observed signal level at the MS fades randomly which can be modeled as a stochastic process.

Another important factor involved in the mobile radio channel is the shadow fading which results from the slower changes in the signal level. These slower variations of the signal level are due to large obstacles such as hills or buildings. Shadow fading is generally modeled as a lognormal random variable.

The received signal power also decays with a power of the direct path length (d) between the BS and the MS. The power of the path length may vary according to the density of obstacles in the region. This is known as the path loss. Theoretical path loss models such as power of distance decay are generally not suited to real-life channel modeling so many empirical models have been developed by curve fitting experimental data. These models are generally geography dependent models.

Radio channels also exhibit characteristics based on the carrier frequency of the signal that is used in the wireless system. Channels may be classified as being frequency-selective

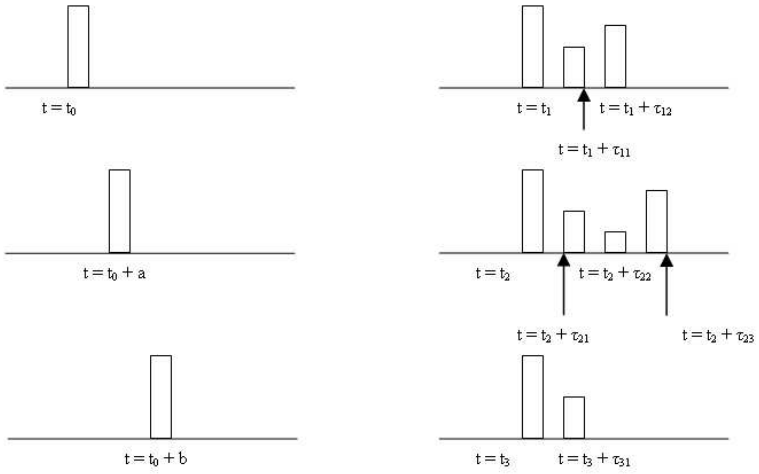

Figure 4.2: An example of the response of a time variant multipath channel to a narrow pulse

or frequency-non-selective (flat). Details on the frequency selectivity of the channels will be discussed later in this chapter.

4.1.1 Multipath Propagation (Flat)

The signal transmitted from the BS arrives at the MS in several different paths. Along these paths the individual rays are exposed to varying amplitude scaling factors and different delays proportional to the distance they travel along that specific path.

Transmitted signal can be represented as:

$$s(t) = Re\{s_l(t)e^{jw_c t}\} \tag{4.1}$$

where $s_l(t)$ is the low-pass equivalent of the signal $s(t)$ and w_c is the carrier frequency.

The received bandpass signal can be represented as:

$$r(t) = \sum_n \alpha_n(t)s[t - \tau_n(t)] \tag{4.2}$$

where $\alpha_n(t)$ is the time-varying attenuation coefficient and $\tau_n(t)$ is the the time-varying delay for path n. Substituting $s(t)$ in (4.1) into (4.2) the following result is obtained

$$r(t) = Re\{[\sum_{n} \alpha_n(t) e^{-jw_c\tau_n(t)} s_l(t - \tau_n(t))] e^{jw_c t}\} \tag{4.3}$$

$r(t)$ can be represented using its low-pass equivalent form as

$$r(t) = Re\{r_l(t) e^{jw_c t}\} \tag{4.4}$$

where

$$r_l(t) = \sum_{n} \alpha_n(t) e^{-jw_c\tau_n(t)} s_l[t - \tau_n(t)] \tag{4.5}$$

Following the fact that $r_l(t)$ is the response of the low-pass channel to the low-pass signal $s_l(t)$, the channel is described by the time-variant impulse response as

$$c(\tau; t) = \sum_{n} \alpha_n(t) e^{-jw_c\tau_n(t)} \delta[\tau - \tau_n(t)] \tag{4.6}$$

Supposing an unmodulated carrier is transmitted ($sl(t) = 1$)

$$r_l(t) = \sum_{n} \alpha_n(t) e^{-j\phi_n(t)} \tag{4.7}$$

where

$$\phi_n(t) = w_c\tau_n(t) \tag{4.8}$$

From the above expression it can easily been seen that the received signal is a sum of time-variant vectors having amplitudes $\alpha_n(t)$ and phases $\phi_n(t)$. Since the delays of different paths change in a random manner $r_l(t)$ can be modeled as random process. When a large number of paths are considered, the Central Limit Theorem [17] may be applied and $r_l(t)$ can thus be modeled as a complex valued Gaussian random process. This also means $c(\tau; t)$ is a complex valued Gaussian random process thus the envelope $|c(\tau; t)|$ at instant t is Rayleigh distributed. Hence the channel is said to be *Rayleigh fading channel*. The Rayleigh probability density function (PDF) is illustrated in Figure 4.3.

4.1.2 Shadow Fading

When the signal transmitted from the BS encounters large obstacles like buildings and hills the signal level fades for a longer duration of time. The change of signal level due to such

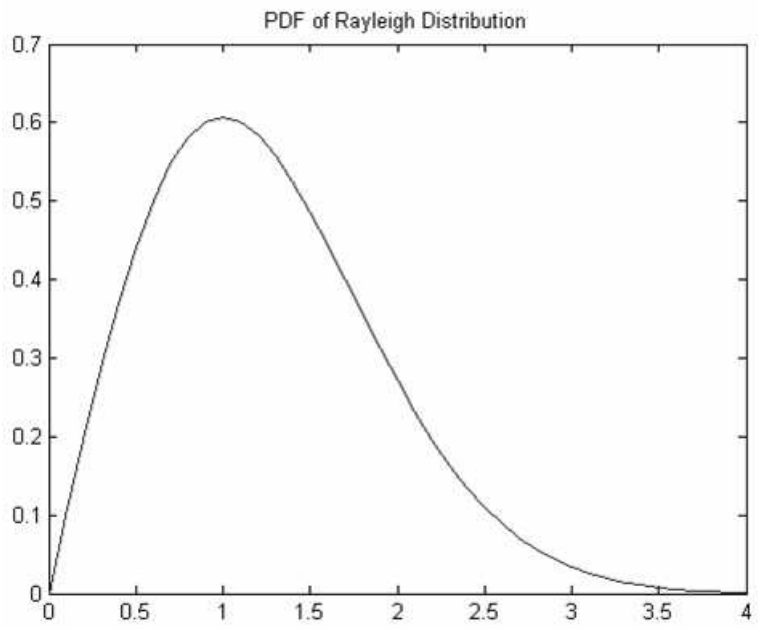

Figure 4.3: Rayleigh PDF

large obstacles is quite slow when compared to Rayleigh Fading. The variations of the signal level in dB about its mean have been observed to demonstrate normal distribution. This implies the signal envelope levels are log-normally distributed around their means.

4.1.2.1 Correlation Model for Shadow Fading

In the design of wireless systems a better understanding of the correlation properties of shadow fading is required. Based on experimental data, Gudmundson [37] proposed a simple correlation model for shadow fading. With this simple model the effect of shadowing can easily be integrated into the overall wireless channel model.

In the model the correlation is given by

$$R_A(k) = \sigma^2 a^{|k|} \tag{4.9}$$

where

$$a = \varepsilon_D^{vT/D} \tag{4.10}$$

In (4.9) σ^2 is the variance and is usually in the range 3-10 dB. In (4.10) ε_D is the correlation

between two points separated by a distance D.

Figure 4.4 shows the normalized autocorrelation in urban environment. Correlation at a distance of $D = 10$m is taken to be $\varepsilon_D = 0.3$ with standard deviation $\sigma = 4.3$ dB [37].

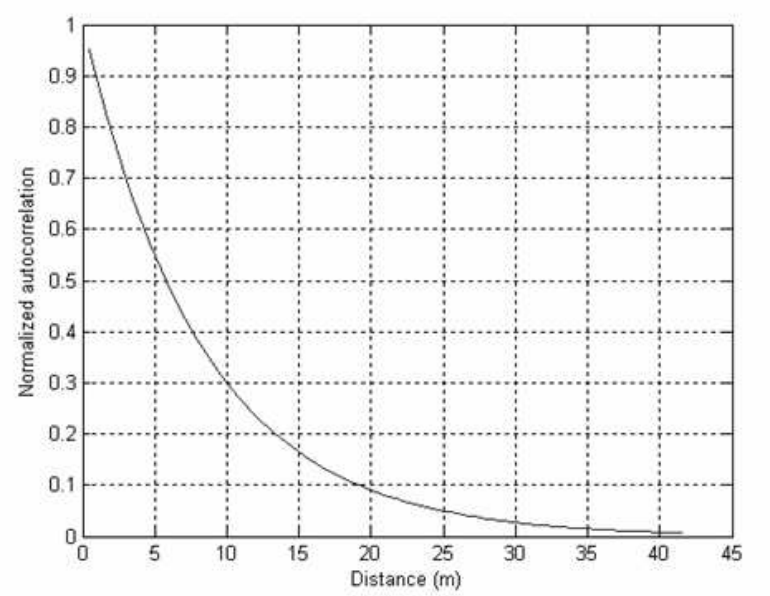

Figure 4.4: Normalized autocorrelation

4.1.3 Path Loss

In the design of wireless systems the mean level of received signal power is representative of the users' average channel conditions. Several useful empirical models have been developed for large-scale path loss by experimentation and curve fitting. Some of these rules are

- Okumura-Hata Model [38]
- Lee's Area-to-Area Model [39]
- COST231-Hata Model [40]
- COST231-Walfisch-Ikegami Model [40]
- ITU-R M.1225 Path Loss Model [41]

In this thesis the ITU-R M.1225 Path Loss model has been chosen since it is both easy to implement and also quite accurate for outdoor channel types.

Using [41] we can state that

$$L(dB) = 30log_{10}(f_{c,MHz}) + 40log_{10}(d_{km}) + 49 \tag{4.11}$$

for the pedestrian channel and

$$\begin{aligned} L(dB) &= -18log_{10}(H_{BS,m}) + 21log_{10}(f_{c,MHz}) \\ &\quad + 40(1 - 0.004H_{BS,m})log_{10}(d_{km}) + 80 \end{aligned} \tag{4.12}$$

for the vehicular channel. In (4.11) and (4.12) $L(dB)$ stands for the overall received signal power in dB, $f_{c,MHz}$ is the carrier frequency in MHz, d_{km} is the distance of the MS from the BS, and $H_{BS,m}$ is the height of the BS antenna in meters.

Table 4.1 summarizes the ITU-R channel models with their respective parameters

Table 4.1: ITU-R Channel Models and Parameters

Pedestrian Channel Model	
Parameter	**Value**
Path Loss (dB)	$L(dB) = 30log_{10}(f_{c,MHz}) + 40log_{10}(d_{km}) + 49$
Speed	3 km/h
Number of paths	1
Multipath normalized	[0.97]
Uncaptured power	[0.03]
Vehicular Channel Model	
Parameter	**Value**
Path Loss (dB)	$L(dB) = -18log_{10}(H_{BS,m}) + 21log_{10}(f_{c,MHz})$ $+40(1 - 0.004H_{BS,m})log_{10}(d_{km}) + 80$
Speed	120 km/h
Number of paths	3
Multipath normalized	[0.7774 0.0301 0.0574]
Uncaptured power	[0.1351]

In Table 4.1, the label "multipath normalized" corresponds to the percentage of the transmitted power that is captured by the MS and the label "uncaptured power" denotes the percentage of power that cannot be captured. In the pedestrian channel, only one direct path is assumed and in the vehicular channel there are 3 distinguishable paths that can be recovered by the Rake receiver. The amount of power received by each finger of the Rake

is indicated by the label "multipath normalized" in the vehicular channel model.

4.1.4 Channel Modeling for MC Approach

In [10] it is shown that serving one user at a time is the optimal method to attain system capacity. The optimality of this scheme is proved for the flat-fading channel. When a broader bandwidth is of concern (like in the MC case) certain design methodologies need to be followed. Multiple accessing over frequency selective fading channels has been studied in [42] and in this paper it has been shown that applying water filling in frequency, just as in time, offers the optimal system performance for frequency selective fading. Following the results of [42], serving one user at a given frequency and at a given time achieves the optimum performance from an information theoretic point of view and hence the basis for our study of 3xHDR has stemmed from the optimality of this scheme. Considering flat fading on each of the separate carriers, different carriers may serve different users at a given time hence increasing overall system throughput and decreasing the overall latency. The resource sharing is demonstrated in Figure 4.5 the for 3xHDR system. In the SC case, there are two resources to be shared: time and code (user). The MC approach adds a third dimension in resource sharing problem adding frequency as the third dimension. The shaded blocks demonstrate the scheduled users to be served by the carriers. One important thing is that each carrier can serve only one user in a single slot, but a user may be served by more than one carrier in that slot.

In the general M subcarrier MC approach, the bandwidth of each subcarrier is chosen such that individual subcarriers undergo flat fading. If the signal faces frequency selective fading, ISI is observed which degrades the overall system performance. Furthermore, the one user at a time scheme would no longer be optimal.

One important issue when there are side-by-side carriers is the envelope correlation between these carriers. It is shown in [43] that the correlation at any instant of time between the fade envelopes of i^{th} and j^{th} subcarriers is

$$E\{\alpha_{k,i}\alpha_{k,j}\} = \frac{1}{1+[\frac{\Delta f}{B_c}]^2} \equiv \rho^{(k)}(f_i - f_j) \tag{4.13}$$

where $\alpha_{k,i}$ and $\alpha_{k,j}$ denote the envelopes of the side-by-side carriers i and j at instant k, $\Delta f = f_i - f_j$ is the frequency separation of the i^{th} and j^{th} carriers expressed in MHz, and

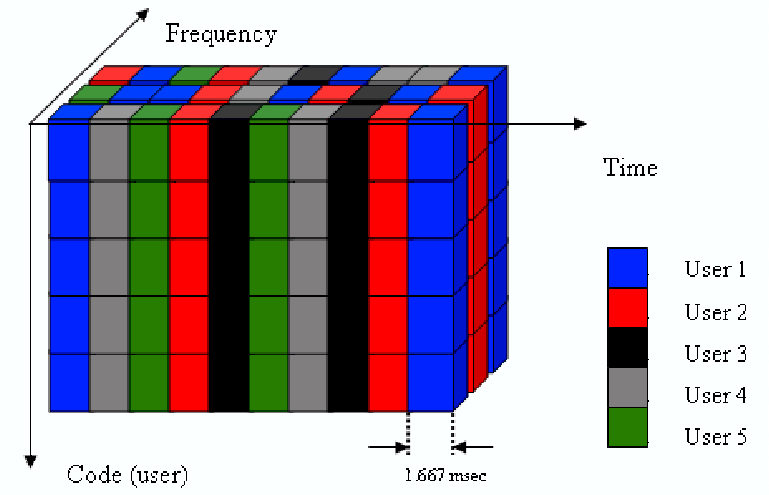

Figure 4.5: Illustrative resource allocation scheme for the MC HDR

B_c is the coherence bandwidth of the channel.

Coherence bandwidth is the range of frequencies over which the channel is considered to be "flat" (constant gain over the all the signal frequencies) and it determines frequency selectivity of the channel

$$B_c = \frac{1}{\sigma_\tau} \tag{4.14}$$

where σ_τ is the rms delay spread of the channel. Each channel exhibits unique properties and hence is identified by its power delay profile (PDP). A sample PDP is presented in Figure 4.6.

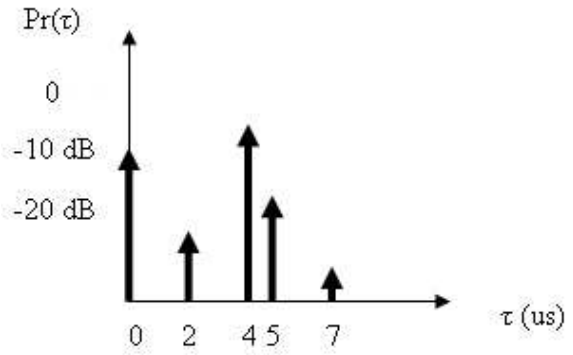

Figure 4.6: A sample PDP

In this thesis, the wideband parameters given in Table 4.2 for the ITU-R test channels have been assumed [41].

Table 4.2: RMS Delay Spread and Channel Coherence Bandwidths

Test Environment	Channel A		Channel B	
	σ_τ (ns)	B_c (MHz)	σ_τ (ns)	B_c (MHz)
Indoor	35	7.89	100	2.76
Outdoor to Indoor and Pedestrian	45	6.13	750	0.368
Vehicular	370	0.746	4000	0.069

In order to generate correlated Rayleigh fading envelopes, the method in [44] has been followed and the details are given in Appendix B.

4.2 Simulations

In order to evaluate the performance of the proposed algorithms a detailed simulation framework has been developed. The main stages of the simulation framework can be summarized as follows:

- Physical Layer Simulations
- System Level Simulations
- Resource Management Simulations (Scheduling)

4.2.1 Physical Layer Simulations

The HDR system makes use of adaptive coding and modulation to support the data rates presented in Table 4.3. Comprehensive simulations have been performed of the IS-856 physical layer using Agilent's Advanced Design System (ADS 2002C) in order to obtain the minimum required E_c/I_o values for 1% packet error rate (PER) which is the assumed target throughout the thesis. E_b/N_t values are obtained from system processing gain (PG) and E_c/I_o values using the equality:

$$E_c/I_o(dB) + 10log_{10}(PG) = E_b/N_t(dB) \tag{4.15}$$

and are presented in Table 4.3.

Table 4.3: Required E_c/I_o Values for 1% PER

Rate (kbps)	Slots	Bits	Number of Chips	Processing Gain	Min. Req. E_c/I_o (dB)	Min. Req. E_b/N_t (dB)
38.4	16	1,024	24576	24	-11.68	2.12
76.8	8	1,024	12288	12	-9.31	1.48
153.6	4	1,024	6144	6	-6.14	1.64
307.2	2	1,024	3072	3	-2.96	1.81
614.4	1	1,024	1536	1.5	-0.77	0.99
307.2	4	2,048	6272	3.06	-3.94	0.92
614.4	2	2,048	3136	1.53	-0.88	0.97
1,228.8	1	2,048	1536	0.75	3.55	2.30
921.6	2	3,072	3136	1.02	1.58	1.67
1,843.2	1	3,072	1536	0.5	7.73	4.72
1,228.8	2	4,096	3136	0.77	3.62	2.46
2,457.6	1	4,096	1536	0.38	11.19	6.93

The simulation setup that has been utilized in ADS has been built on the 1xEV example project available in the software. ADS simulates the AWGN performance of the forward traffic channel via discrete time execution. The simulation setup is shown in Figure 4.14. This setup shows the system blocks used to evaluate forward demodulation performance of the HDR system. Several modifications have been made on the original example to save simulation time and to obtain more accurate results. The simulation has been performed at the baseband level without RF modulation. Effects due to RF characteristics of the received signal have been taken into consideration in the system level simulations. One major modification has been on the block "1xEV_TurboDecoder". The original block consists of 4 Maximum Aposteriori Probability (MAP) decoders. In order to increase the performance of turbo codes, the number of iterative decodings should be sufficiently large [19]. Hence to obtain a good decoding performance the number of MAP decoders have been increased to 12. The "1xEV_TurboDecoder" block is shown in Figure 4.13.

There are 12 different data rate options in the HDR which are differentiated by the variable "DataRate" as shown in Figure 4.12. This variable takes on values from 0 (corresponding to 38.4 kbps) to 11 (corresponding to 2457.6 kbps) to account for the different data rate options. The purpose of performing physical layer simulations is to obtain the C/I values which correspond to 1% PER. To account for the interference power, AWGN has been used in the simulation setup. By sweeping the parameter I_{oc}, which corresponds

to the white noise spectral density (dBm/1.25 MHz), PER values are obtained. The total BS transmitter power is taken to be 16 dBm. The I_{oc} value which gives 1% PER is used to obtain the C/I as follows:

$$C/I(dB) = 16 - I_{oc}(dB) \tag{4.16}$$

The C/I values giving 1% PER are then used in the resource allocation simulations to map the received signal powers of the MSs to data rates of the HDR system.

Figure 4.7 is the signal source and transmitter part of the 1xEV-DO system. As the signal source, random bits are generated with probability of 1's and 0's being equal. Depending on the data rate value, forward link packets are formed by combining the corresponding number of bits for each packet. The packets pass through the CRC encoder, tail former followed by the Turbo encoder. Later scrambling and interleaving are applied to the packets. The block 1xEV_FwdSrc performs the time division multiplexing of forward preamble, pilot, traffic and MAC channels. In Figure 4.8 modulation is performed at the baseband level. The modulated signal is sent through the AWGN channel and then demodulated. Figure 4.9 shows the receiving section of the HDR system. The inverse operations with respect to the ones performed in Figure 4.7 are performed here. Figure 4.10 shows the scrambling code generation and the delay element needed to compare the original bitstream with the decoded bitstream. Finally, Figure 4.11 shows the blocks for PER and BER calculation. The parameters and variables needed in performing the simulations are shown in Figure 4.12. An overall view of the ADS simulation platform is shown in Figure 4.14.

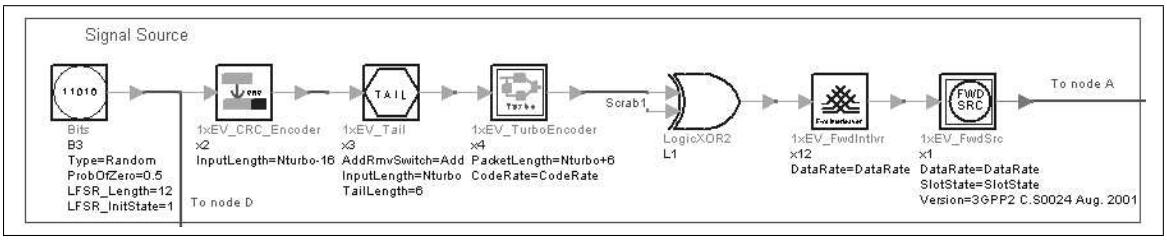

Figure 4.7: 1xEV Transmitter

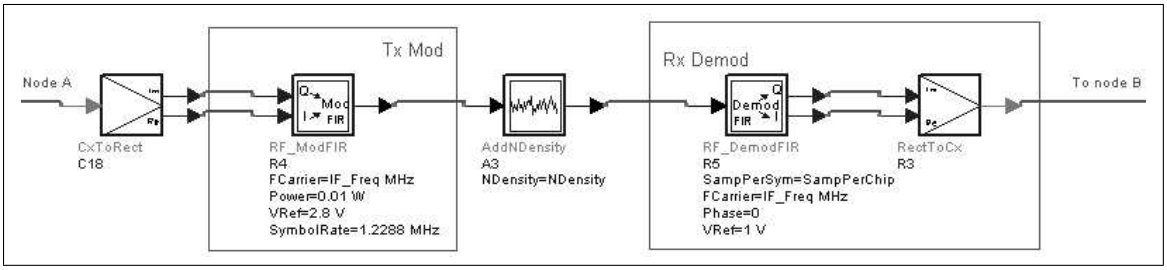

Figure 4.8: Modulation, AWGN and demodulation

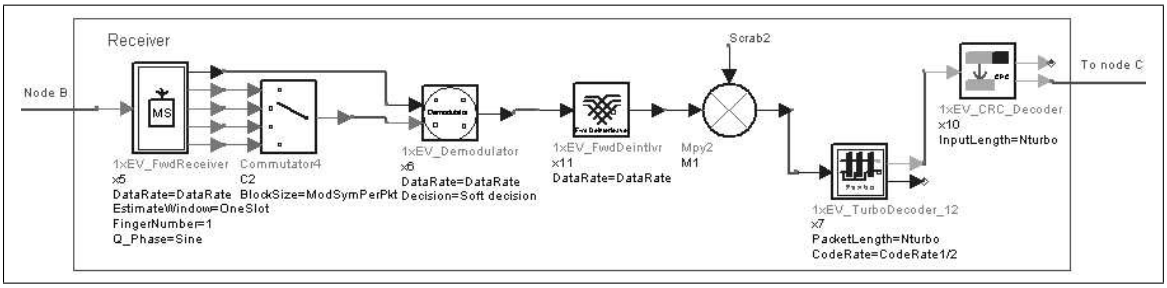

Figure 4.9: 1xEV Receiver

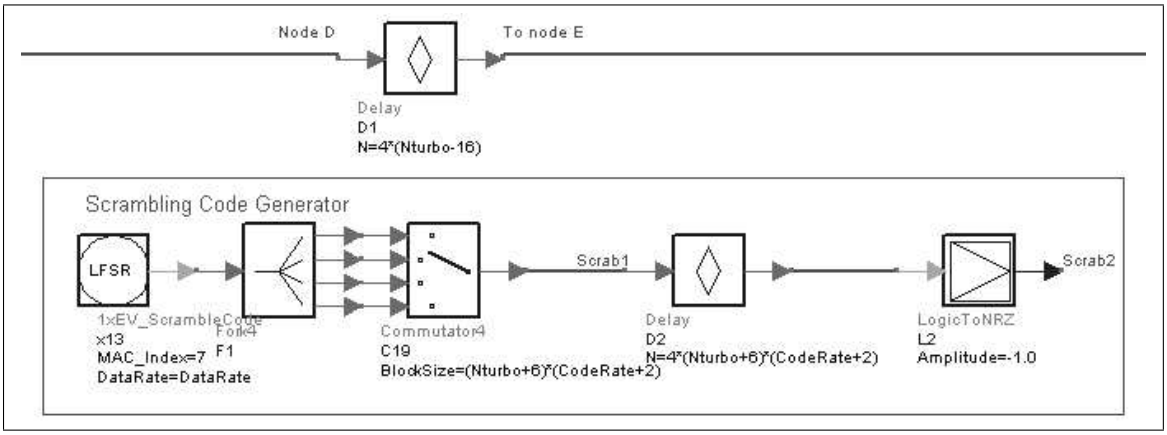

Figure 4.10: Scrambler and delay element for PER calculation

4.2.2 System Level Simulations

System level simulations include network planning and propagation modeling and have been performed in MATLAB. The thesis is concerned only with the forward link of the HDR system. In this light the BS is the transmitter and the MSs are the receivers.

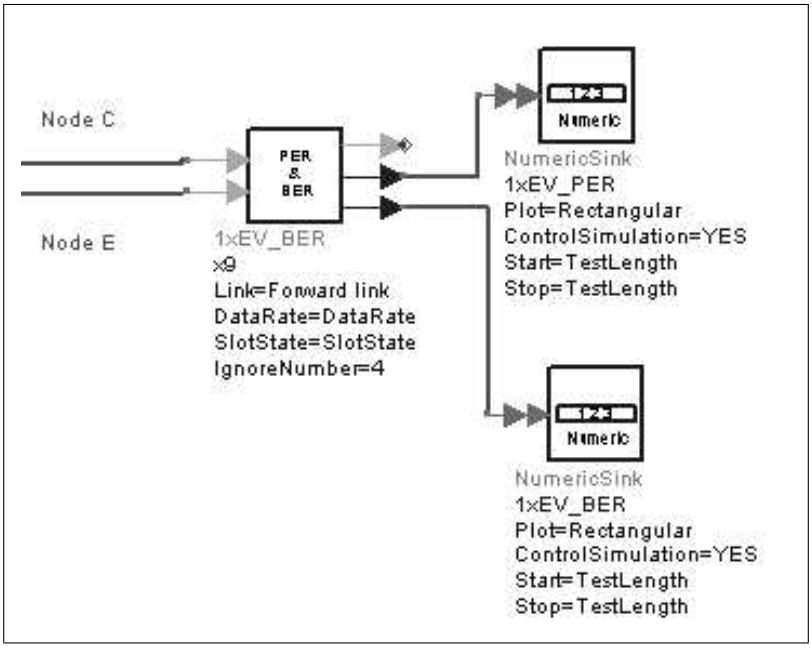

Figure 4.11: BER and PER calculation

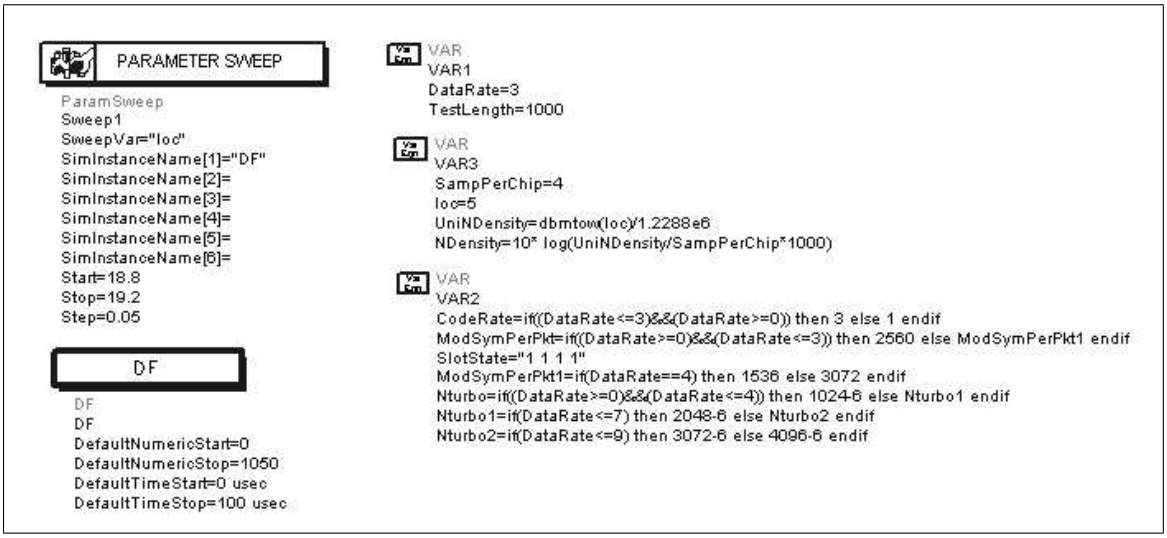

Figure 4.12: Simulation parameters and variables

4.2.2.1 Network Planning

In the simulations a 3-tier cellular layout has been considered (Figure 4.1). The simulations have been performed with the mobile users uniformly distributed throughout the center cell. A sample drop of 32 users is shown in Figure 4.15. After uniformly distributing the

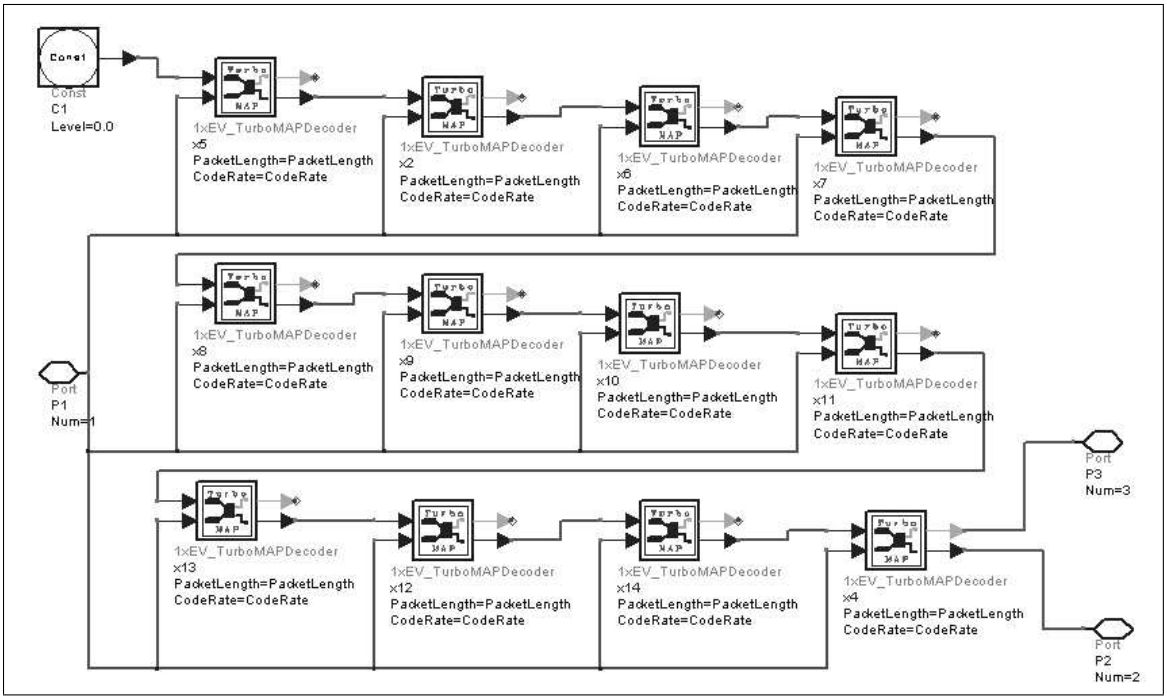

Figure 4.13: Modified turbo decoder with 12 MAP decoders

users in the center cell, signal power for each mobile is calculated from (4.19). $SINR_i$ for each mobile i is calculated taking into account the interference from the neighboring cells and the thermal noise and given as in (4.17). Since pedestrian A channel is utilized single path Rayleigh fading is assumed with a 97% path capture factor. Remaining 3% accounts for interference.

$$SINR_i = \frac{P_r^i}{\sum_{k=1}^{n} P_{t,k} L_k + N} \tag{4.17}$$

where n is total number of interfering BSs ($n = 36$ for the simulations), L_k is the path loss for k^{th} interfering BS and N is the thermal noise which is calculated using:

$$N = F + 10log_{10}(kTB) \tag{4.18}$$

where F is the receiver noise figure (taken as 9 dB [45]), k is Boltzmann's constant (1.38e-23 J/K), T is the operating temperature ($T = 290$ K) and B is the receiver bandwidth ($B =$ 1.25 MHz).

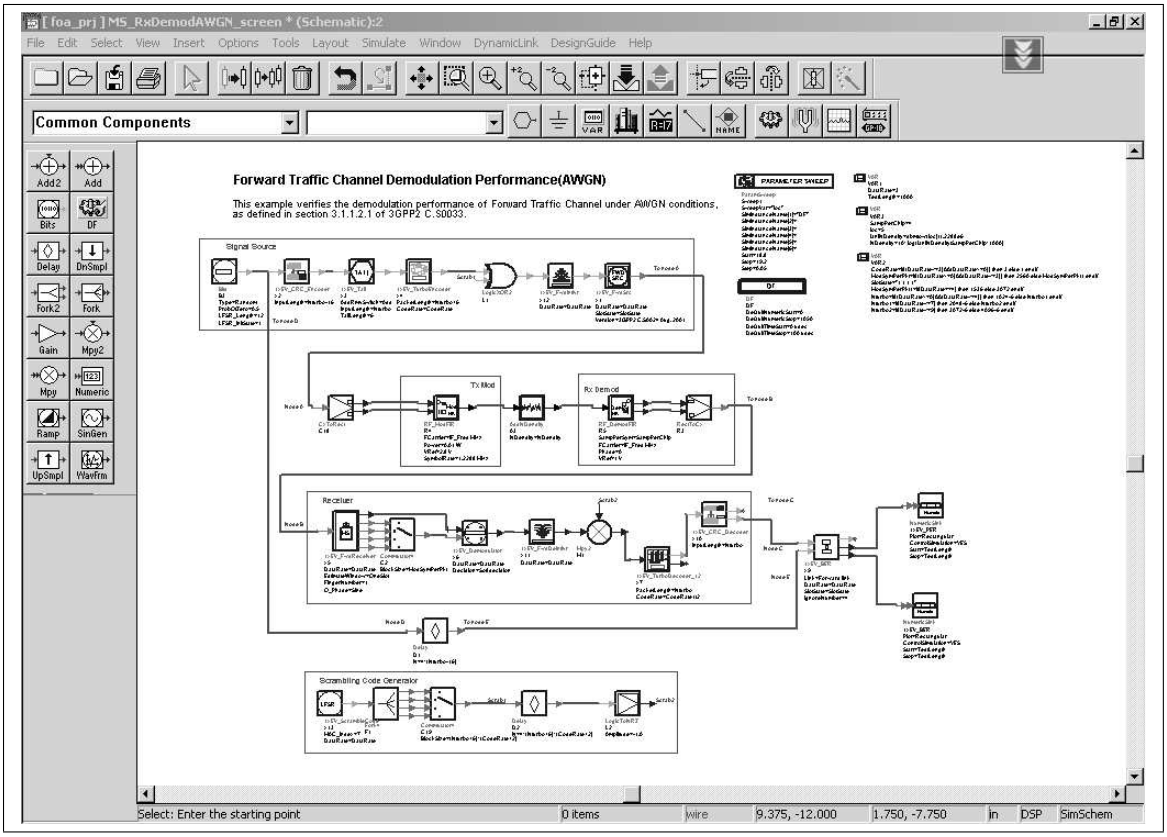

Figure 4.14: Overall view of the ADS simulation platform

From the above values the thermal noise is obtained to be -104 dBm. In practice, these $SINR$ values are reduced by the implementation imperfections and hence are normalized to 13 dB which is the maximum attainable $SINR$ value. Figure 4.16 shows the CDF of user $SINRs$.

The network parameters and link budget are summarized in Table 4.4.

4.2.2.2 Propagation Modeling

The received signal power levels at the user terminals may be expressed as:

$$P_r^i = P_t(dB) - L_i(dB) + X_\sigma^i(dB) + R^i(dB) \tag{4.19}$$

where P_r^i is the received signal power for user i (in dB), P_t is the BS transmit signal power (in dB), X_σ^i is log-normal shadow fading for user i with variance σ in dB and R_i is the

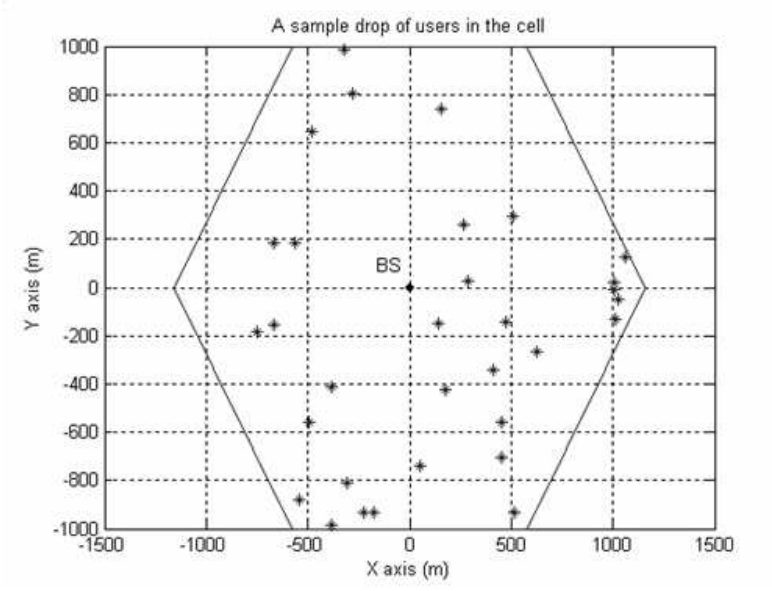

Figure 4.15: A sample drop of 32 users in the center cell

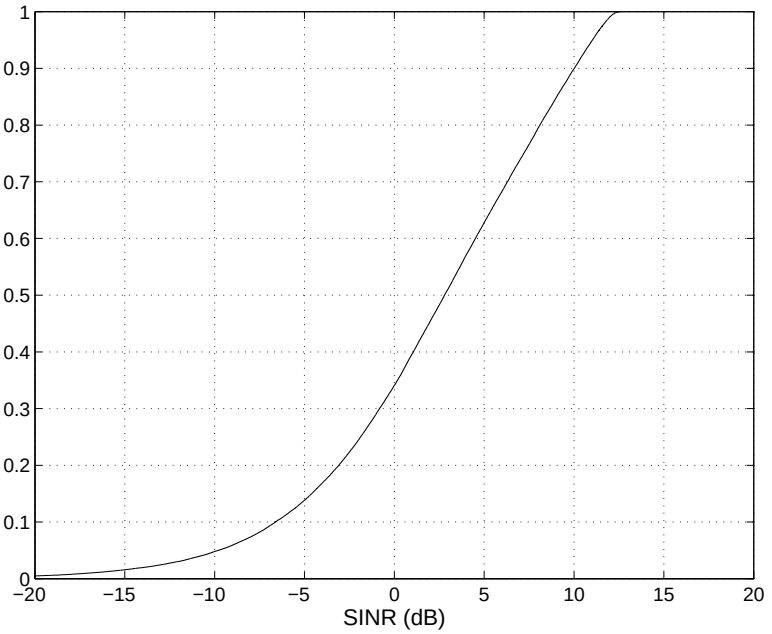

Figure 4.16: CDF of user SINRs in the pedestrian A channel

Rayleigh fading coefficient for user i (in dB).

In propagation modeling the following models have been utilized:

Table 4.4: System Parameters and Forward Link Budget.

Carrier Frequency	2 Ghz
Chip Rate	1.2288 Mcps
Cell Layout	Hexagonal, 3 Tier
BS-to-BS Distance	2000m
Radiation Pattern	Omnidirectional
Path Loss Model (dB)	$30\log_{10} f_c + 49 + 40\log_{10} d$ $d(km), f_c(MHz)$
Log-normal Shadowing	Gudmundson Model (4.3 dB variance)
Short term fading	Rayleigh with Jakes spectrum
User distribution	Uniform
BS Output Power (K)	41.8 dBm
TX Antenna Gain (L)	17 dBi
Cable Loss (M)	3 dB
Body Loss (N)	3 dB
Total Forward Traffic Channel Tx Power (=K+L-M-N)	52.8 dBm
Thermal Noise	-104 dBm

Path Loss Model The path loss model for the ITU pedestrian test environment has been used [41] and it is given as:

$$L(dB) = 30log_{10}(f_c) + 49 + 40log_{10}(d) \tag{4.20}$$

where f_c is the carrier frequency (MHz), d is the distance (km) from the BS to the MS.

Slow (Shadow) Fading In order to model the slow variation of the user signal powers, shadow fading has been generated using log-normal random process with autocorrelation properties from Gudmundson model [37]. The shadow fading model can be expressed as a white noise process that is filtered by a first order low-pass filter [46] as shown in (4.21)

$$X_{k+1}(dB) = aX_k(dB) + (1-a)w_k \tag{4.21}$$

where X_k is the mean envelope level (in dB) experienced at time k, w_k is the zero-mean Gaussian random variable and a is the parameter that controls the spatial correlation of the shadows. From [37]:

$$a = \varepsilon_D^{vT/D} \tag{4.22}$$

ε_D is the correlation between two points separated by a distance D (m), v is the mobile speed (m/sec) and T (sec) is the sampling period of the signal envelope.

Rayleigh Fading For small-scale Rayleigh fading the Filtered Gaussian Noise method from [46] has been used. In the pedestrian A channel, it is assumed that the mobiles have fixed velocities at 3 km/h. At this speed a fading rate of $f_m = 5.56$ Hz is obtained from:

$$f_m = \frac{f_c v}{c} \tag{4.23}$$

where f_m is the maximum doppler shift (Hz), f_c is the carrier frequency (Hz), v is speed of the mobile (m/sec) and c is the speed of light (m/sec).

The generation of Rayleigh fading envelopes and the correlated envelopes will be explained in the Appendix A and B.

4.2.3 Resource Allocation Simulations

After $SINR_i$ is calculated for each user from (4.17), the $SINR$ values are mapped to the data rates supported in HDR by using the table 4.3. These data rates are the user data requests to be used in the reverse DRC channel. For perfect rate estimation, an error free reverse link is assumed. Figures 4.17 and 4.18 show the user $SINRs$ for a sample of 3 users out of 32 users present in the cell. The duration is 1200 and 60 slots corresponding to 2 sec. and 100 ms. of real-time respectively. Figure 4.19 shows the mapped data rates for these users based on their $SINRs$.

As it can been from Figure 4.20, users 2 and 3 request 0 kbps as their DRC values. This means, these users have $SINR$ values that cannot even satisfy the lowest data rate of 38.4 kbps so they are assigned 0 kbps by the BS meaning they will not be served in that particular slot. Assignment of 0 kbps to the users also correspond to the outage of the users and in the simulations an outage value of 4.61% is observed.

The sampling rate for the simulations is 600 Hz which also corresponds to the DRC update rate in HDR. (1 slot duration = 1.667 msec) The scheduling simulations have been

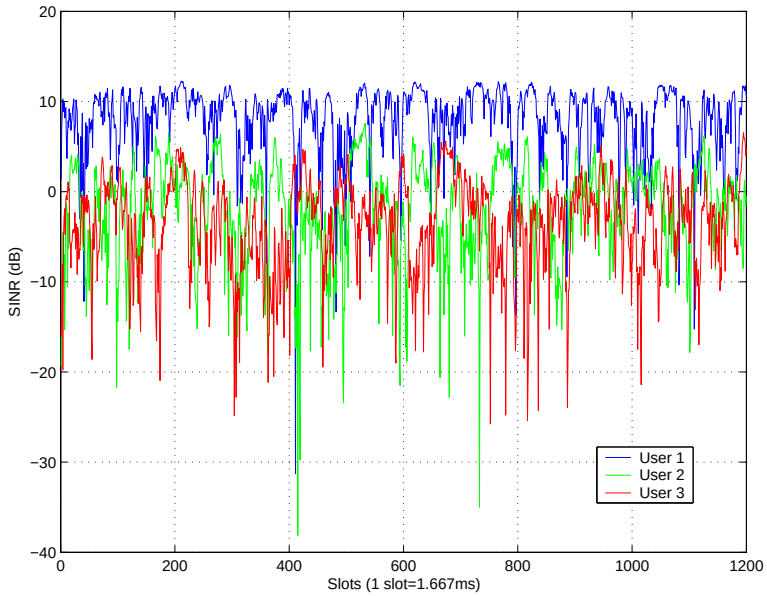

Figure 4.17: User $SINR$ values for a sample of 3 users - 1200 slots

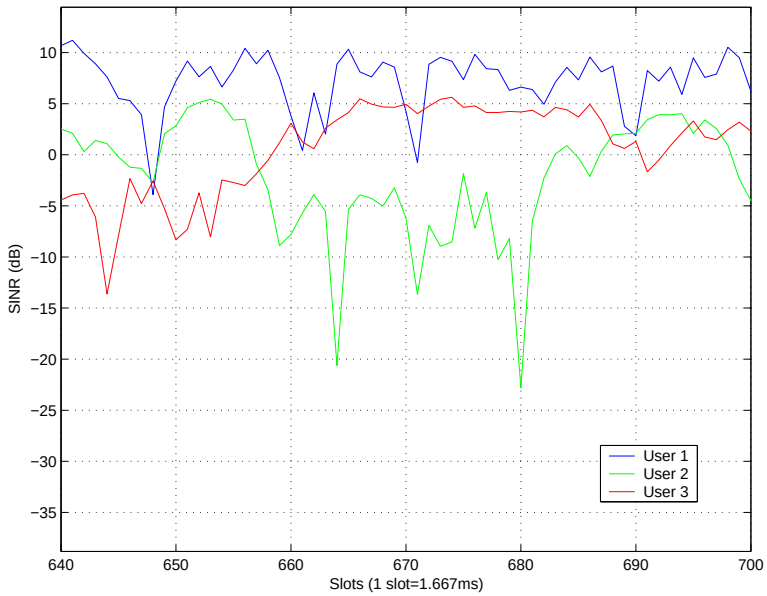

Figure 4.18: User $SINR$ values for a sample of 3 users - 60 slots

performed for 18000 slots corresponding to 30 sec. of real time taking into account the 4 slot interlaced multi-slot transmission of packets [9].

In the scheduling simulations of 3xHDR it is observed that the performance of 3xHDR

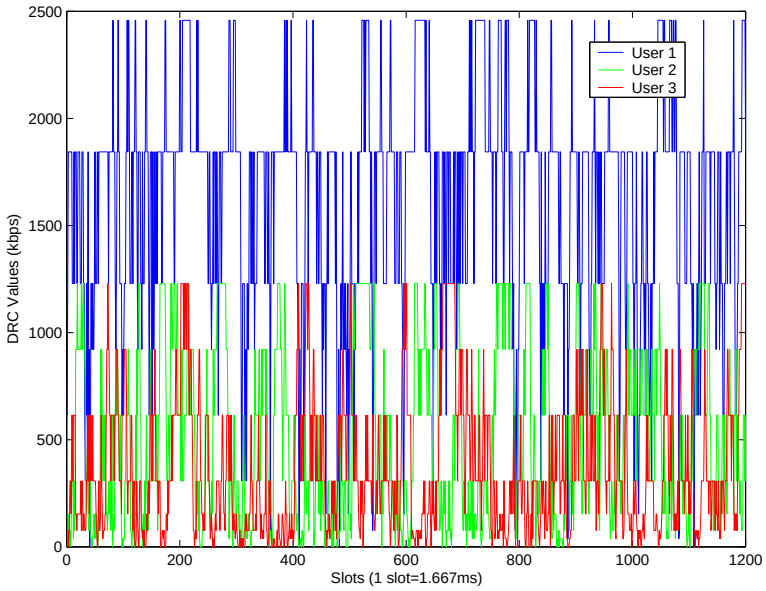

Figure 4.19: Mapped DRC values for the 3 users - 1200 slots

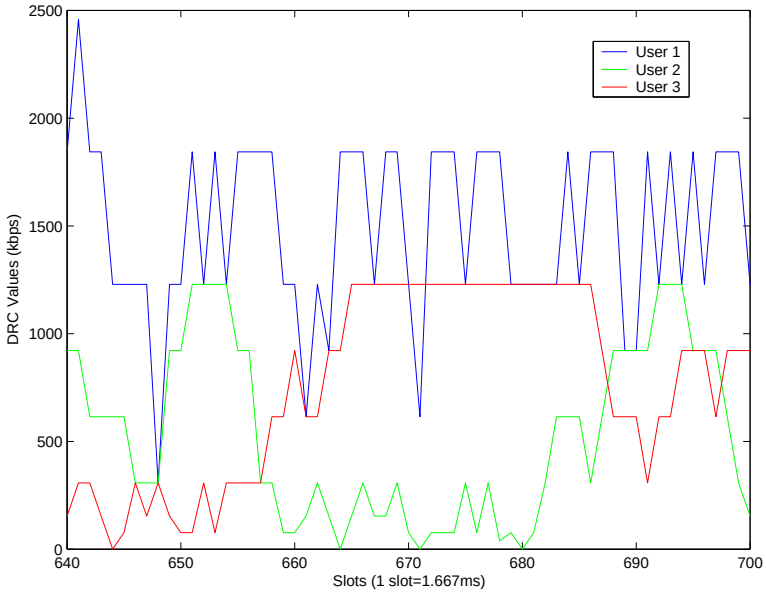

Figure 4.20: Mapped DRC values for the 3 users - 60 slots

outperforms 1xHDR since users have the chance to get service from multiple carriers in a time-slot. The overall system latency is also reduced since more than one user may be served in the same slot by different carriers.

In the scheduling of 3xHDR one important issue is the propagation of average data rate value through time-slots taking into account the scheduling of other carriers. The average data rate of a user should be the sum of served rates on all carriers. Average data rate is a metric that is commonly used in the scheduling algorithms.

4.3 Simulation Results

An extensive set of simulations have been performed to evaluate both overall system throughputs and latencies when various scheduling algorithms have been employed at the BS. The statistical performances together with the variances of user average data rates from the required QoS values are presented here. Statistical results will presented in two formats: a) The QoS parameter will be fixed and the guaranteed percentage will be presented as a function of number of active users. b) The statistical assurance (PoT) will be fixed and the QoS values will be presented with varying number of active users.

In the first set of simulations the overall system performance of the HDR system is investigated in terms of throughput and latency. Figures 4.21 and 4.22 show the overall throughput (in kbps) and overall latency (in slots) of the system for the single carrier pedestrian A channel. One striking fact is the increase of overall throughput with the increasing number of active users in the system. Except for the RR scheduler, all other scheduling algorithms exploit the multi-user diversity of the Rayleigh fading channel. The maximum system performance is obtained with the MaxR rule since this rule selects the user with the best channel condition. As a major drawback, this algorithm performs the worst in terms of overall system latency. Users are not served in a fair manner by using MaxR. This can readily be seen in Figure 4.22 with the MaxR having the worst latency performance. Best latency performance is obtained with the RR algorithm, however since RR does not exploit channel conditions the overall system throughput suffers greatly especially for high number of users. Figures 4.23 and 4.24 show the results of the MC scheduling. Since the system can serve at most 3 users at a given time, overall system performance is almost tripled. For instance, for 8 users overall system throughput is very close to 6000 kbps compared to 2000 kbps in the SC case. Another important gain is obtained in terms of latency performance. By serving 3 different users at a time, overall system latency is reduced. Overall latency can be defined as the total latency of all the users in terms of the

number of slots users do not receive any service averaged over the total number of users multiplied by the number of simulation slots. Likewise the system performance graphs have been obtained for the vehicular B channel. In vehicular B channel the MSs are assumed to be moving at speeds of 120 km/h, hence the channels they experience become fast fading with little correlation between the sample points of the received signal envelope. When compared to the pedestrian channel, the performance of the HDR system degrades in terms of throughput in the vehicular channel. It becomes less likely for the mobiles to maintain their good channel conditions for a long time. On the other hand the latency performance slightly increases. For a comparison considering the PF rule, overall system latency is 80 slots in pedestrian channel whereas it is around 60 slots in the vehicular channel. This result follows from the fact that the probability of number of different users that will be served in a certain time window in the vehicular channel is more than that of the pedestrian. Due to almost uncorrelated fading between the envelope samples, a user with a high SNR at a given slot may experience worse performance than another user in the next slot leading to the other user getting service. Figures 4.25, 4.27 show the results of the throughput simulations for SC and MC cases respectively, and Figures 4.26, 4.28 give the overall latency results. In Figure 4.28 it is clearly seen that the overall system latency is very much reduced when compared to pedestrian SC case. The Exp rule gives 15 slots average latency for 30 users in the vehicular MC case compared to about 50 in the pedestrian SC case.

The figures 4.29-4.36 show the statistical performance results obtained with the first proposed QoS aware scheduling scheme, *RExpQoS* Rule with Threshold Extension. The simulation results will be presented in the "PoT QoS not satisfied" format. "PoT QoS satisfied (PoTP)" is simply:

$$PoTQoSsatisfied = 1 - (PoTQoSNOTsatisfied) \tag{4.24}$$

For the bitrates 16, 32, 64 and 128 kbps the proposed algorithm demonstrates better performance in terms of statistical assurance when compared to the other algorithms from the literature. For the specified bitrates (QoS parameters) the *RExpQoS* Rule with Threshold guarantees higher percentage of time the QoS requirements are satisfied. With the increasing QoS values, it becomes harder to satisfy the requirements so the PoTP degrades. For 128 kbps and 20 active users, the PoTP becomes 35 % for the proposed algorithm but it is

still higher than the other algorithms. Figures 4.33-4.36 show the PoTP results for the MC case.

The simulation results for the second proposed algorithm, $R^2ExpQoS$, are presented in Figures 4.37-4.44. The statistical performance of $R^2ExpQoS$ starts to degrade for 64 kbps in the SC case and 256 kbps in the MC case when compared to the other algorithms and this is the drawback of the second algorithm with respect to the first algorithm. Without the threshold extension, it is observed that that the statistical performance of $R^2ExpQoS$ cannot be better for high user count and high QoS requirements. For instance for the SC case and 64 kbps, starting from about 22 active users the algorithm cannot guarantee the QoS better than the other algorithms. Due to this drawback of the second algorithm, this algorithm may only be used for lower QoS requirements and lower number of users for relatively better performance. $R^2ExpQoS$ does not employ a threshold mechanism hence it becomes computationally more efficient to apply this algorithm compared to $RExpQoS$ Rule with Threshold extension. In order to utilize the $RExpQoS$ Rule with Threshold extension a real time computation of the thresholds is needed which necessitates extra computation power.

The second form of simulation results are shown in Figures 4.45-4.56. These results have been obtained by setting the percentage of time values fixed and by evaluating the system performance in terms of the number of users that can be supported. By utilizing QoS aware algorithms it becomes possible to support more users and to guarantee a fixed percent of assurance for a given bitrate. For instance, when the statistical guarantee is 99 %, the $RExpQoS$ Rule with Threshold can support about 14 users at 60 kbps compared to 1 user, 2 and 7 users supported by MaxR, RR and Exp respectively. This can be seen in Figure 4.45. The number of users that can be supported by the $R^2ExpQoS$ rule falls below to that of Exp and PF for the 50 % statistical guarantee. This is the result of the mentioned drawback of this algorithm and can be seen in Figures 4.53 and 4.56.

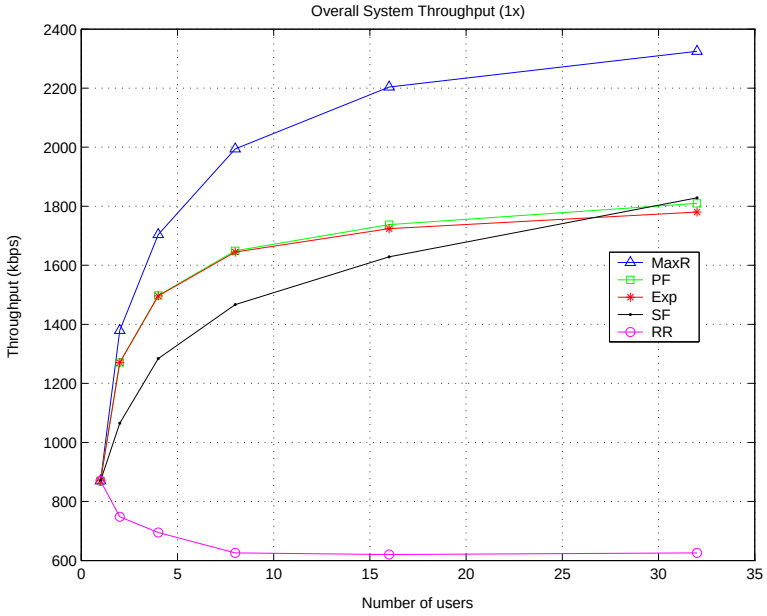

Figure 4.21: Overall System Throughput for SC (1x) System - Pedestrian A

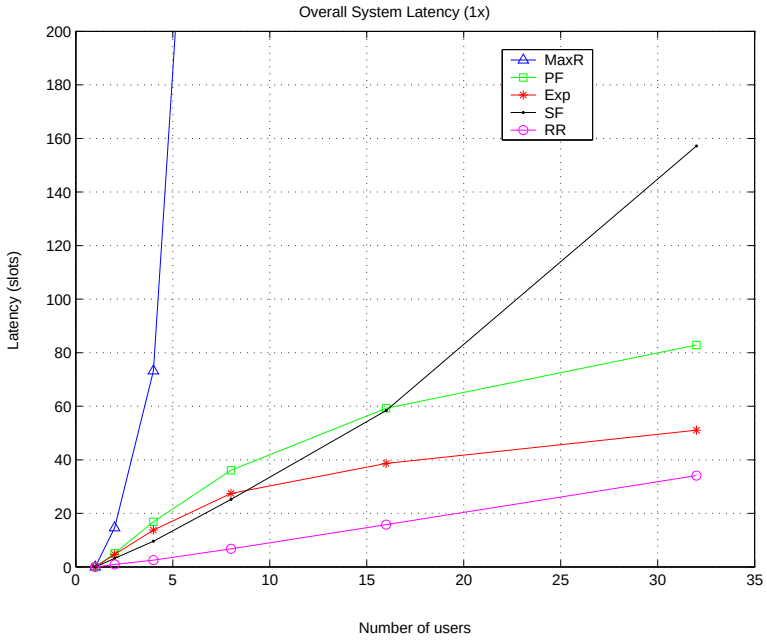

Figure 4.22: Overall System Latency for SC (1x) System - Pedestrian A

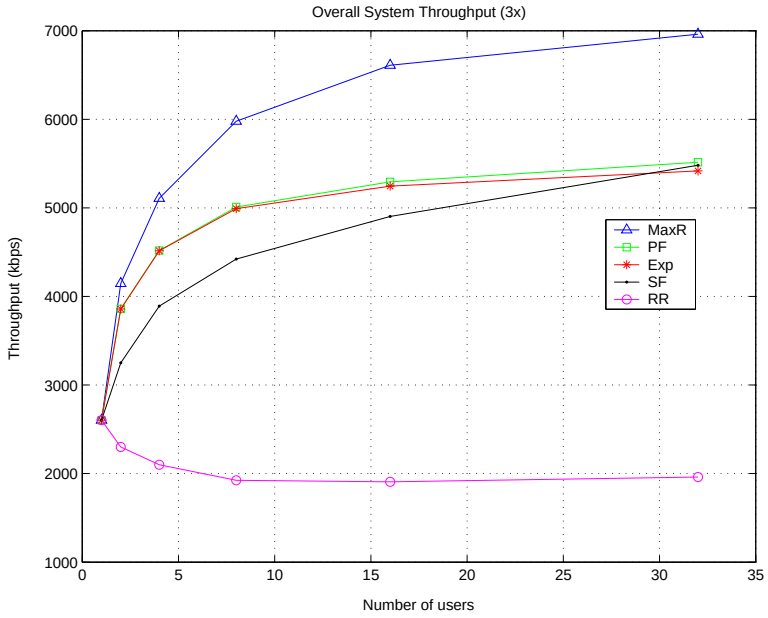

Figure 4.23: Overall System Throughput for MC (3x) System - Pedestrian A

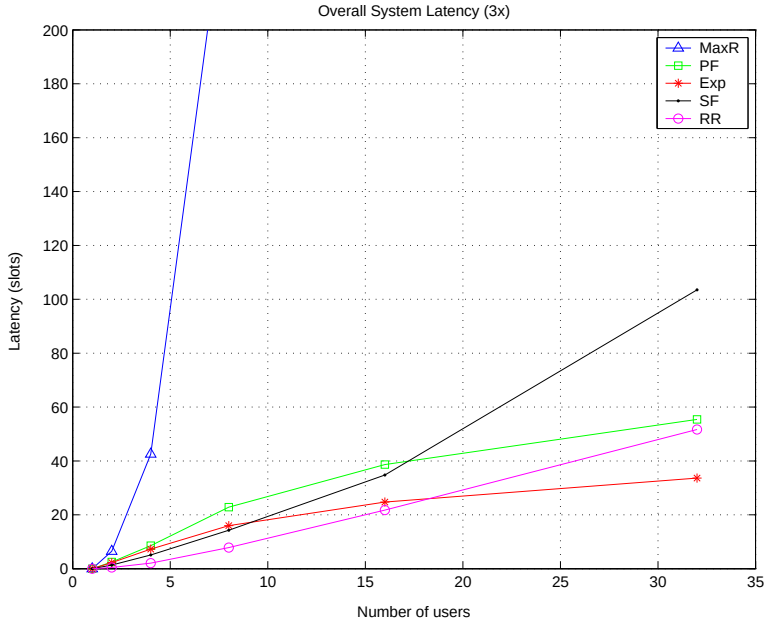

Figure 4.24: Overall System Latency for MC (3x) System - Pedestrian A

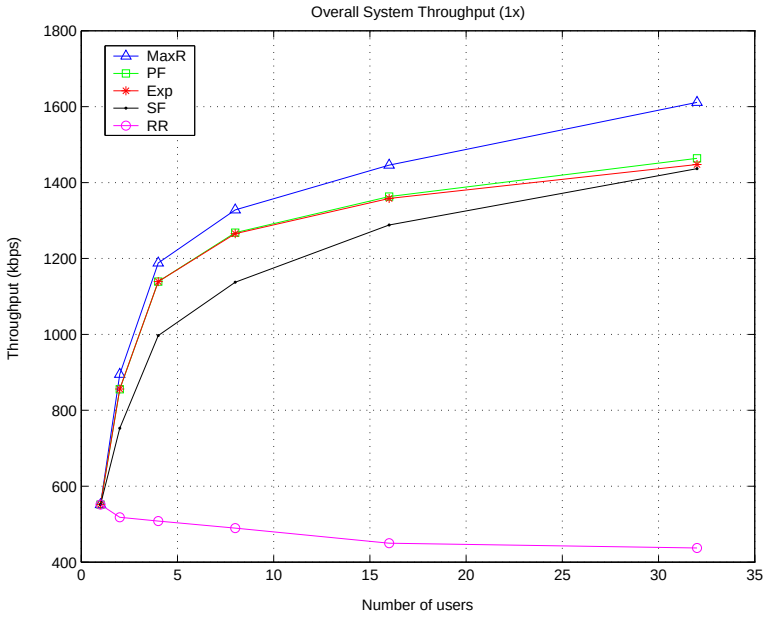

Figure 4.25: Overall System Throughput for SC (1x) System - Vehicular B

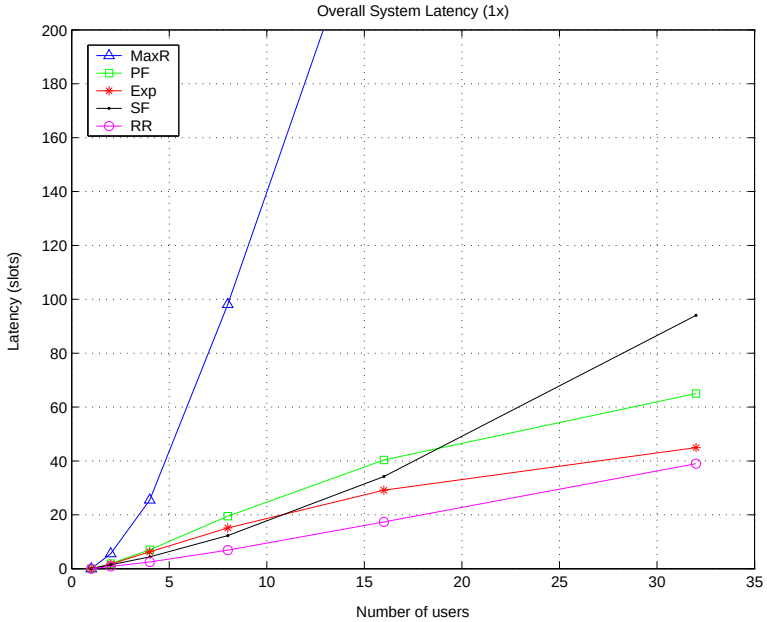

Figure 4.26: Overall System Latency for SC (1x) System - Vehicular B

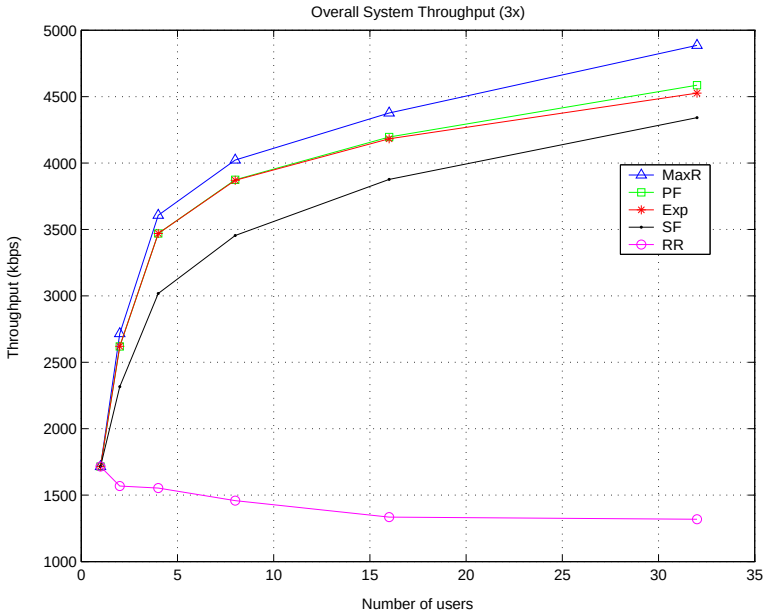

Figure 4.27: Overall System Throughput for MC (3x) System - Vehicular B

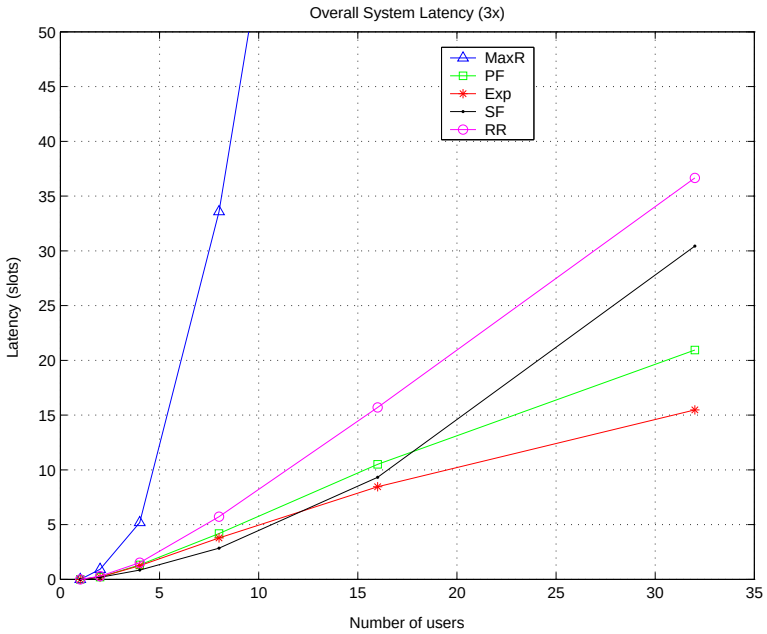

Figure 4.28: Overall System Latency for MC (1x) System - Vehicular B

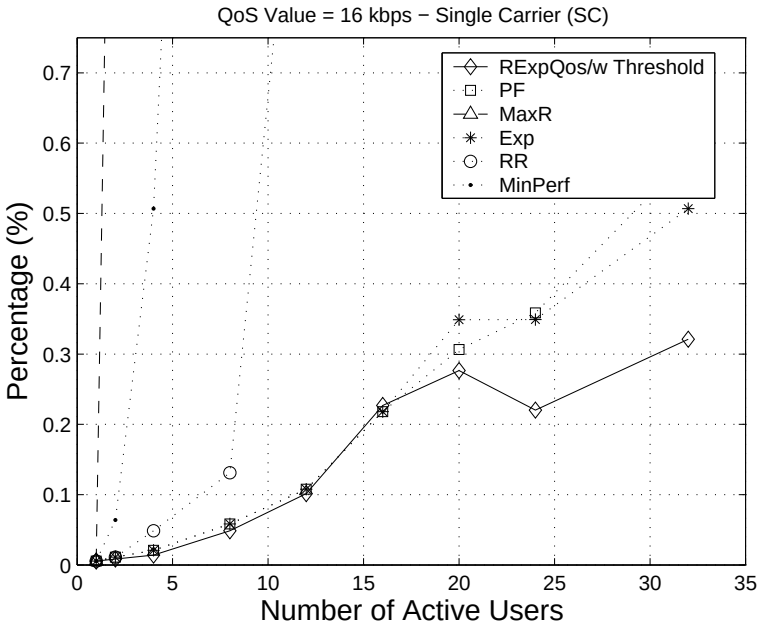

Figure 4.29: SC - Statistical performance for *RExpQoS* /w threshold for 16 kbps

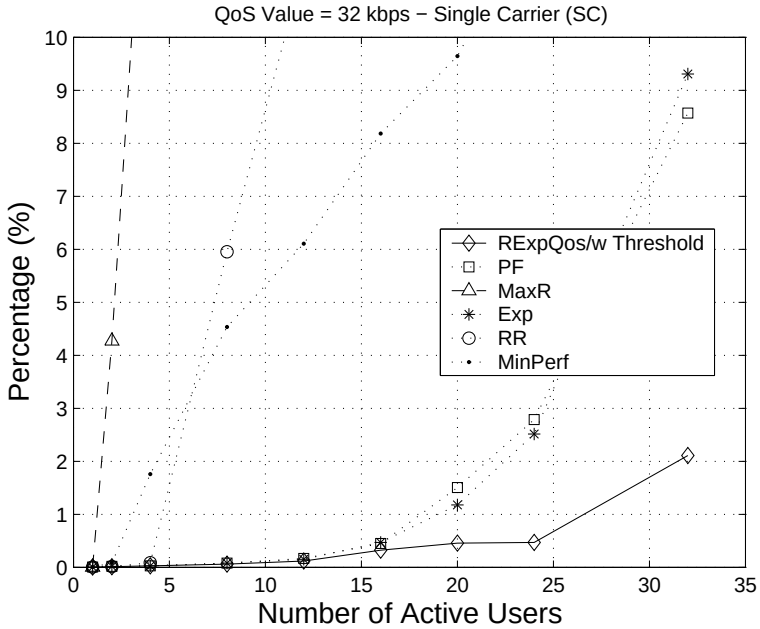

Figure 4.30: SC - Statistical performance for *RExpQoS* /w threshold for 32 kbps

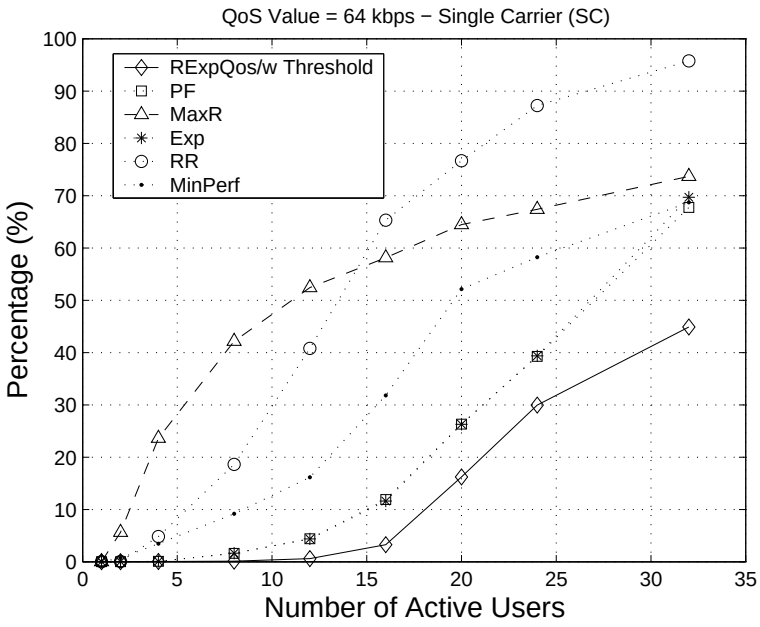

Figure 4.31: SC - Statistical performance for *RExpQoS* /w threshold for 64 kbps

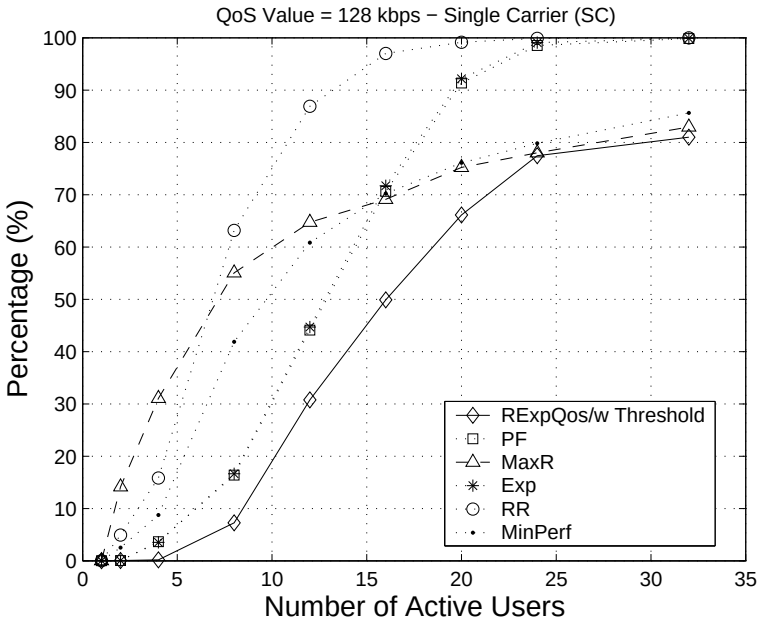

Figure 4.32: SC - Statistical performance for *RExpQoS* /w threshold for 128 kbps

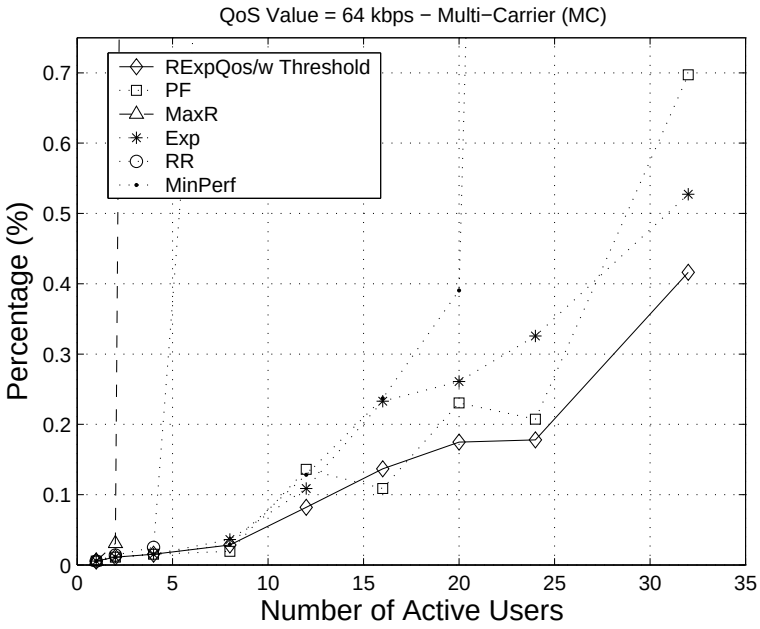

Figure 4.33: MC - Statistical performance for *RExpQoS* /w threshold for 64 kbps

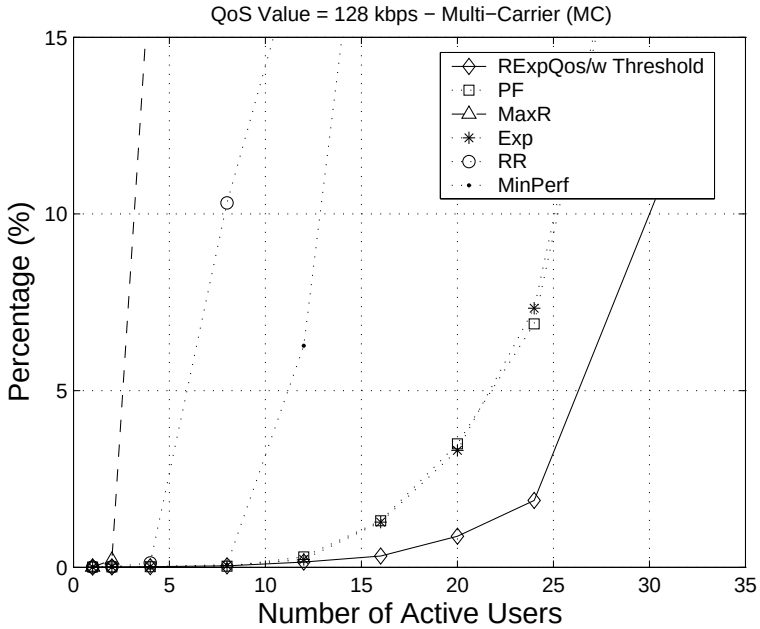

Figure 4.34: MC - Statistical performance for *RExpQoS* /w threshold for 128 kbps

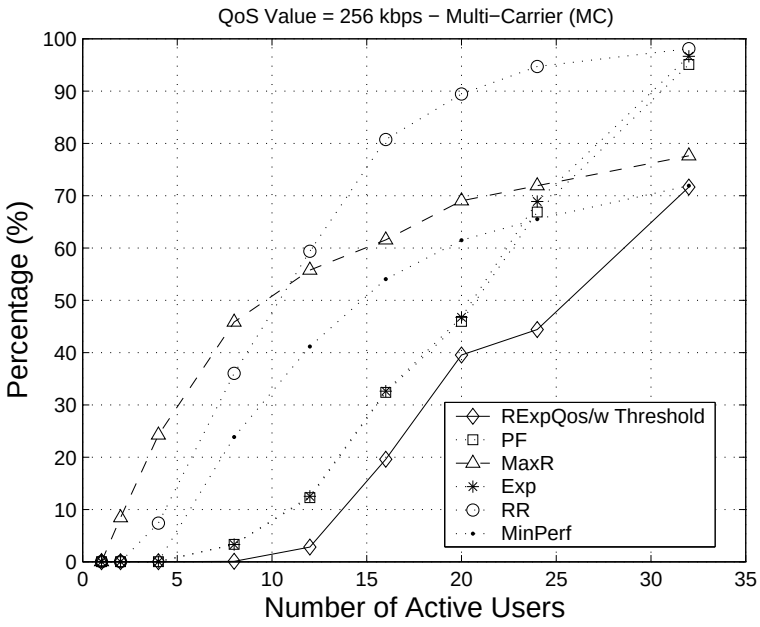

Figure 4.35: MC - Statistical performance for *RExpQoS* /w threshold for 256 kbps

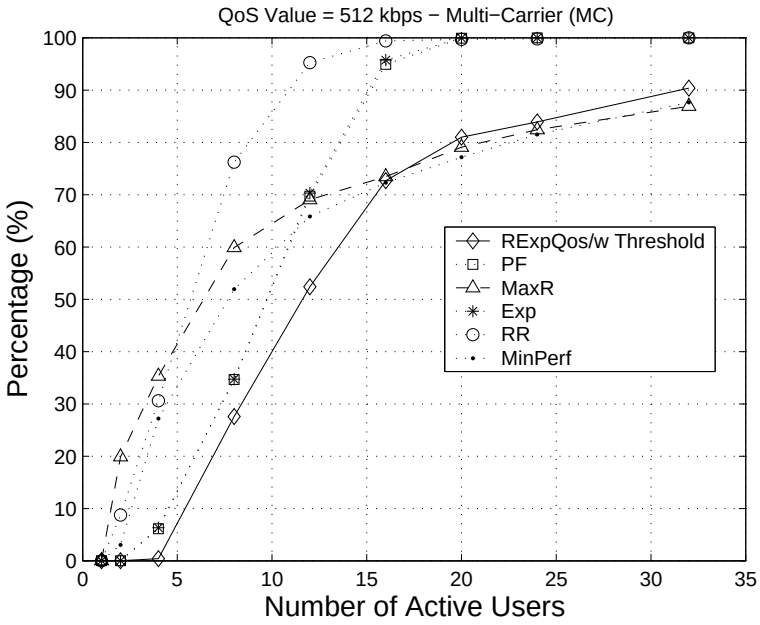

Figure 4.36: MC - Statistical performance for *RExpQoS* /w threshold for 512 kbps

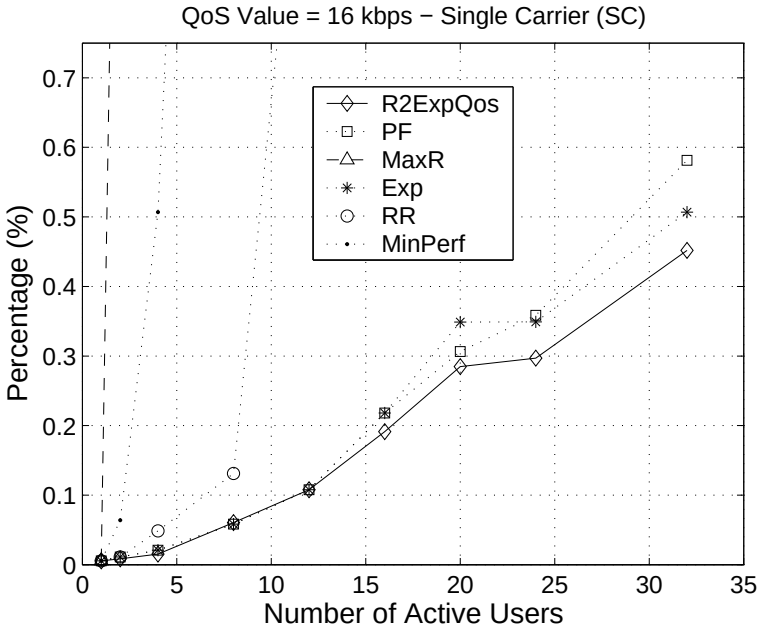

Figure 4.37: SC - Statistical performance for $R^2ExpQoS$ for 16 kbps

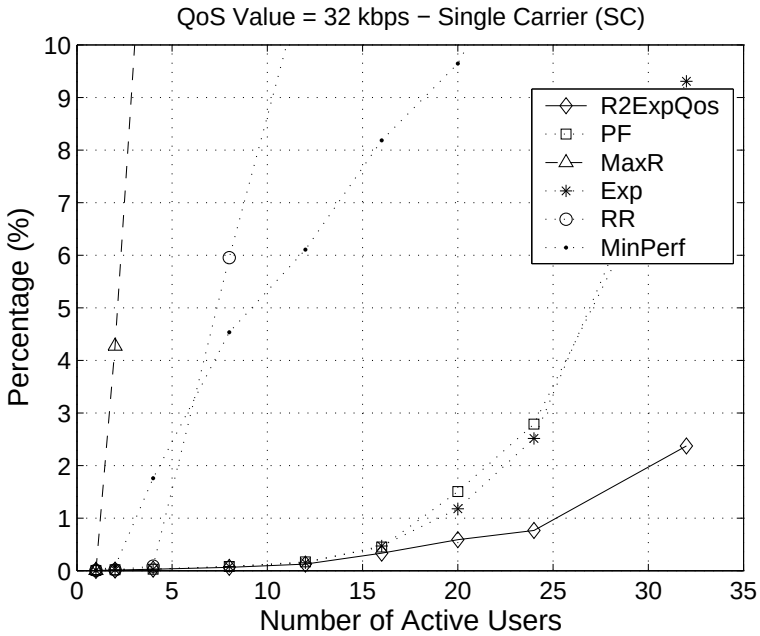

Figure 4.38: SC - Statistical performance for $R^2ExpQoS$ for 32 kbps

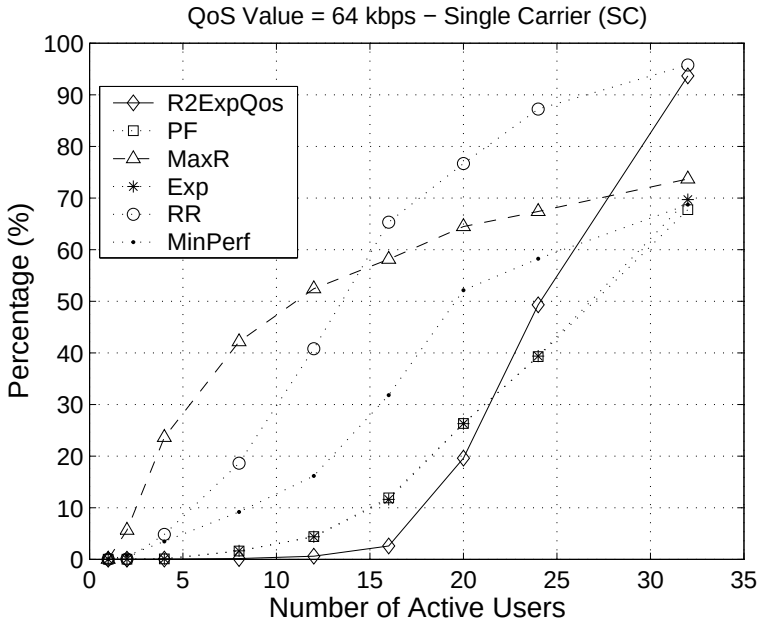

Figure 4.39: SC - Statistical performance for $R^2ExpQoS$ for 64 kbps

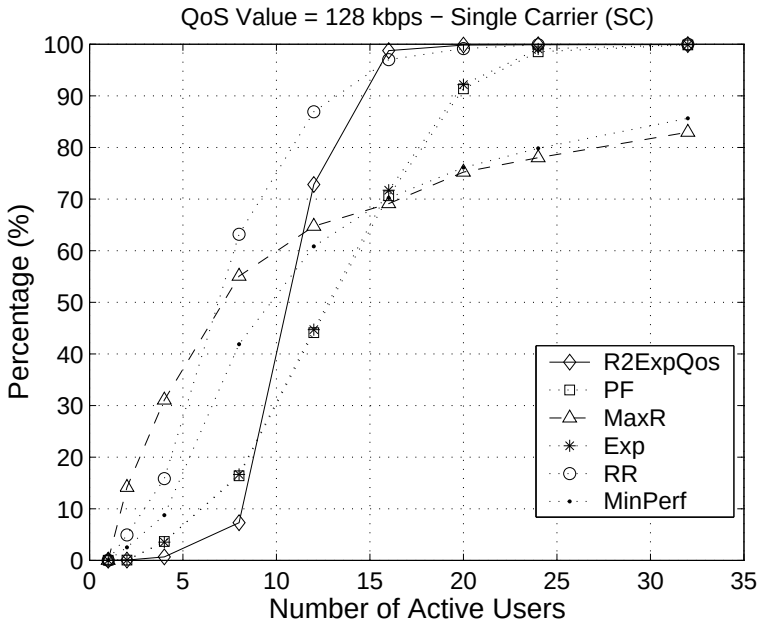

Figure 4.40: SC - Statistical performance for $R^2ExpQoS$ for 128 kbps

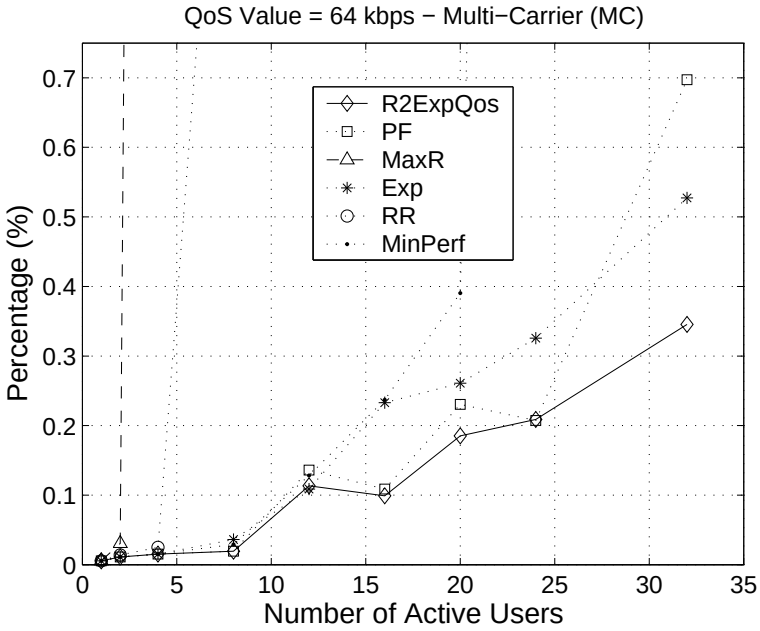

Figure 4.41: MC - Statistical performance for $R^2ExpQoS$ for 64 kbps

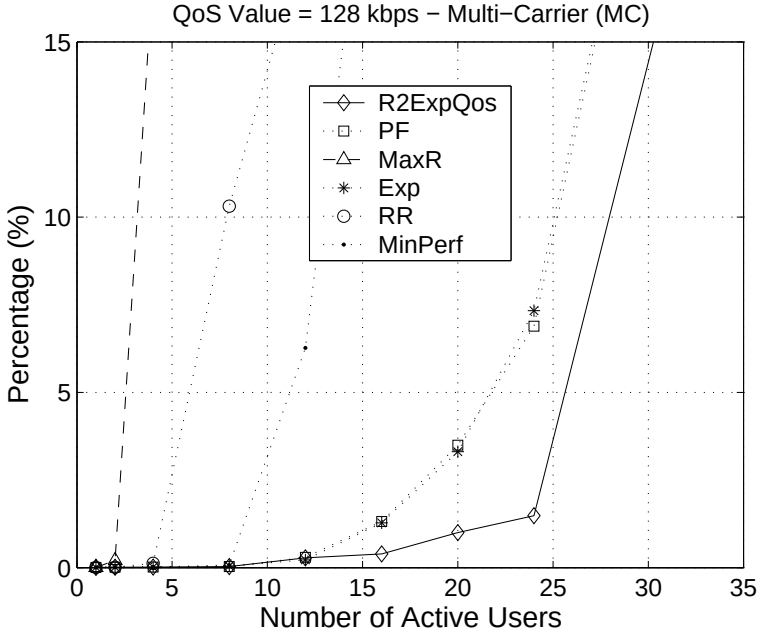

Figure 4.42: MC - Statistical performance for $R^2ExpQoS$ for 128 kbps

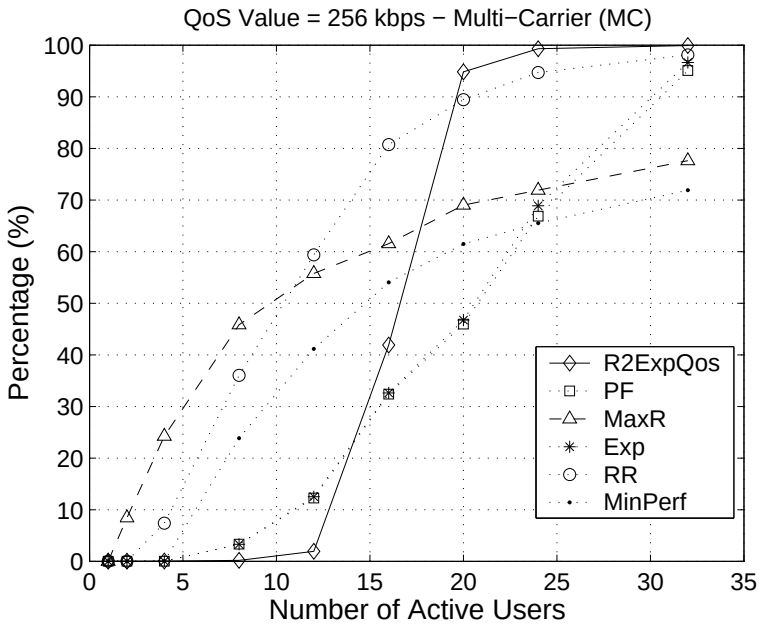

Figure 4.43: MC - Statistical performance for $R^2ExpQoS$ for 256 kbps

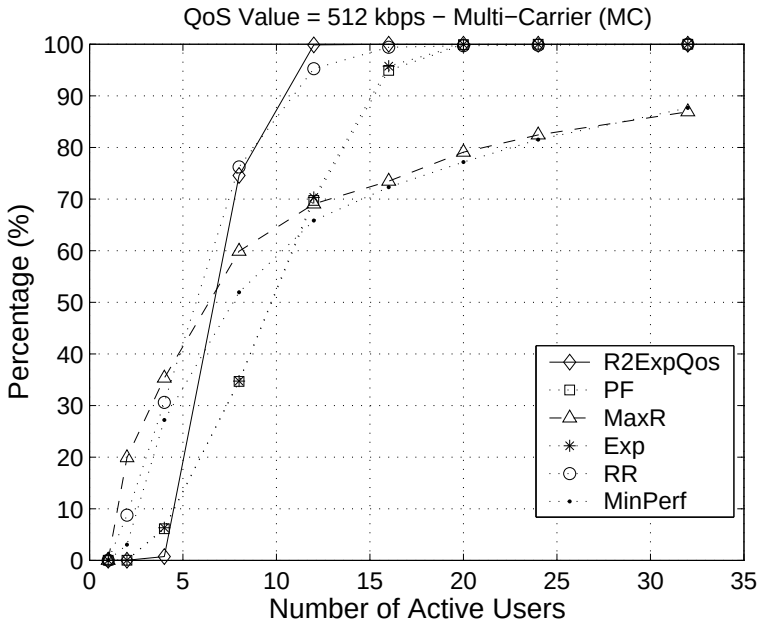

Figure 4.44: MC - Statistical performance for $R^2ExpQoS$ for 512 kbps

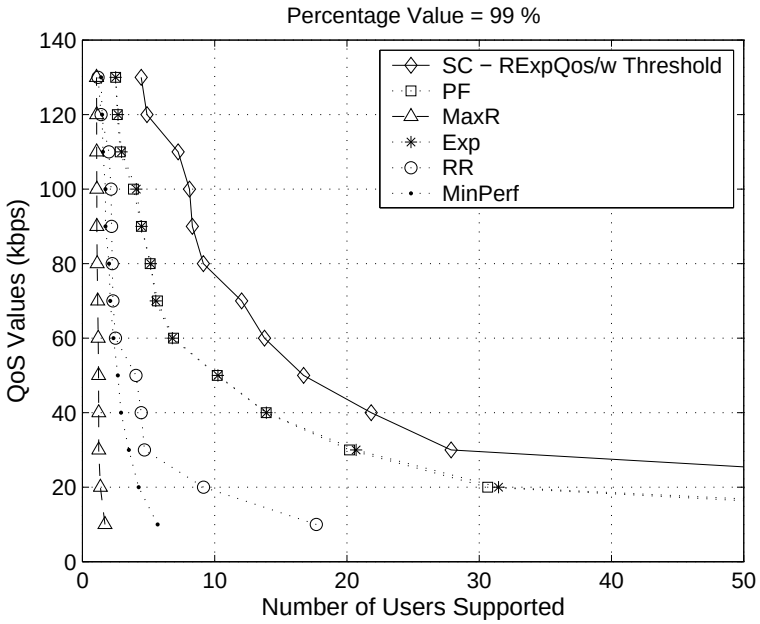

Figure 4.45: SC - Number of supported users for *RExpQoS* /w threshold for 99% statistical guarantee

4.4 Conclusion

In this chapter, a detailed analysis of the wireless channel models have been done and the comprehensive simulation platform has been introduced. QoS performance of the scheduling algorithms that are present in the literature have been compared with that of the proposed ones. The proposed algorithms offer a certain level of service assurance which we regard as the statistical QoS assurance. This type of service can be a desired alternative for service providers since it tries to meet the requirements of both enhanced system performance and also maintain a slightly loose form of service guarantees.

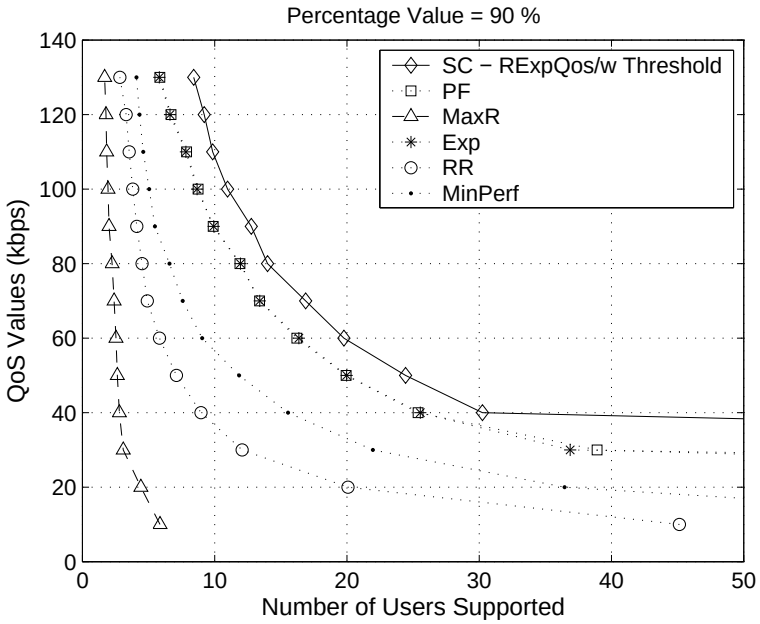

Figure 4.46: SC - Number of supported users for *RExpQoS* /w threshold for 90% statistical guarantee

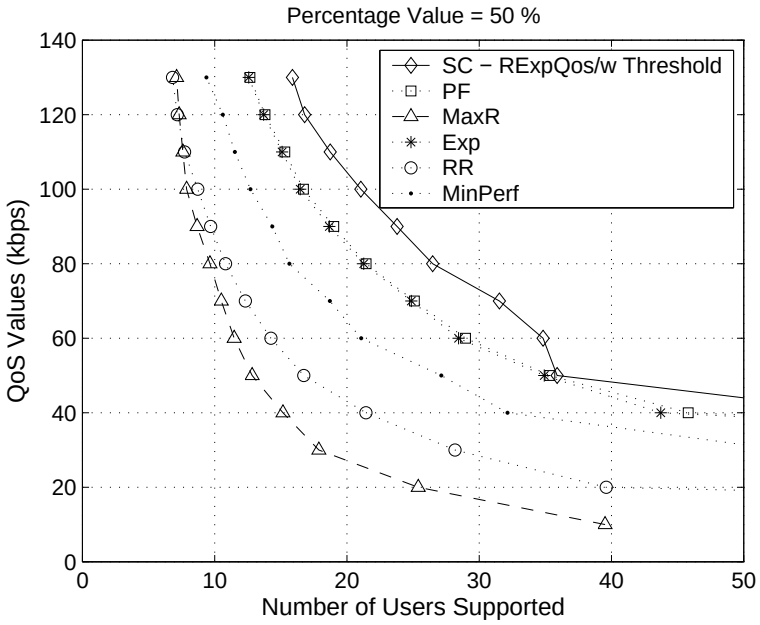

Figure 4.47: SC - Number of supported users for *RExpQoS* /w threshold for 50% statistical guarantee

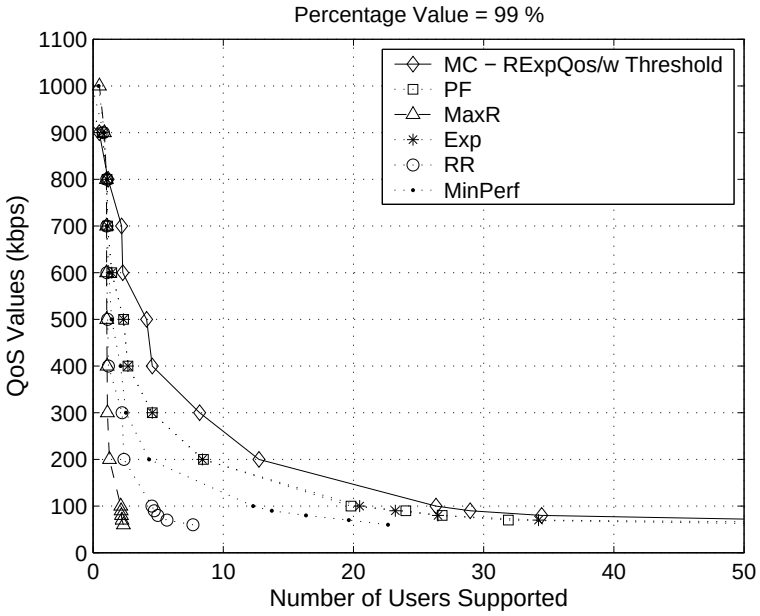

Figure 4.48: MC - Number of supported users for *RExpQoS* /w threshold for 99% statistical guarantee

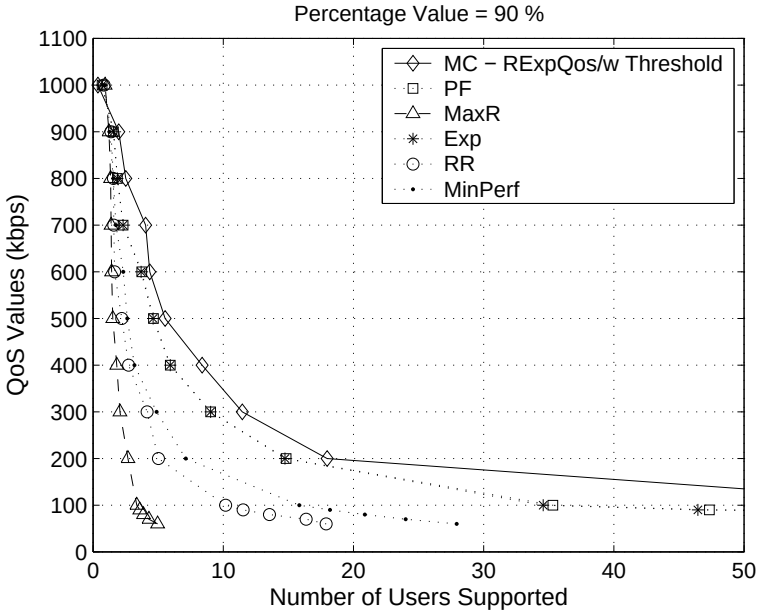

Figure 4.49: MC - Number of supported users for *RExpQoS* /w threshold for 90% statistical guarantee

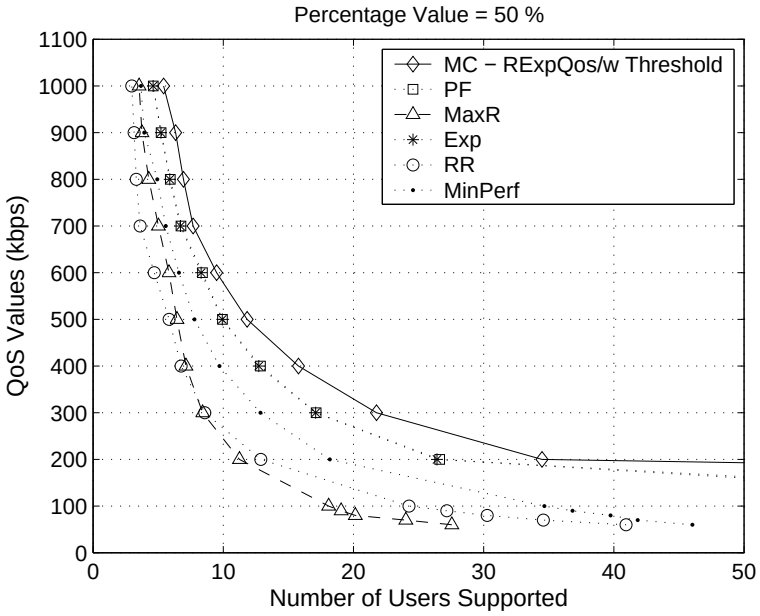

Figure 4.50: MC - Number of supported users for $RExpQoS$ /w threshold for 50% statistical guarantee

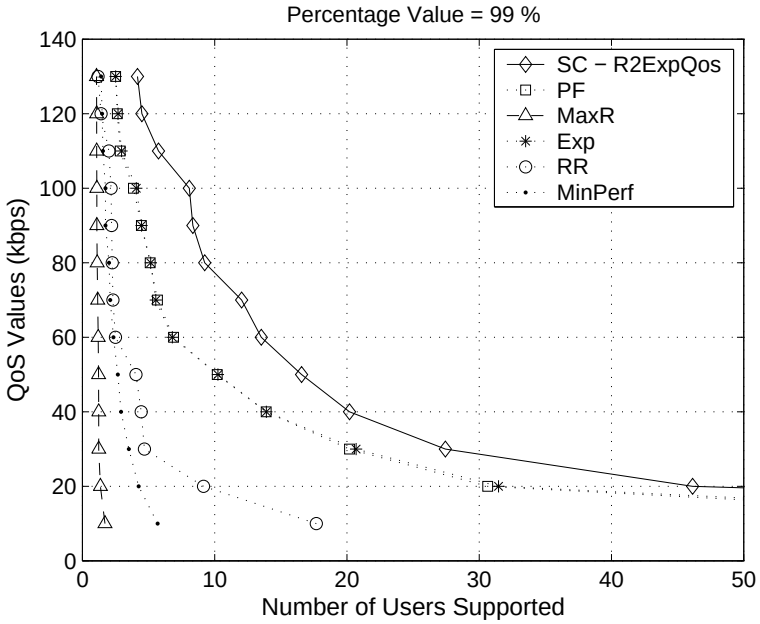

Figure 4.51: SC - Number of supported users for $R^2ExpQoS$ for 99% statistical guarantee

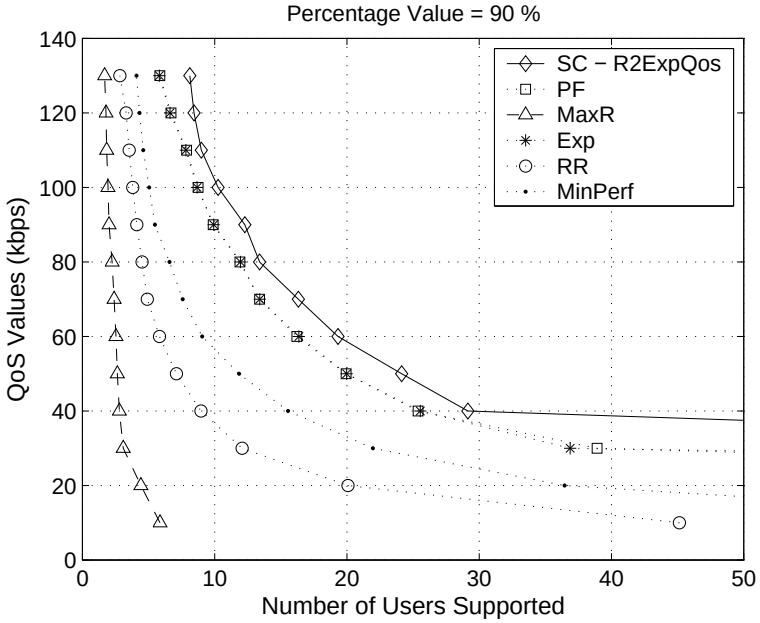

Figure 4.52: SC - Number of supported users for $R^2ExpQoS$ for 90% statistical guarantee

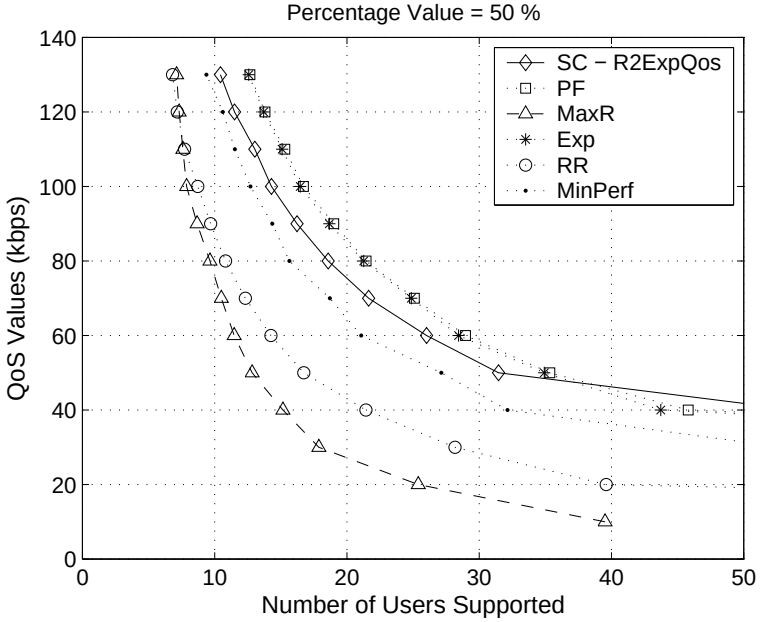

Figure 4.53: SC - Number of supported users for $R^2ExpQoS$ for 50% statistical guarantee

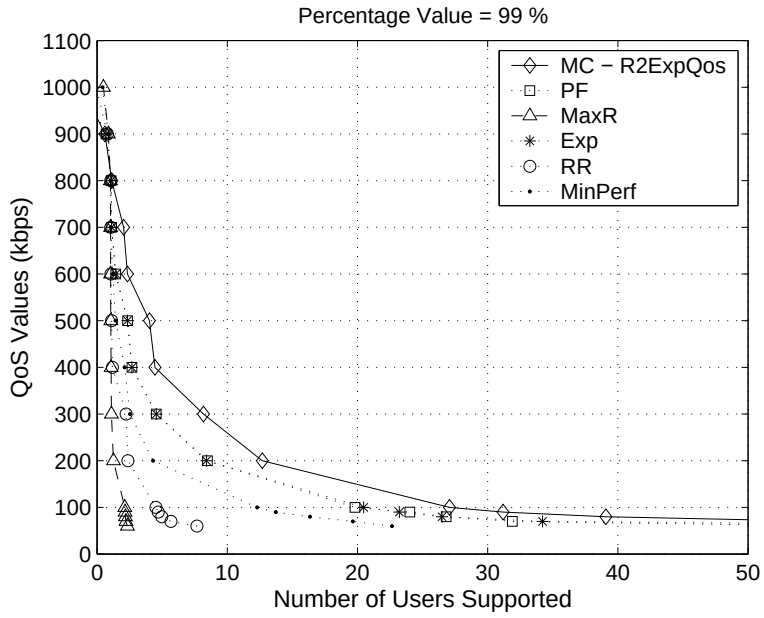

Figure 4.54: MC - Number of supported users for $R^2ExpQoS$ for 99% statistical guarantee

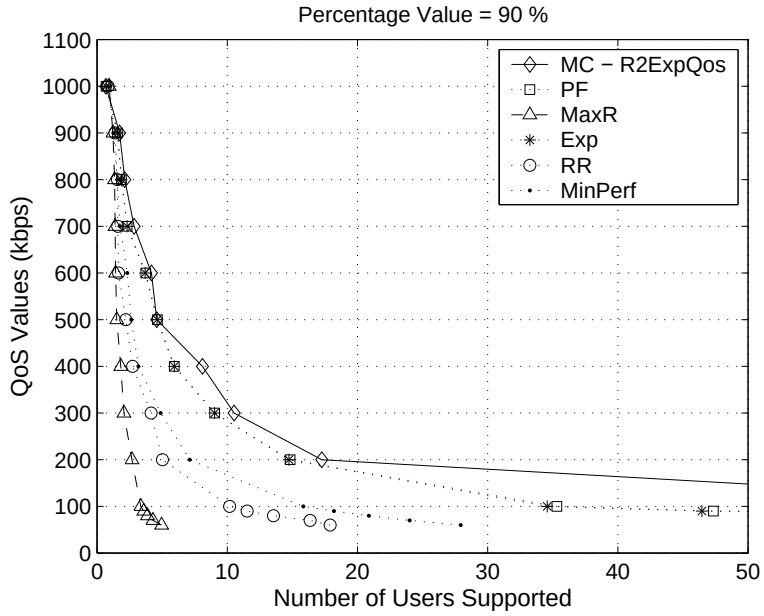

Figure 4.55: MC - Number of supported users for $R^2ExpQoS$ for 90% statistical guarantee

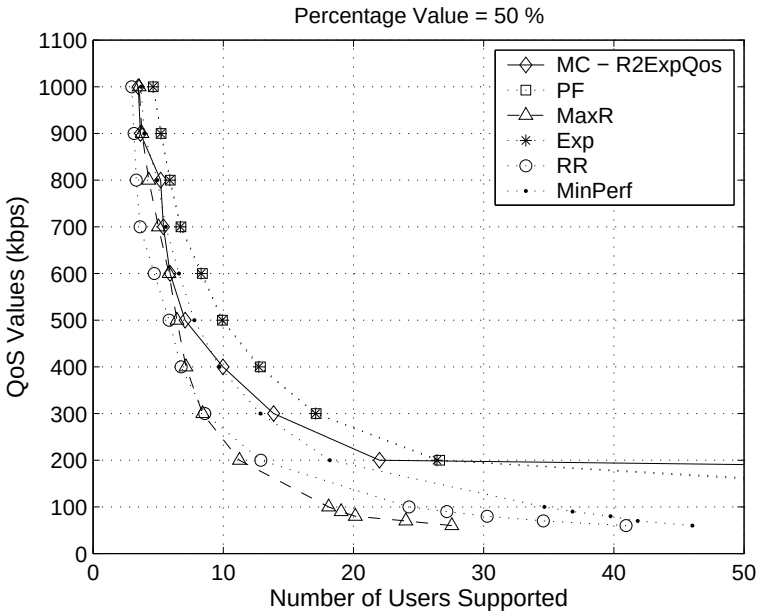

Figure 4.56: MC - Number of supported users for $R^2ExpQoS$ for 50% statistical guarantee

Chapter 5

WIRELESS LOCAL AREA NETWORKS (WLANS) - AN OVERVIEW

The rapid advances in the field of computer networking together with wireless systems have opened up the possibility to access data networks without any wiring at speeds almost equivalent to wired networks and especially with the production of portable computers, WLANs have gained incredible popularity.

WLANs have been standardized under the working group name IEEE 802.11 [47] and there are continuing efforts to enhance the transmission capabilities of WLANs. The IEEE 802.11 standard [48] is an umbrella for a number of different WLAN standards namely IEEE 802.11, IEEE 802.11a [49], IEEE 802.11b [50] and IEEE 802.11g [51] whose specifications will be briefly discussed below.

5.1 IEEE 802.11

The main goal in developing the IEEE 802.11 standard was to provide services equivalent to the ones provided by wired networks like the famous Ethernet or IEEE 802.3. It was also mandatory to develop a high throughput, high reliability system capable of delivering continuous network connection. The IEEE 802.11 standard has been defined at the bottom two layers (physical and data link layers) of the ISO 7-layer architecture [8] as depicted in Figure 5.1.

At the media access control (MAC) sub layer, IEEE 802.11 uses the carrier sense multiple access with collision avoidance (CSMA/CA) protocol [48].

Being standardized in 1997, IEEE 802.11 defines the base level specifications for wireless physical and MAC layers and operates in the 2.4 GHz band which is the band allocated for ISM (industrial, scientific and medical) devices. The ISM band has three frequency ranges: 902-928, 2400-2483.5 and 5725-5850 MHz [52]. Data rate support is for 1 and 2 Mbps.

IEEE 802.11 defines two types of transmission technologies at the physical layer. The first one is the direct sequence spread spectrum (DSSS) [48] and the second is the frequency

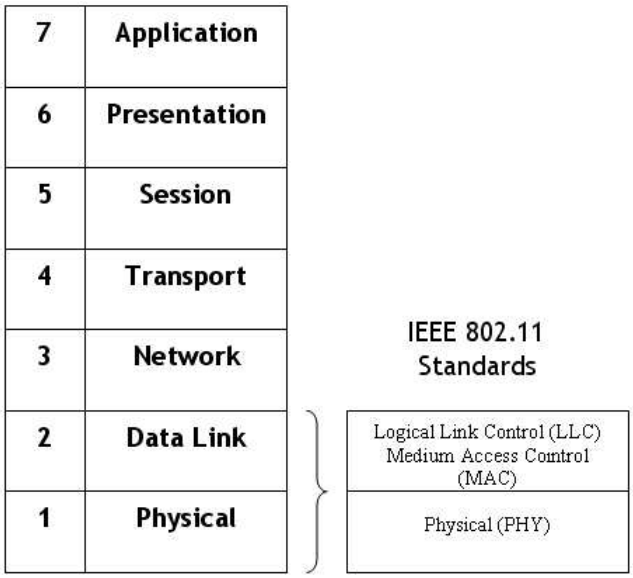

Figure 5.1: ISO 7-layer Architecture

hopping spread spectrum (FHSS) [48]. The extension standards IEEE 802.11a and 802.11g also define a third type of transmission technology called the OFDM [53, 46]. Before commenting on the various aspects of different 802.11 standards, transmission technologies are briefly discussed below:

5.1.1 DSSS

In DSSS, the user signal is multiplied by a higher rate bit sequence (chipping code) thus spreading the user data signal energy over the entire transmission bandwidth. The receiving station only needs to know the chipping code to decode the signal. For other stations the signal of a particular station is received as noise. Using DSSS 802.11 can obtain data rates 1 and 2 Mbps. On top of DSSS, IEEE 802.11b and 802.11g utilizes a complementary code keying (CCK) scheme [54] to achieve higher data rates.

5.1.2 DSSS with CCK

It comprises a set of 64 eight-bit code words used to encode data for 5.5 and 11Mbps data rates in the 2.4GHz band of 802.11b wireless networking. CCK works only in conjunction with the DSSS technology that is specified in the original 802.11 standard. It is not

compatible with FHSS. CCK increases the number of bits represented in each symbol by transforming the DSSS code according to certain mathematical rules. In this way it becomes possible to transmit 11 Mbps as opposed to 2 Mbps defined in the original standard.

5.1.3 FHSS

In FHSS, the user data signal is modulated by a carrier that rapidly changes frequency over a wide range of frequencies in a predefined manner as a function of time. The rapid changing of frequencies is referred to as "hopping". The spread spectrum signal obtained in this way is immune to interference provided that another transmission is not taking place in the same frequency at exactly the same time. The order of the frequencies is determined by a hopping code. The receiver needs to know the same code in order to synchronize with the transmitted signal. According to FCC regulations, the minimum number of frequencies transmitters are allowed to use is 75 and the maximum time spent on each frequency (dwell time) is 400 ms.

5.1.4 OFDM

The history of OFDM dates back to 1960's. The idea of using separate carriers to transmit and receive information was first proposed in R.W Chang's paper [53]. With the advances in digital signal processors it became possible to implement OFDM systems.

In OFDM, a communications channel is divided into a number of equally spaced frequency bands. In each band a portion of the user information is carried by a subcarrier (a tone). The design of the waveforms is made such that each subcarrier is orthogonal with any other subcarrier. Unlike in FDM, the bands are allowed to overlap thus reducing the total bandwidth as in Figure 5.2. Since the subcarriers are orthogonal, retrieving signals from the individual subcarriers is easily implemented.

In OFDM, user data is modulated onto tones. Modulating onto a tone is established by adjusting a tone's phase (PSK), amplitude (QAM) or both. An OFDM system takes a data stream and splits it into N parallel data streams, each at a rate $1/N$ of the original rate. Each stream is then mapped to a tone at a unique frequency and combined together using the IFFT to yield the time-domain waveform to be transmitted. Figure 5.4 shows the block diagram of an OFDM system.

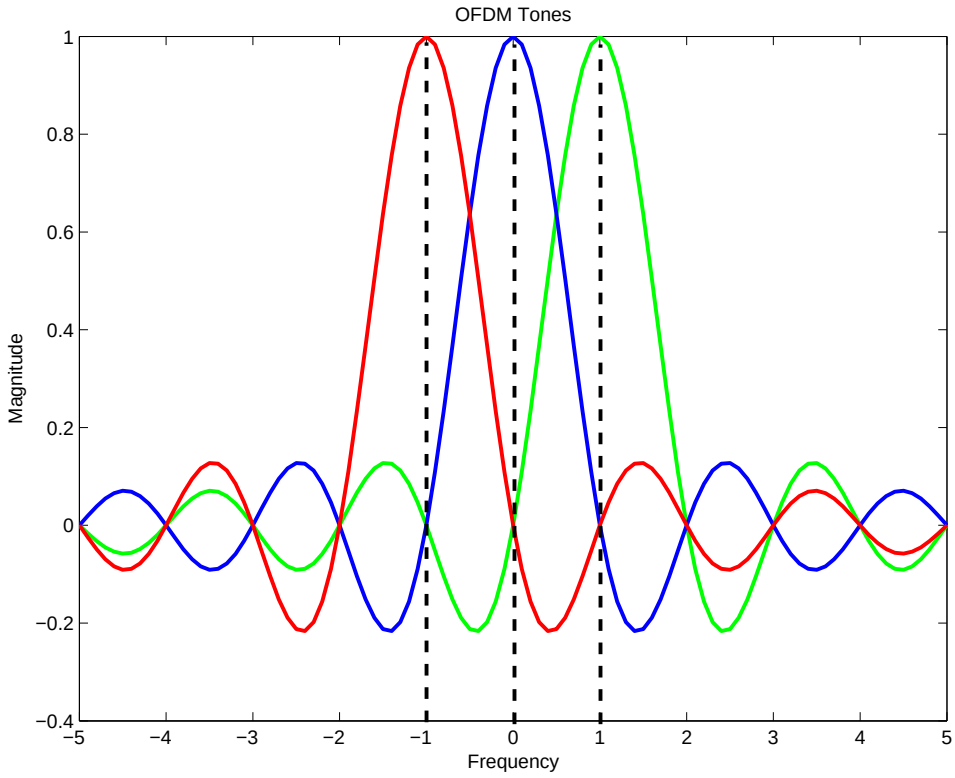

Figure 5.2: OFDM Tones

An OFDM symbol comprises of a guard interval (cyclic prefix) in order to prevent ISI together with ICI. Guard interval should be chosen to be longer than the maximum delay component of the wireless channel but should also be short enough in order not to decrease effective data rate since guard interval acts as an overhead. Figure 5.3 shows the configuration of the OFDM symbol. The effective symbol length is the FFT integration time.

Considering a 256-tone system, a single data stream with a total data rate of 1 Mbps would span 256 parallel data streams each with 4 kbps. The slower data streams decrease the bandwidth of modulation symbols by a factor of the number of tones. Decreased bandwidth leads to much reduced ISI since multipath delays occupy a very small portion of the symbol time. In other words, for each stream the channel behaves as flat channel thus eliminating the need for complex time-domain equalizers.

OFDM represents a different system-design approach. It is a combination of modulation and multiple-access schemes that segments a communications channel in such a way that

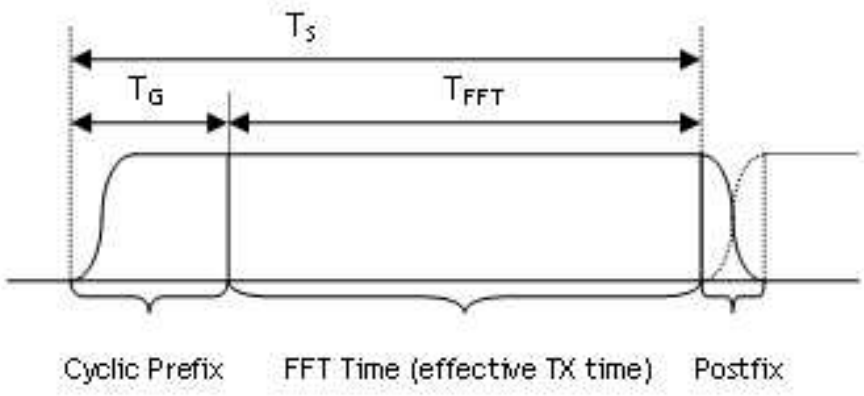

Figure 5.3: OFDM Symbol

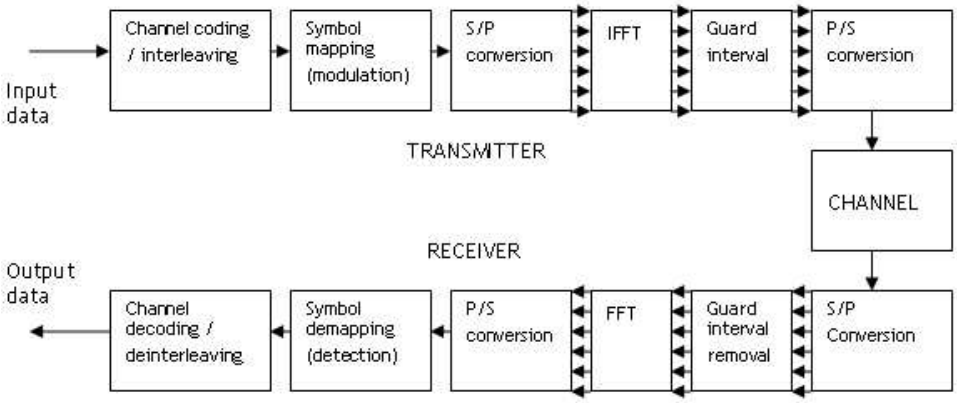

Figure 5.4: OFDM System Block Diagram

many users can share it. The multiple access scheme utilizing OFDM is called the OFDMA. The assignment of set of tones to individual users is controlled by the MAC layer resource management algorithms. As a comparison, TDMA divides resources in time, CDMA in code and OFDM in frequency.

OFDM is a promising technology for the future high speed wireless networks and it is also dubbed as the key ingredient for the upcoming 4^{th} generation systems. Major advantages of OFDM can be listed as:

- Simple equalization at the receiver due to near flat frequency response on each sub-

carrier.

- Can be easily combined with a number of multiple access methods (FDMA, TDMA, CDMA).
- Inherent support for Multiple Input Multiple Output (MIMO) systems.

Besides these advantages OFDM has also some drawbacks. These can be listed as:

- Requires perfect time and frequency synchronization.
- Due to high Peak-to-Average Power Ratio (PAPR) very linear power amplifiers (expensive and inefficient) must be used in OFDM transmission.

5.2 IEEE 802.11a

This standard is defined to operate in the 5GHz band to deliver data rates up to 54 Mbps and uses OFDM encoding scheme rather than FHSS or DSSS.

5.3 IEEE 802.11b (also referred to as 802.11 High Rate or Wi-Fi)

This is the widely accepted and deployed extension to 802.11 and provides speeds up to 11 Mbps (with a fallback to 5.5, 2 and 1 Mbps) in the 2.4 GHz band. 802.11b uses only DSSS. 802.11b was a 1999 ratification to the original 802.11 standard, allowing wireless functionality comparable to Ethernet.

5.4 IEEE 802.11g

This relatively new standard is also defined to operate in the 2.4 GHz band promising data rates up to 54 Mbps. It is backward compatible with IEEE 802.11b. Rates lower than 20 Mbps are obtained with DSSS with CCK and rates above 20 Mbps are obtained with OFDM scheme.

Table 5.1 summarizes the key aspects of the wireless standards mentioned above.

5.5 Conclusion

The WLANs will be the key components in the high speed wireless data evolution hence the studies focus on various aspects of the WLANs. One key study topic is the integration

Table 5.1: IEEE 802.11 Standards

IEEE Standard	**802.11a**	**802.11b**	**802.11g**
Data Rates (Mbps)	54, 48, 36, 24, 12, 6	11, 5.5, 2, 1	54, 48, 36, 24, 12, 6
Operating Frequency	5 GHz (unlicensed)	2.4 GHz	2.4 GHz
Modulation Scheme	OFDM	DSSS with CCK	OFDM and DSSS with CCK
Typical Range[a]	Up to 55m	Up to 90m	Up to 90m
Security	WEP and WPA	WEP and WPA	WEP and WPA
Remarks	Standardized in 1999, not widely deployed due to incompatibility	Standardized in 1999, widely deployed and accepted	Standardized in 2003, expected to replace 802.11b

[a]Depends on manufacturer and geography.

of next generation cellular systems (3G) with the WLANs and the next chapter will discuss the integration issues together with the contribution of this thesis for a possible integration methodology.

Chapter 6

3G/WLAN INTEGRATION

In order to provide mobile users with high data rate wireless access to data networks and the Internet, efficient integration of 3G systems and WLANs has been at the heart of these research efforts [55, 56, 57]. Emerging dual-mode MSs can serve to provide enhancements to the performance of 3G systems with proper integration methodologies. One possible architecture for the integration of these systems is the relay of information from the 3G BS to the WLAN end user by utilizing these dual-mode terminals as the relay nodes. For such a system, the WLAN is configured to operate in ad-hoc mode [48].

Since wireless systems rely on the mobility of terminals, an important aspect in the design of these systems is the minimal usage of MSs' batteries. WLANs operating in ad-hoc mode should employ power (battery) aware routing algorithms on the relay nodes in order to find the optimal route to the end user.

With the deployment of WLANs inside 3G cells, it becomes possible to serve users having poor channel conditions with relatively higher data rates by relaying the information via nodes that have better channel conditions. Serving users with better channel conditions increases the overall system performance of the 3G system since these users will benefit from higher 3G data rates. From this point onwards, we will regard WLANs inside a 3G cell as the HSs.

Figure 6.1 depicts the deployment of a HS with D nodes within the 3G system. The lower dotted arrow represents the traditional 3G system scheduling. If the node to be served by the BS (end node) is in the HS, a performance enhancement may be achieved by directing the 3G BS to another node in the HS that has better channel conditions. The upper solid arrow shows the integrated scheduling/routing process.

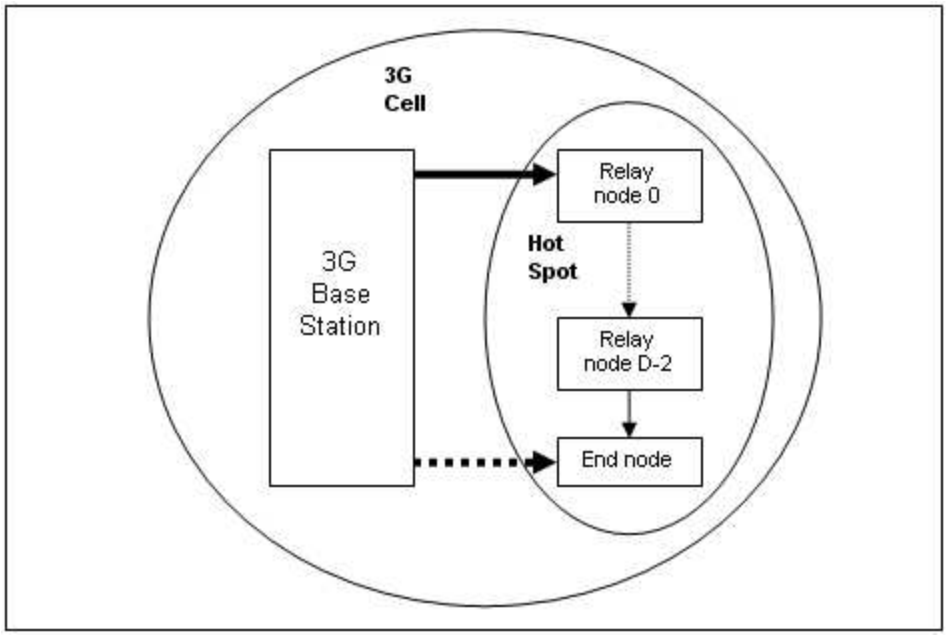

Figure 6.1: HS deployment within a 3G cell

6.1 Overview of Ad-Hoc Routing Protocols

The routing process among the nodes within a HS needs to be done in such a way as to maximize the lifetime of the nodes as well as to provide the fastest route to the end user. In determining the best route out of all possible routes within the HS, it should also be a design constraint to make the overall performance of the 3G system better.

There are some common routing algorithms used in ad-hoc networks [58]. The routing algorithms that will be briefly discussed are as follows:

6.1.1 Minimum Total Transmission Power Routing (MTTPR)

This algorithm tries to find a route on which the total transmission power is a minimum with respect to other possible routes [58]. In order to realize reliable communication between any two given nodes, the SNR should be greater than a certain threshold γ. SNR is directly related to BER. The SNR should satisfy the following equation for successful transmission:

$$SNR_j = \frac{P_i G_{i,j}}{\sum_{k \neq i} P_k G_{k,j} + \eta_j} \gamma \tag{6.1}$$

where P_i is the transmission power of node n_i, $G_{i,j}$ is the path gain between nodes n_i and n_j, and η_j is the thermal noise at node n_j. The transmission power $P(n_i, n_j)$ between nodes n_i and n_j can be used as a metric [59] to obtain the route with the minimum total transmission power. For a route l the total transmission power P_l can be written as:

$$P_l = \sum_{i=0}^{D-1} P(n_i, n_{i+1}) \tag{6.2}$$

where n_0 and n_D are the source and destination nodes respectively. The desired route m can be obtained from:

$$P_m = \min_{l \in A} P_l \tag{6.3}$$

where A is the set containing all possible routes. Dijkstra's shortest path algorithm [60] is modified to obtain minimum total power route [61]. Since transmission power is proportional to d_n (usually $n = 2, 3, 4$ depending on the terrain) this algorithm tries to select the route with more hops than other routes. When more hops are involved in a route, end-to-end delay also increases. Another drawback of this scheme is the possibility that the selected route will be unstable since, as the number of nodes involved in the route increases, the possibility that one of them will be off the ad-hoc network also increases which does not make MTTPR an attractive choice for routing in ad-hoc networks.

6.1.2 Minimum Battery Cost Routing (MBCR)

MTTPR utilizes total transmission power on a specific route for the best route selection [58]. Total transmission power is an important metric since it is related to the lifetime of the nodes, however it does not address the factors that directly affect the lifetime of nodes. The remaining battery capacity on each node can be considered as a more accurate metric to develop battery efficient routing protocols [62]. In this way, extended lifetime for the nodes can be provided.

In order to develop the routing algorithm a battery cost function $f_i(c_i^t)$ is defined for node n_i where c_i^t is the battery capacity of node n_i at time t. The tendency of a node to forward packets is a function of its remaining battery capacity. One possible choice for battery cost function is:

$$f_i(c_i^t) = \frac{1}{c_i^t} \tag{6.4}$$

As the battery of a node decreases its battery cost function increases. The battery cost function R_l of a route l consisting of D_l nodes is given as:

$$R_l = \sum_{i=0}^{D_l-1} f_i(c_i^t) \tag{6.5}$$

In order to find the route with the maximum remaining battery capacity, the route m with the minimum battery cost is selected:

$$R_m = \min(R_l | l \in A) \tag{6.6}$$

where A is the set containing all possible routes.

This algorithm selects the routes based on the total remaining battery capacities of the nodes on the route. It does not account for the individual nodes that are at critical battery levels. For instance, a route with a node at a critical battery capacity is selected if the total remaining battery capacity on this route is maximum. In order to overcome the problem of node overuse, another algorithm is proposed and is briefly discussed below.

6.1.3 Min-Max Battery Cost Routing (MMBCR)

The cost function given in (6.5) is modified [62] to overcome the problem of node overuse. Battery cost R_l is redefined as:

$$R_l = \max_{i \in route_l} (f_i(c_i^t)) \tag{6.7}$$

The desired route m is thus obtained from:

$$R_m = \min(R_l | l \in A) \tag{6.8}$$

Since this metric tries to avoid the routes with nodes having the least battery capacity, batteries of nodes will be used more fairly when compared to previous algorithms.

6.2 A New Approach in Battery Efficient Routing: Exponential Ad-Hoc Routing

Previously mentioned routing algorithms in mobile ad-hoc networks perform routing based on the lifetime of intermediate nodes within the HS but do not take into account the overall performance of the combined 3G/WLAN system. Building on the original exponential scheduling rule [32] for the 3G CDMA systems, we propose an exponential ad-hoc routing (ExpAR) algorithm. This algorithm tries to evaluate the battery capacities of each possible route in the HS in a comparative fashion with regard to the mean battery capacity of all the routes and selects the route with the highest argument according to:

$$s_l = \arg\max_i R_l(t) \exp\left(\frac{batt_l(t) - \overline{batt(t)}}{1 + \sqrt{\overline{batt(t)}}}\right) \tag{6.9}$$

where $R_l(t)$ is the normalized route throughput ($R_l(t) \in [0,1]$) calculated by the average route throughput divided by the maximum possible throughput (11 Mbps) between the source and the end nodes. For example considering a 2 hop scenario with route throughput 5.5 Mbps between the source and the relay node and 11 Mbps between the relay node and the end node, the average route throughput would be 8.25 Mbps and the normalized route throughput, $R_l(t)$, would be $8.25Mbps/11Mbps = 0.75$. $batt_l(t)$ is the normalized total battery capacity of route l ($batt_l(t) \in [0,1]$) and $\overline{batt(t)}$ is the average of the total battery capacity of all the routes. Figure 6.2 shows the argument as a function of $R_l(t)$ and $batt_l(t)$ corresponding to x and y axes respectively. For comparison purposes the plane representing the function $R_l(t)$ is also given. As the graph clearly indicates for routes with high total battery, the increase in the exponential term dominates the throughput term thus favoring high total battery capacity routes leading to battery efficient route selection within the ad-hoc network. The $R_l(t)$ term is also an important parameter in the cost function since it directly relates to source-to-end node latency as well as the link utilization of a particular route within the HS. Relaying the packets for the end node on a route with the highest throughput available means disturbing the internal communications of WLAN in the least way possible.

The motivation underlying this rule follows a similar approach as discussed in [32]. In choosing the best route to relay BS data to the end node, average data rate of the route

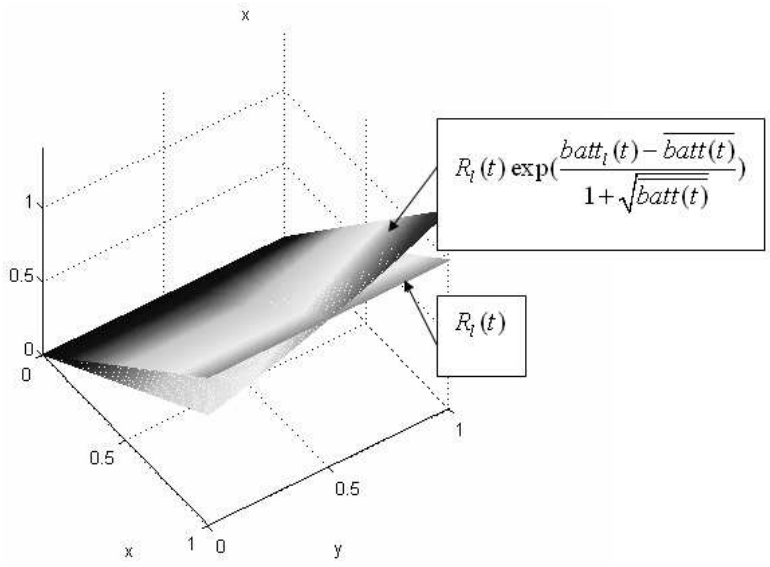

Figure 6.2: Mathematical Representation of the Cost Function

is also accounted for, thus making a compromise between choosing the highest data rate route and the route with the highest total battery capacity. When the total battery of a certain route is higher than the average total battery of all the routes by more than order $\sqrt{\overline{batt(t)}}$ the exponential term overrides the average route throughput and this route is selected. For routes that have lower battery capacity than the average total battery of all the routes, argument is dominated by the average throughput term. When a certain route has significantly lower total battery, this route will be less likely to be chosen even if it has a high average throughput.

6.2.1 General Structure of the Combined 3G Scheduling and Ad-Hoc Routing System

The operation of the combined scheduling and routing algorithm for the 3G/WLAN system is summarized below:

STEP 1: The BS selects a user within the 3G cell by employing the HDR exponential scheduler.

STEP 2: If the selected user is in HS, a central station (may be a separate system from the HS nodes) in the WLAN is notified and HS routing is initiated.

STEP 3: The first user that will be the source node of the route is selected using:

$$s_{wlan} = \arg \max_i R_i(t) \tag{6.10}$$

This first user is also the user that will be served by the 3G BS and hence needs to be selected in such a way to increase the overall 3G system performance as well as being battery efficient. Ties are broken in such a way that the node with the highest battery capacity is chosen.

STEP 4: After determining the first node of the route, all the possible routes between the source node s_{wlan} and the destination node (originally 3G selected user) are evaluated and the route with the maximum argument of (6.11) is selected for ad-hoc routing.

$$s_l = \arg \max_i R_l(t) \exp\left(\frac{batt_l(t) - \overline{batt(t)}}{1 + \sqrt{\overline{batt(t)}}}\right) \tag{6.11}$$

The system we consider in our proposal and simulations is a closed network system, in which the total number of users in the cell, N_{3G}, will be constant. This means, as the number of users in the HS increases, the number of users outside the HS but in the 3G cell decreases. This can be shown as:

$$N_{3G} = N_{HS} + N'_{HS} \tag{6.12}$$

6.3 Simulation Environment

In performing the simulations, the base level simulation model for the HDR is utilized. A detailed explanation on the simulation model for the HDR system is given in Chapter 3. The number of users in the HS has been taken to vary from 2 to 16 users out of a total of 32 users in the 3G cell. The radius of the HS and the distance of the HS from the 3G cell center have also been taken as variables in the performance evaluations. In the simulations the following have been assumed for the HSs:

- The set of radii: $S_r = \{50m, 100m, 200m\}$
- The set of HS distances corresponding to each radius:
  $S_{D_{r=50m}} = \{100m, 250m, 500m, 750m\}$

$$S_{D_{r=100m}} = \{100m, 250m, 500m, 750m\}$$
$$S_{D_{r=200m}} = \{250m, 500m, 750m\}$$

There have been 30 drops for the positions of the users throughout the course of the simulation and the users in the cell have been redistributed uniformly at the beginning of each drop to create sufficient geographical diversity. Pedestrian A channel has been assumed with the same constant velocity for each mobile throughout the simulation. Figures 6.3, 6.4 and 6.5 show the sample distributions of users in the HS and the 3G cell covering all the 30 uniformly distributed drop locations. The HS has been identified as a circle located at the distances chosen from the set S_{D_r}.

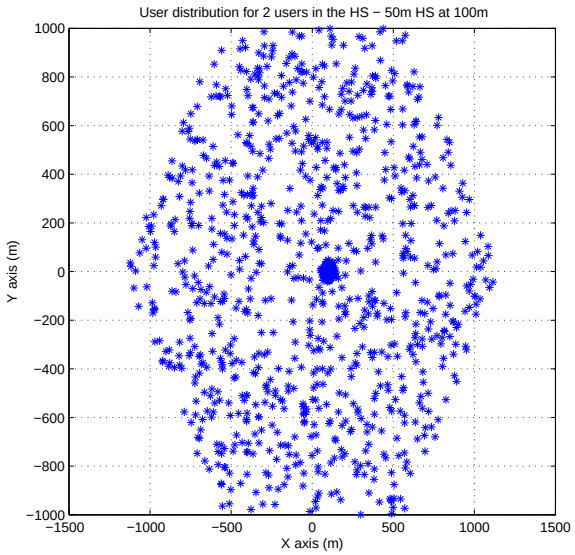

Figure 6.3: HS with 50m radius at 100m from cell center - 2 users in the HS

The scheduling algorithms that have been used in the 3G HDR system are:

- Exponential (Exp)
- Round Robin (RR)
- Maximum Rate (MaxR)

These algorithms have been chosen since they provide benchmark results for throughput (MaxR) and latency (RR). Exp scheduling represents the best-effort service.

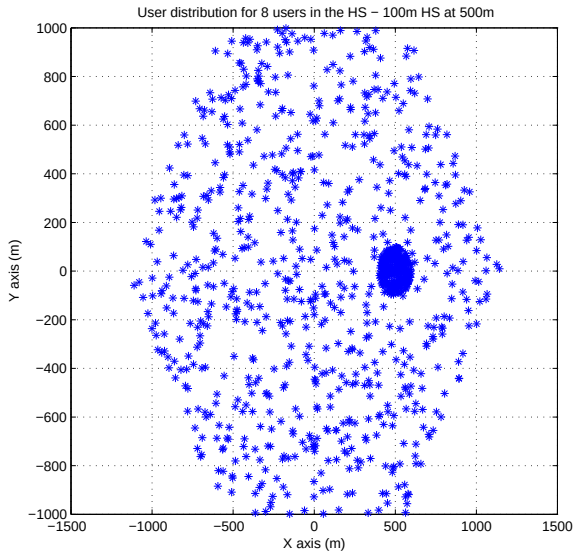

Figure 6.4: HS with 100m radius at 500m from cell center - 8 users in the HS

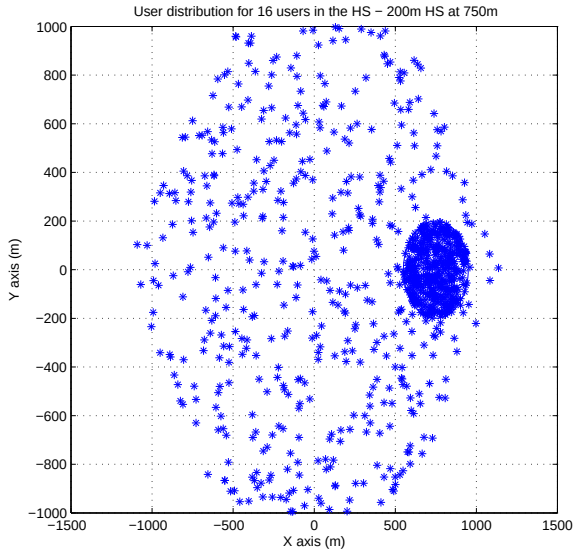

Figure 6.5: HS with 200m radius at 750m from cell center - 16 users in the HS

When a user in the HS is selected by the BS the routing algorithm in the HS is initiated. The total number of 3G users is fixed at 32 and the maximum number of users in the HS has been set to 16. In the simulations we have investigated the performance of the scheduling/routing system starting from 2 up to 16 active users in the HS. 16 users account for the 50 % of the total number of users in the 3G cell. Figure 6.6 shows the flow diagram

for combined 3G/WLAN scheduling/routing.

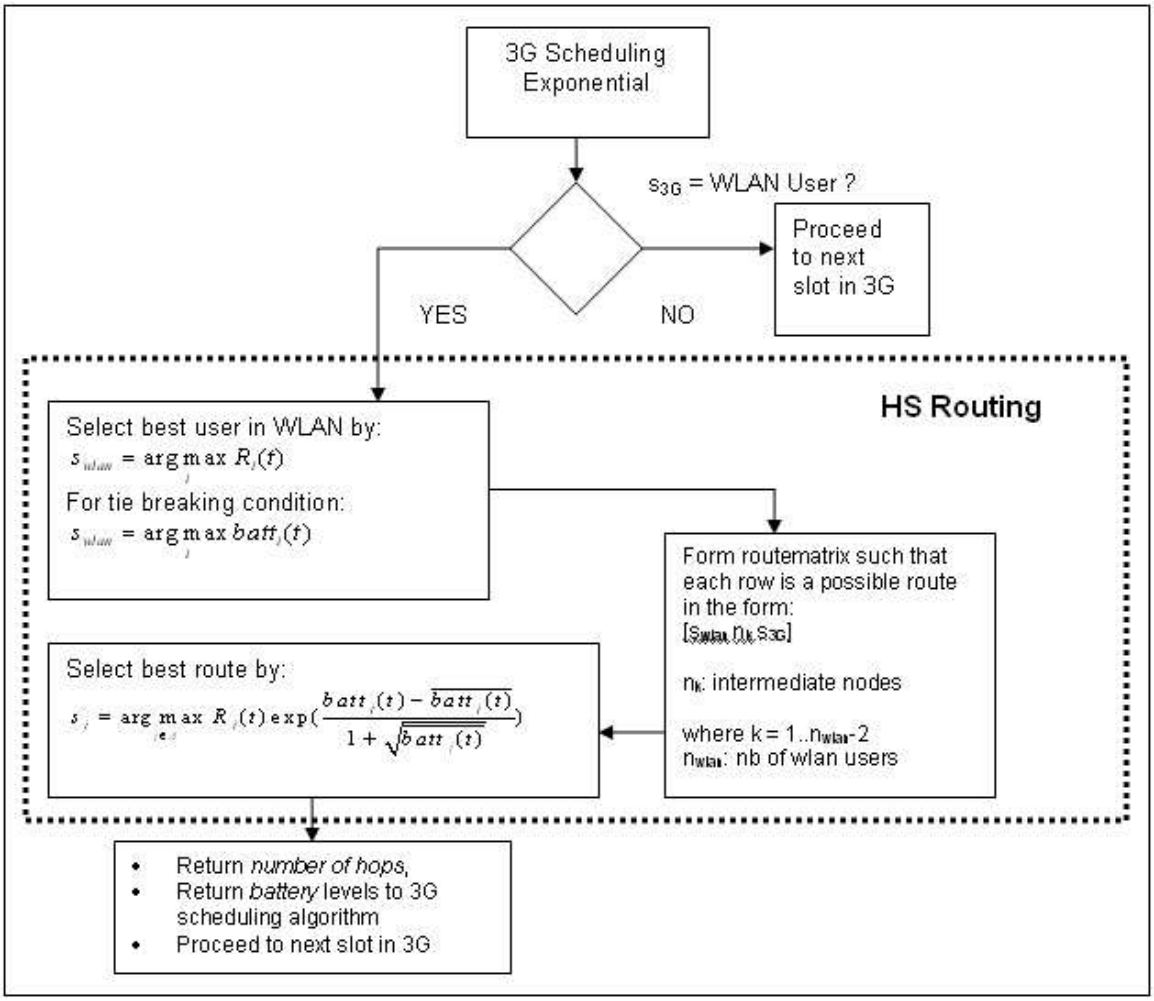

Figure 6.6: 3G/WLAN scheduling/routing algorithm

In the above mentioned algorithm, if the best user in the HS is the user that is also selected by the 3G system the user is served without using HS resources, which corresponds to a 0 hop routing.

In the HS we have simulated the IEEE 802.11b WaveLAN system which has been studied in the literature in detail and which is widely available in the market.

Table 6.1 summarizes the performance data of the WLAN system [63].

Table 6.1: Performance data for WaveLAN

Date Rate	**Estimated Range (Open Office)**	**Estimated Range (Open Field)**
11 Mbps	55m	160m
5.5 Mbps	70m	270m
2 Mbps	85m	400m
1 Mbps	105m	550m

6.4 Simulation Results

This section includes the performance graphs obtained from the simulation environment. Due to a high volume of graphs available only certain representative graphs will be presented. Figures 6.7-6.17 and 6.18-6.28 present the performance enhancement of the proposed battery efficient routing algorithm for the overall 3G cell throughput for Exp and RR 3G scheduling respectively. MaxR scheduling has also been evaluated but since MaxR inherently selects the best user in the cell, no performance enhancement is obtained by using a HS. If the selected user in HS, it will be the highest data rate user in the HS, hence no routing will take place.

As it can be seen from the figures, the utilization of HSs inside 3G cells increases the overall throughput values of the 3G cell. One striking result is the decrease of the system throughput when the HS is further away from the BS. This is quite an expected result since by forcing more users in the HS situated further away from the BS, we are decreasing the mean requested data rates of the users due to lower SNRs as a result of greater path loss.

It is also apparent that the performance increase due to HS is greater when the RR scheduling is utilized at the 3G BS. This is also a reasonable result since RR scheduling does not exploit the channel conditions.

Figures 6.29-6.34 show the normalized battery levels of individual HS users. By utilizing the ExpAR, the routes with relatively higher total battery levels and higher throughput values are chosen thus balancing the use limited batteries of the MSs and providing fairness. The algorithm performs quite satisfactorily since even for 16 users in the HS, battery distribution is fair for different HS distances and radii. Due to limited space, battery graphs for the HS with 100m radius at 500m are considered for both Exp and RR 3G scheduling. Since MaxR does not lead to HS routing, batteries of the nodes are not consumed.

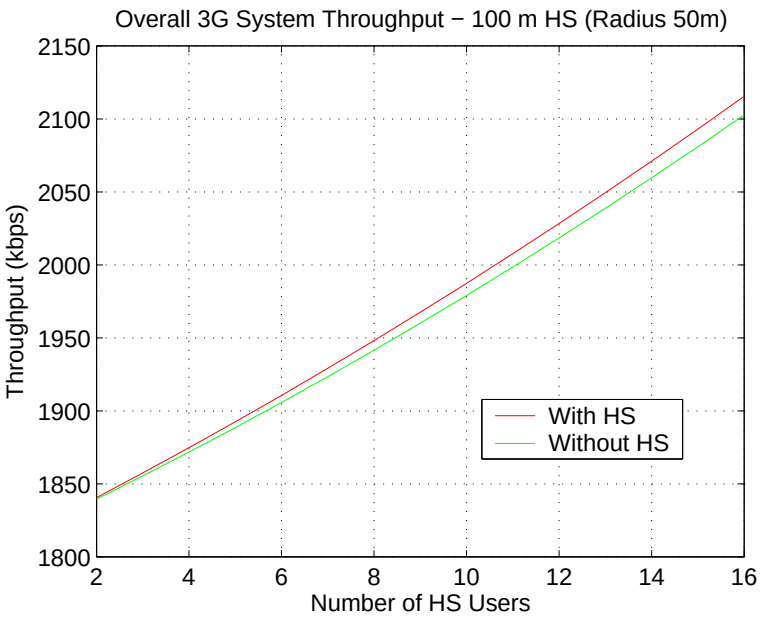

Figure 6.7: Overall 3G System Throughput for Exp 3G scheduling - HS (with 50m radius) at 100m

A detailed table is given in Appendix D that presents the percentage of occurrence of hop numbers inside the HS for the whole range of HS distances and radii employing Exp, RR and MaxR scheduling at the 3G BS. In this table NoHS indicates that a user outside the HS is scheduled. 0 hop row indicates that the selected user in the HS is also the end user that will be served without any routing.

Figures 6.35-6.40 show the throughput of the 3G/WLAN system when QoS aware scheduling algorithm is utilized in the 3G system. The figures give a comparison of the throughputs between the HS assisted 3G system with respect to HS non-assisted system. The results are also evaluated against the best effort scheduling scheme, the Exp algorithm. These results are shown for the 100m and 200m radius HSs. One immediate result obtained from these figures is that with the increasing QoS requirement the overall system performance values also increase however this corresponds to worse statistical performance for the 3G users. For the different QoS requirements, especially for the HS at 750m from the BS, WLAN assisted performance of the scheduling algorithm at lower QoS starts to beat that of the WLAN non-assisted at a higher QoS requirement. This can be clearly seen in Figure 6.40. The overall system performance of the 16 kbps QoS scheduling algorithm

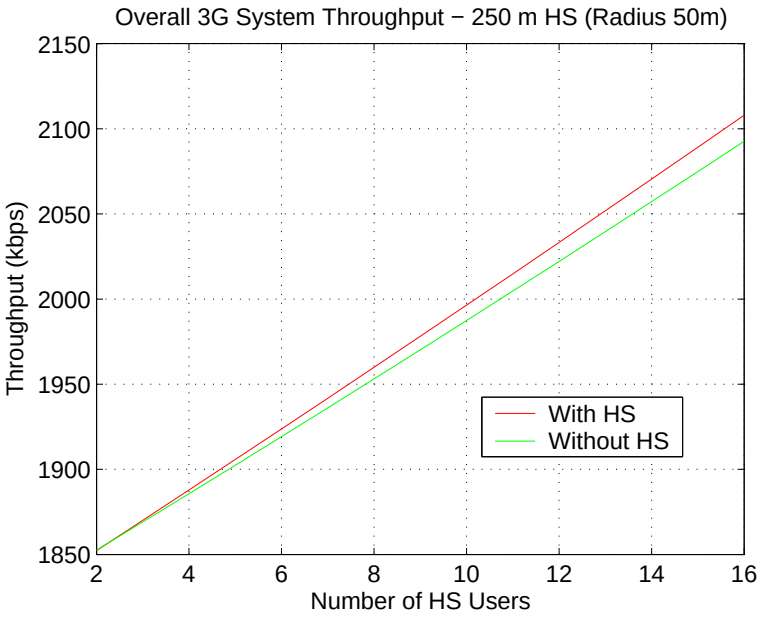

Figure 6.8: Overall 3G System Throughput for Exp 3G scheduling - HS (with 50m radius) at 250m

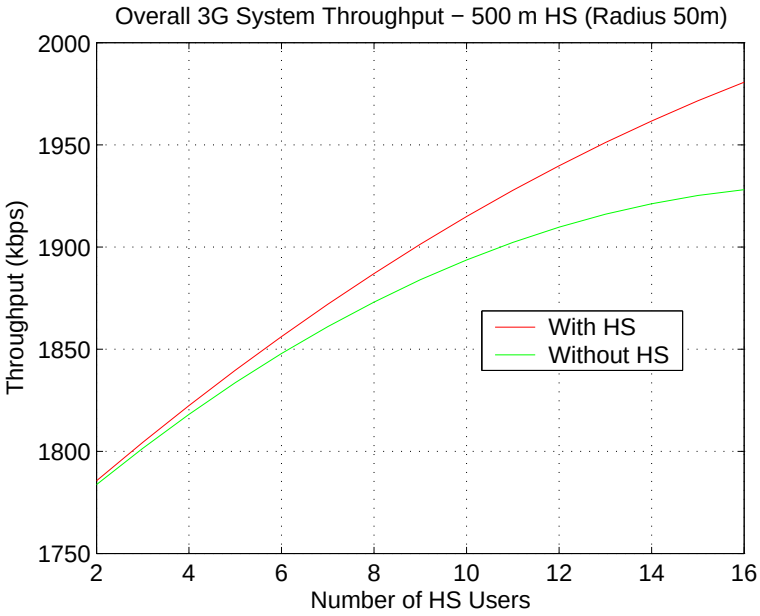

Figure 6.9: Overall 3G System Throughput for Exp 3G scheduling - HS (with 50m radius) at 500m

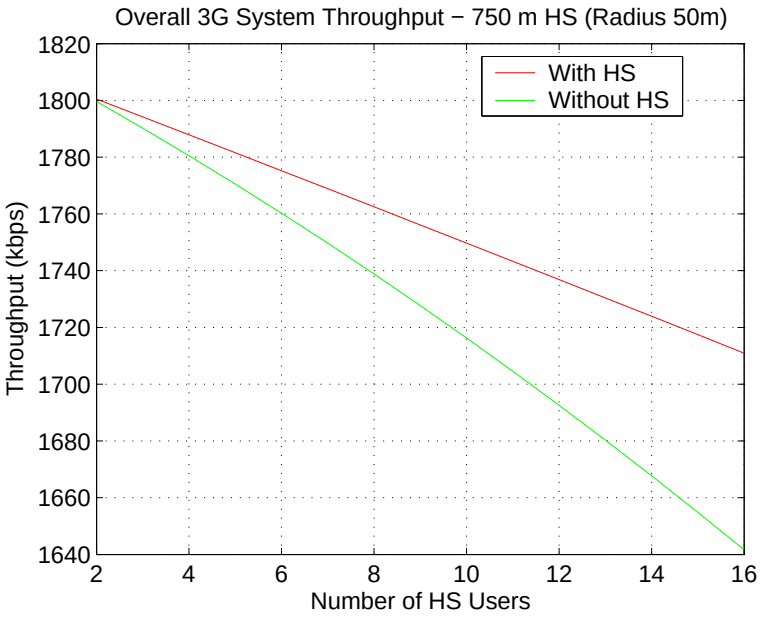

Figure 6.10: Overall 3G System Throughput for Exp 3G scheduling - HS (with 50m radius) at 750m

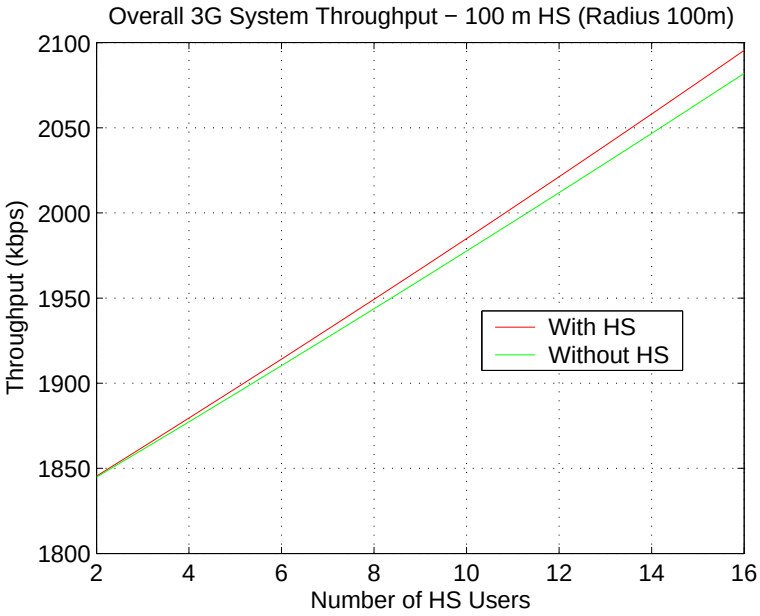

Figure 6.11: Overall 3G System Throughput for Exp 3G scheduling - HS (with 100m radius) at 100m

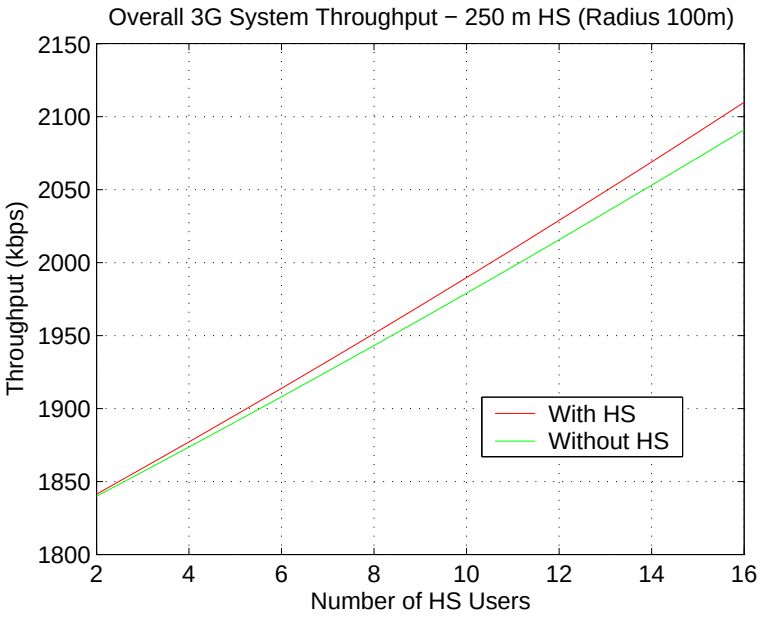

Figure 6.12: Overall 3G System Throughput for Exp 3G scheduling - HS (with 100m radius) at 250m

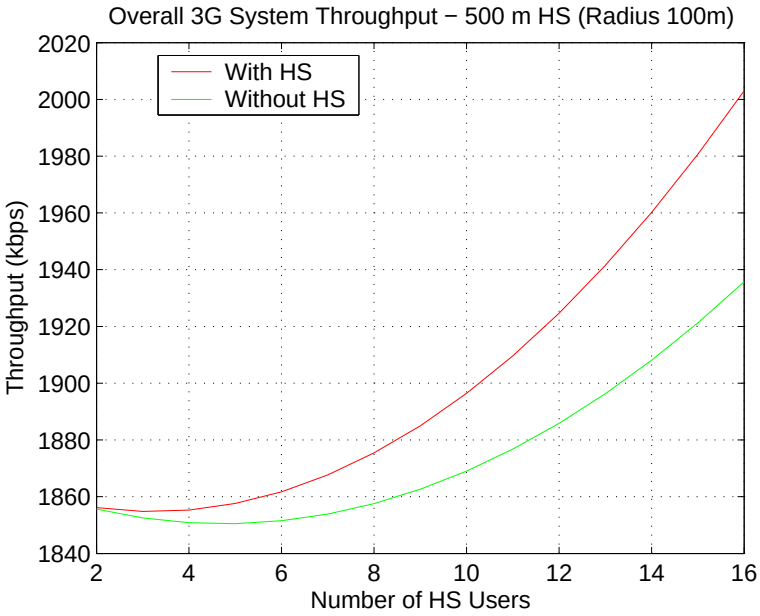

Figure 6.13: Overall 3G System Throughput for Exp 3G scheduling - HS (with 100m radius) at 500m

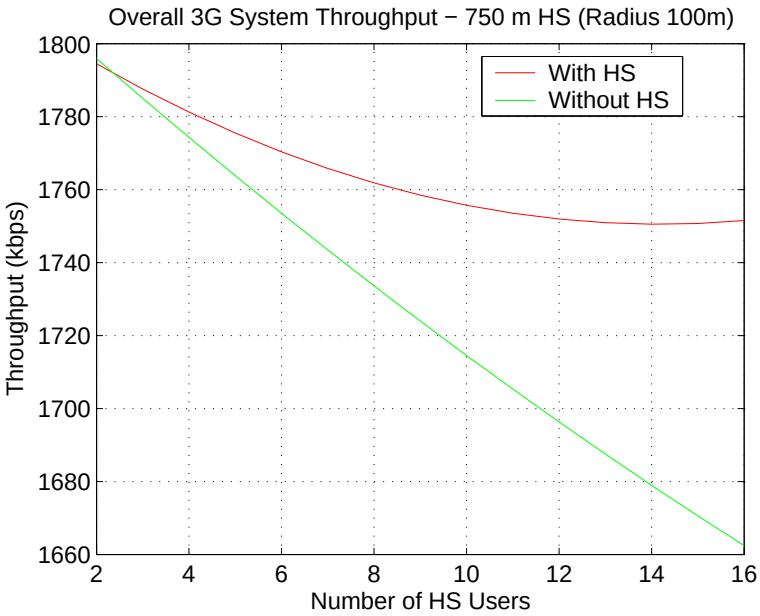

Figure 6.14: Overall 3G System Throughput for Exp 3G scheduling - HS (with 100m radius) at 750m

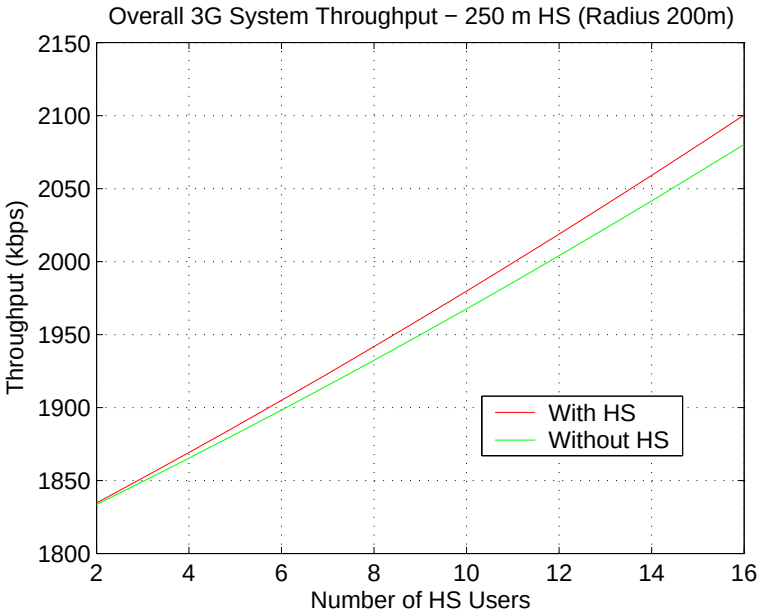

Figure 6.15: Overall 3G System Throughput for Exp 3G scheduling - HS (with 200m radius) at 250m

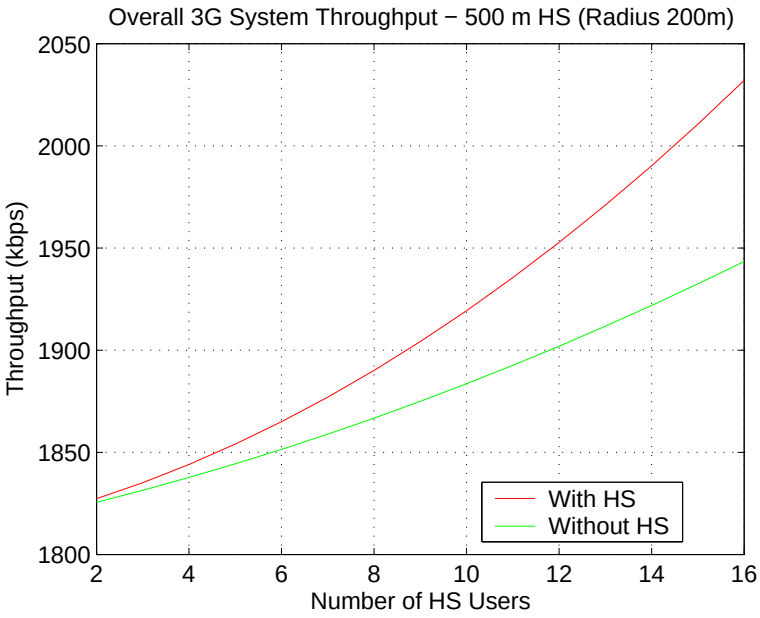

Figure 6.16: Overall 3G System Throughput for Exp 3G scheduling - HS (with 200m radius) at 500m

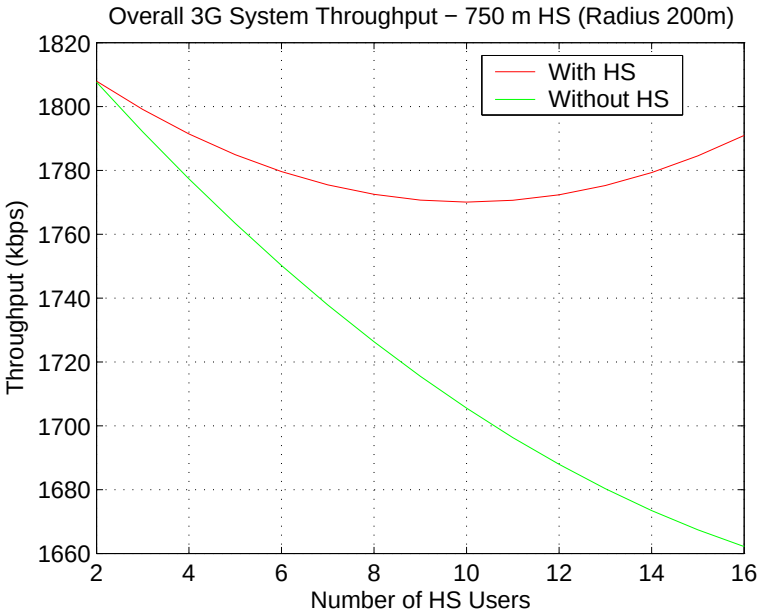

Figure 6.17: Overall 3G System Throughput for Exp 3G scheduling - HS (with 200m radius) at 750m

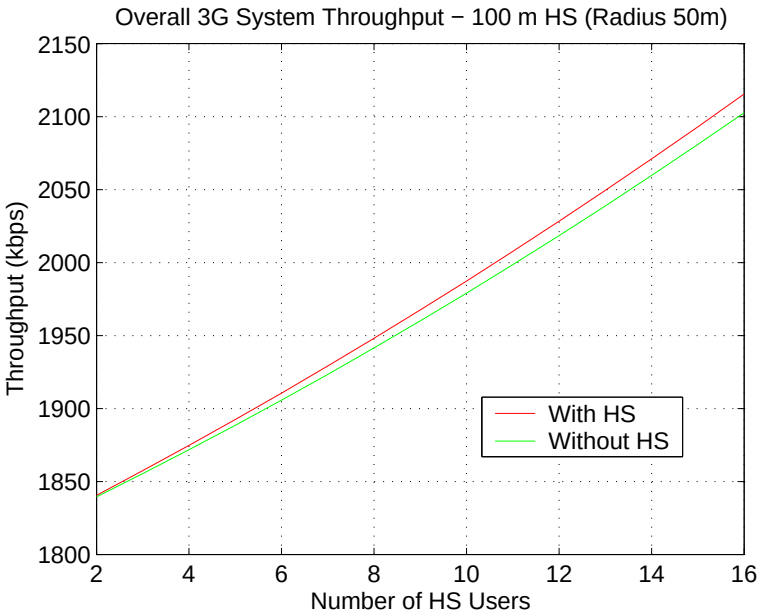

Figure 6.18: Overall 3G System Throughput for RR 3G scheduling - HS (with 50m radius) at 100m

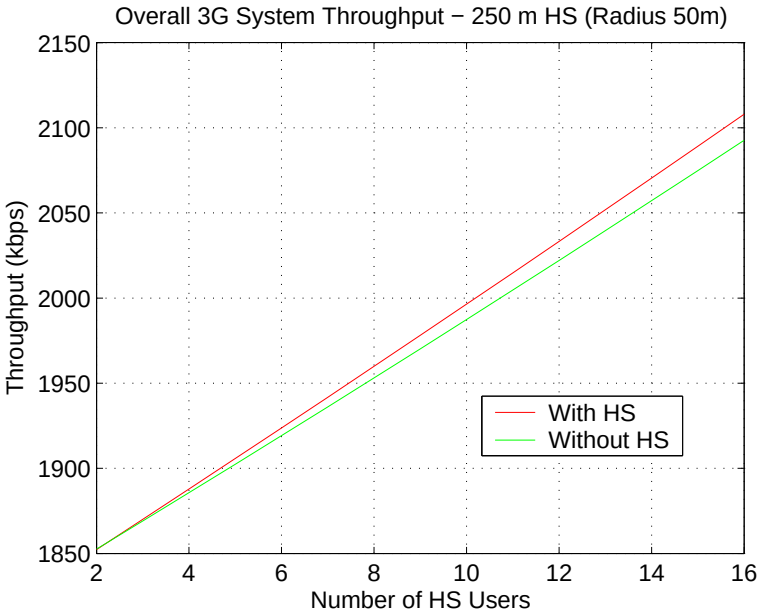

Figure 6.19: Overall 3G System Throughput for RR 3G scheduling - HS (with 50m radius) at 250m

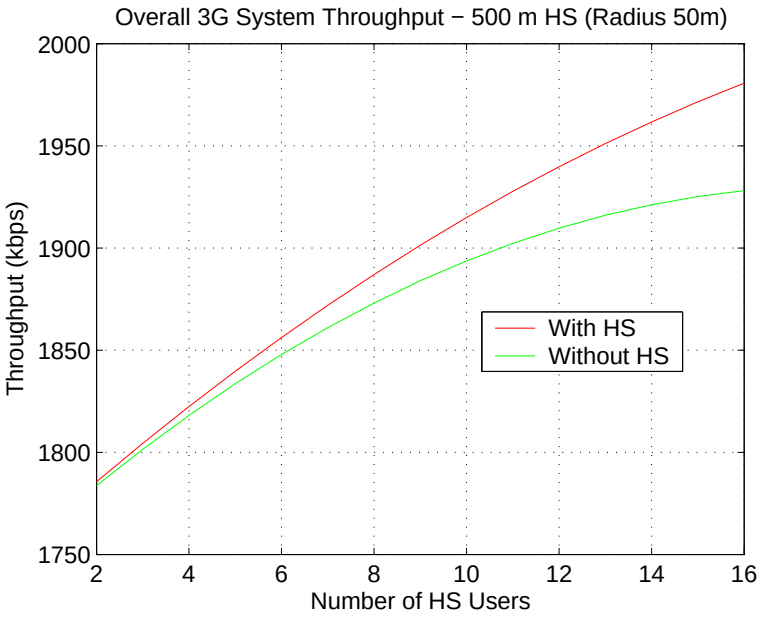

Figure 6.20: Overall 3G System Throughput for RR 3G scheduling - HS (with 50m radius) at 500m

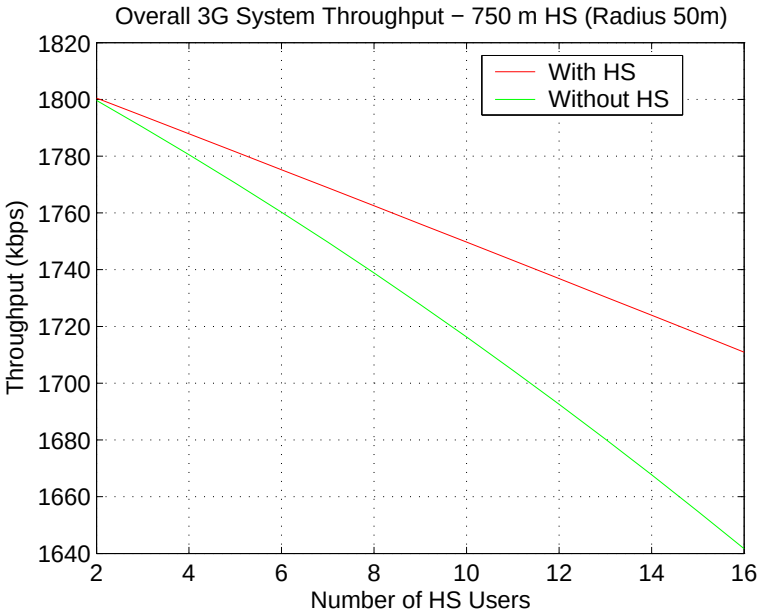

Figure 6.21: Overall 3G System Throughput for RR 3G scheduling - HS (with 50m radius) at 750m

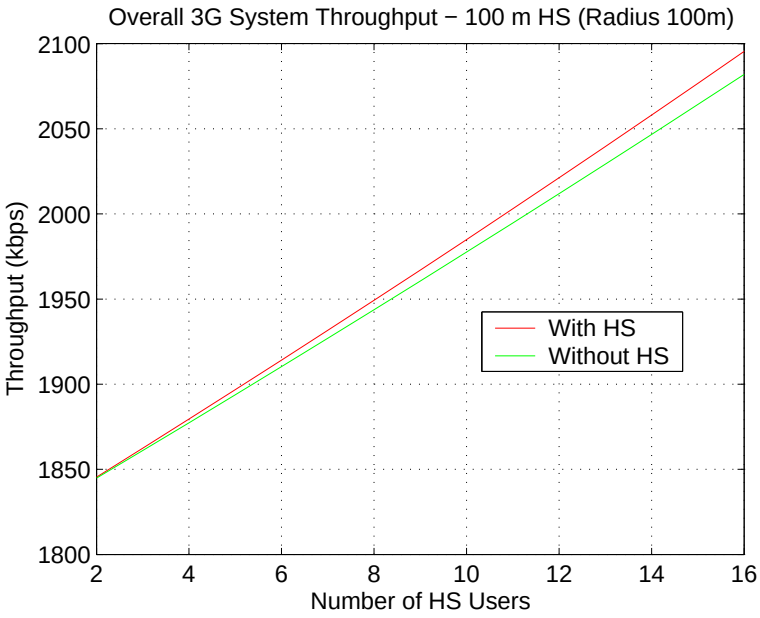

Figure 6.22: Overall 3G System Throughput for RR 3G scheduling - HS (with 100m radius) at 100m

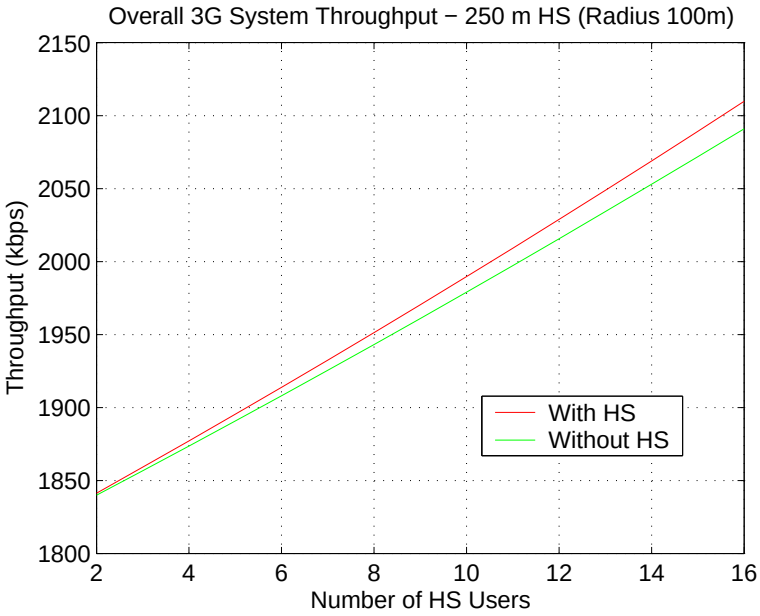

Figure 6.23: Overall 3G System Throughput for RR 3G scheduling - HS (with 100m radius) at 250m

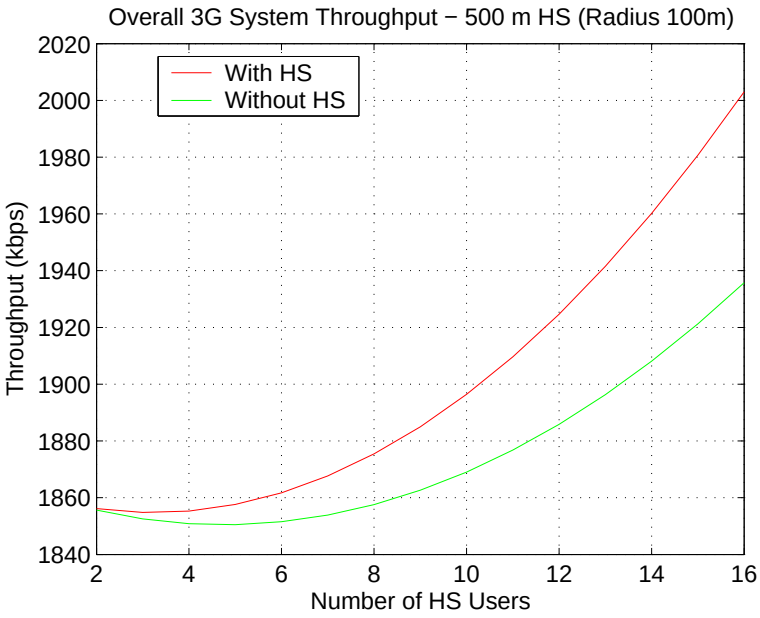

Figure 6.24: Overall 3G System Throughput for RR 3G scheduling - HS (with 100m radius) at 500m

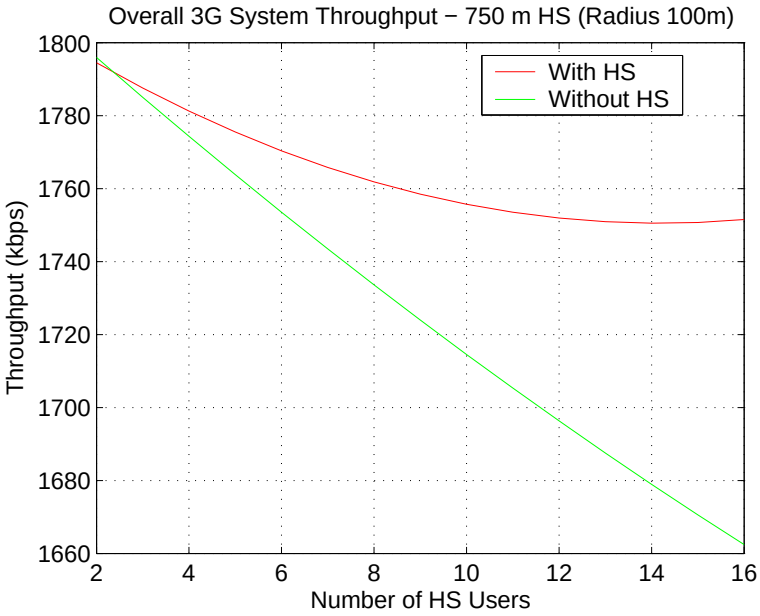

Figure 6.25: Overall 3G System Throughput for RR 3G scheduling - HS (with 100m radius) at 750m

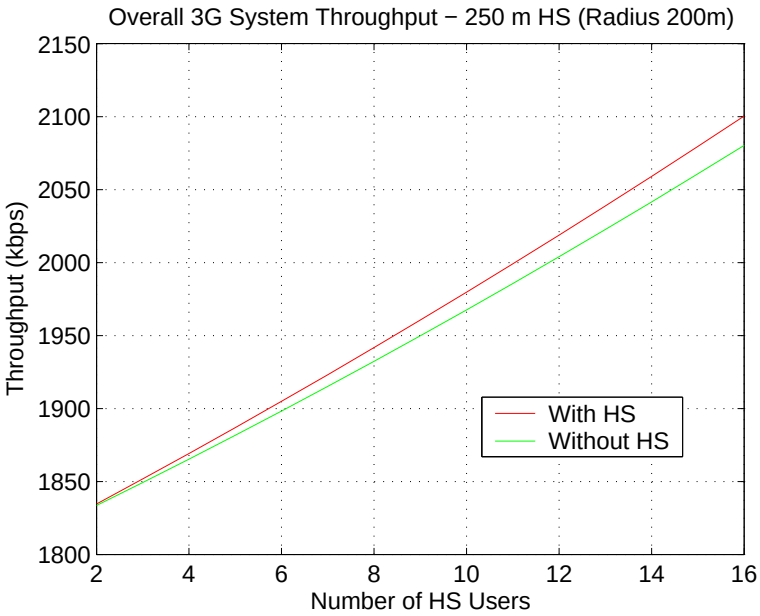

Figure 6.26: Overall 3G System Throughput for RR 3G scheduling - HS (with 200m radius) at 250m

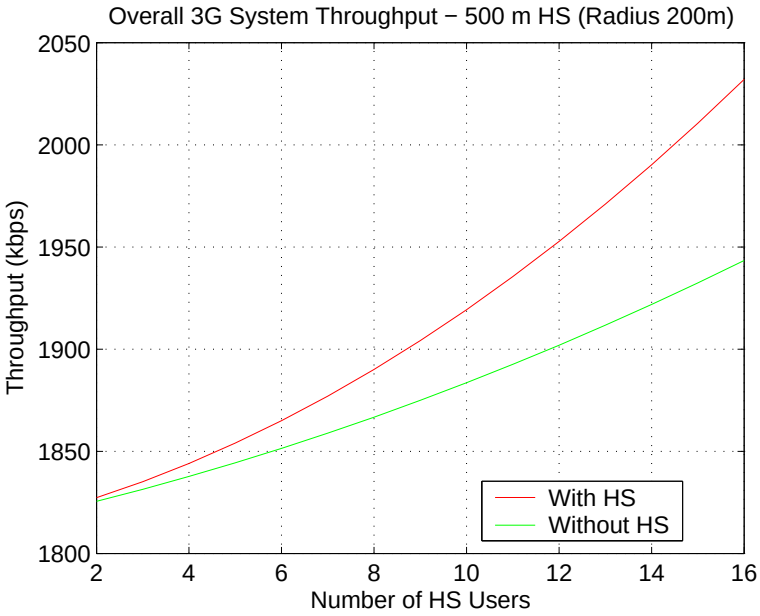

Figure 6.27: Overall 3G System Throughput for RR 3G scheduling - HS (with 200m radius) at 500m

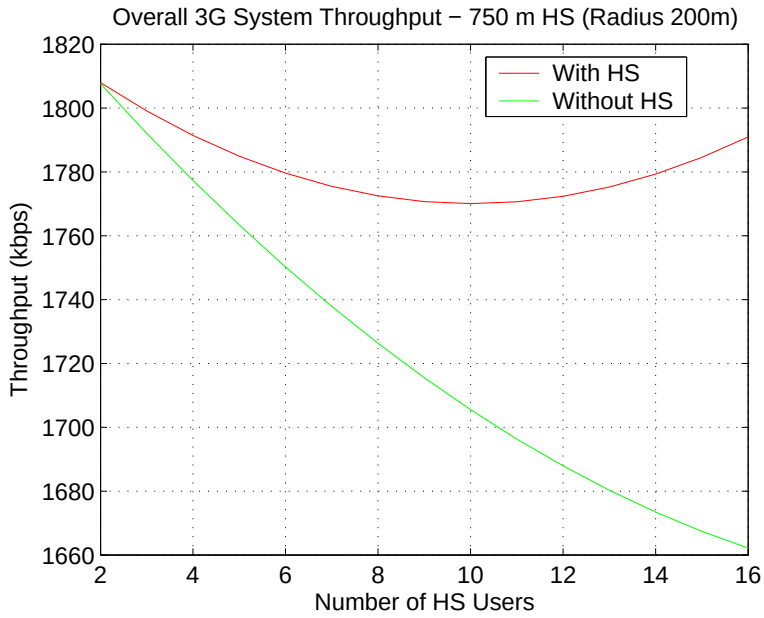

Figure 6.28: Overall 3G System Throughput for RR 3G scheduling - HS (with 200m radius) at 750m

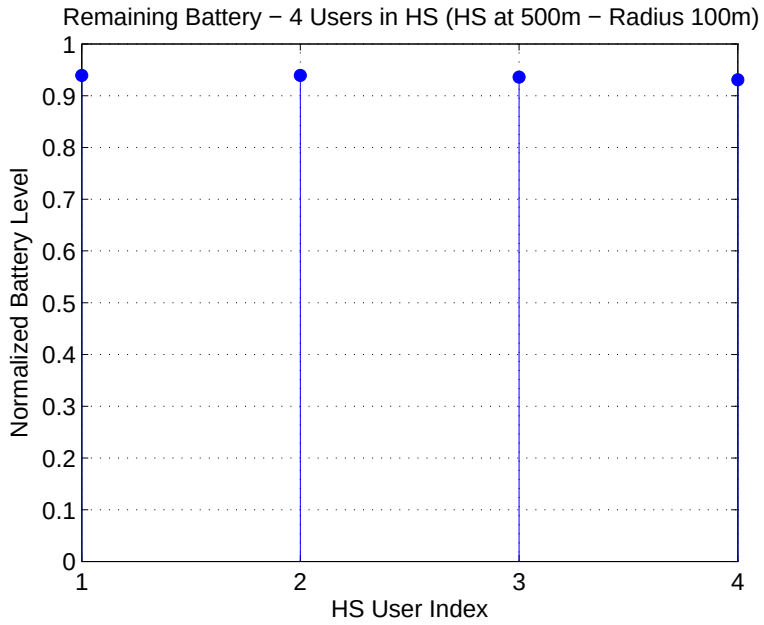

Figure 6.29: Battery Levels of the Nodes - HS (with 100m radius) at 500m - 4 active users - Exp 3G Scheduling

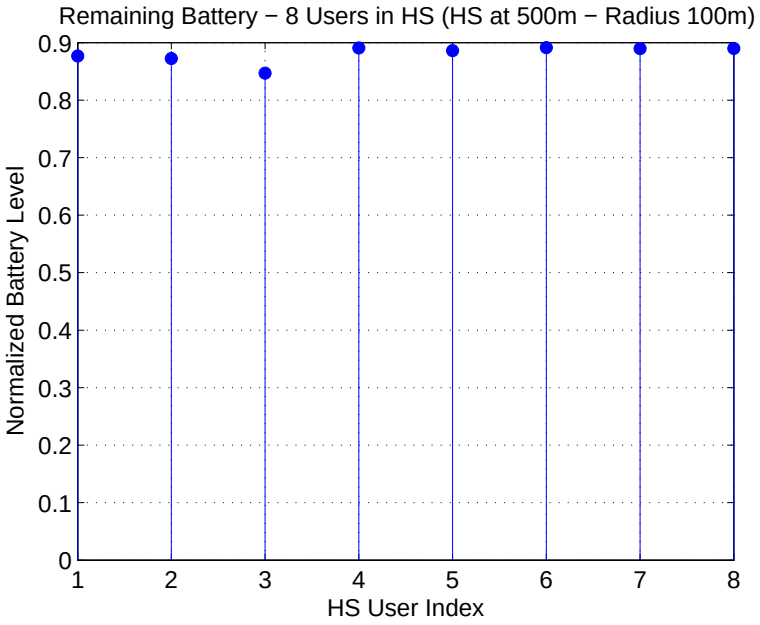

Figure 6.30: Battery Levels of the Nodes - HS (with 100m radius) at 500m - 8 active users - Exp 3G Scheduling

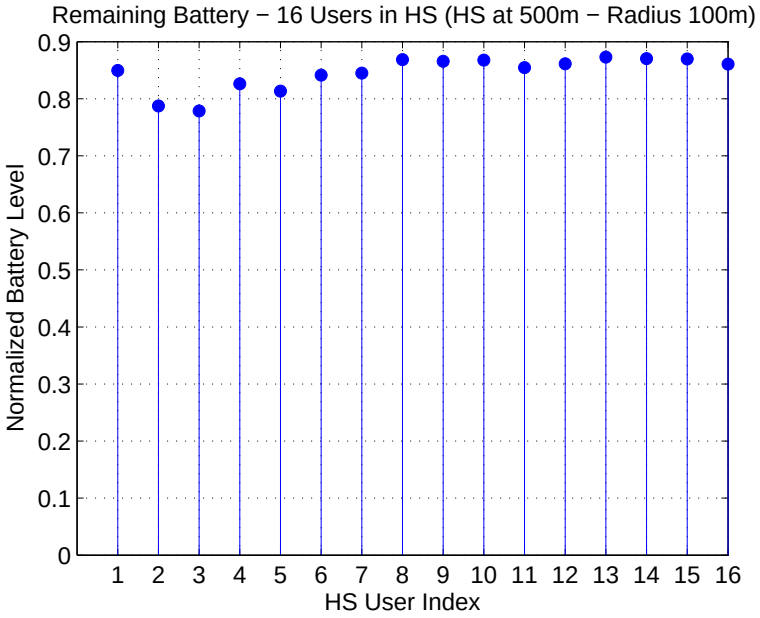

Figure 6.31: Battery Levels of the Nodes - HS (with 100m radius) at 500m - 16 active users - Exp 3G Scheduling

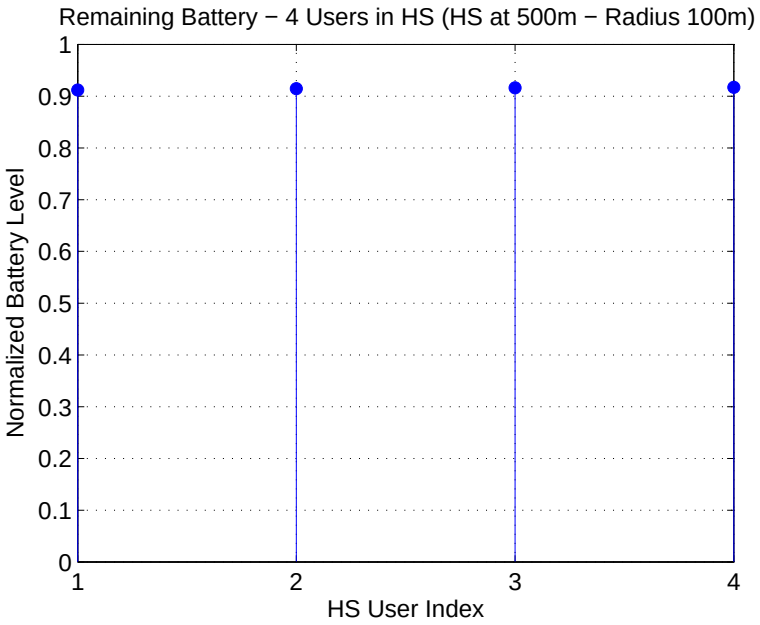

Figure 6.32: Battery Levels of the Nodes - HS (with 100m radius) at 500m - 4 active users - RR 3G Scheduling

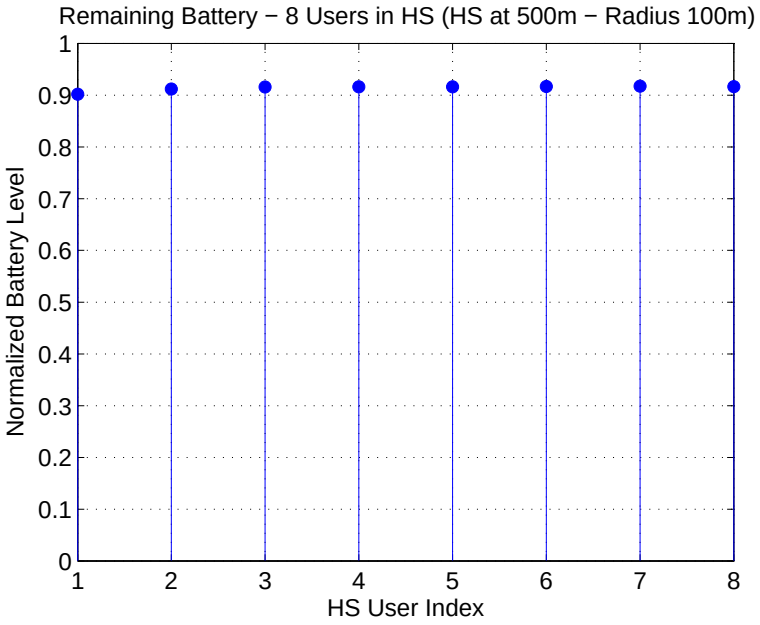

Figure 6.33: Battery Levels of the Nodes - HS (with 100m radius) at 500m - 8 active users - RR 3G Scheduling

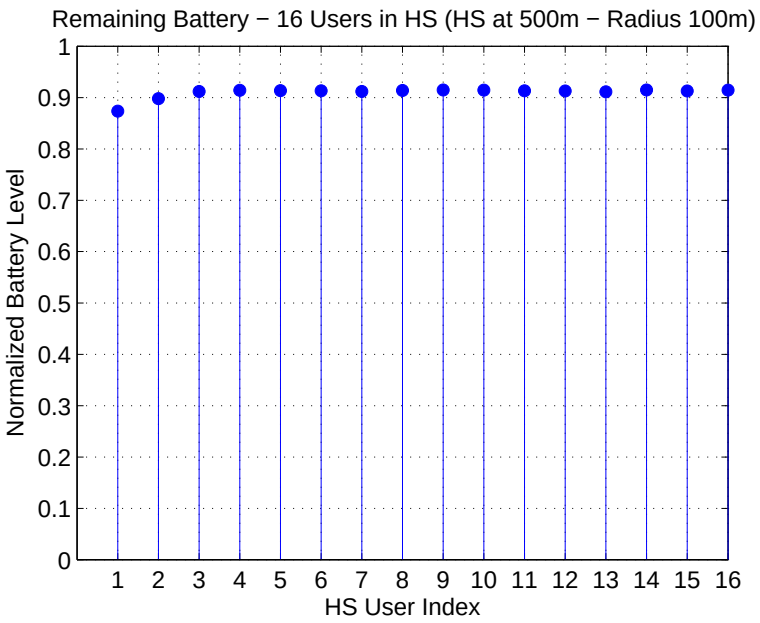

Figure 6.34: Battery Levels of the Nodes - HS (with 100m radius) at 500m - 16 active users - RR 3G Scheduling

with WLAN assistance equals to the performance of the 128 kbps QoS scheduling without WLAN assistance.

6.5 Conclusion

Integration of 3G systems with WLANs will be the next step in forming seamlessly integrated ubiquitous networks. In this chapter, a possible system integration method between the 3G CDMA system and the IEEE 802.11 WLAN has been proposed. In developing the system we have taken into account two important constraints: 3G system performance enhancement and efficient routing based on the battery capacities of the nodes within the HS. The proposed algorithm not only enhances the 3G system performance but also utilizes HS nodes fairly via efficient routing.

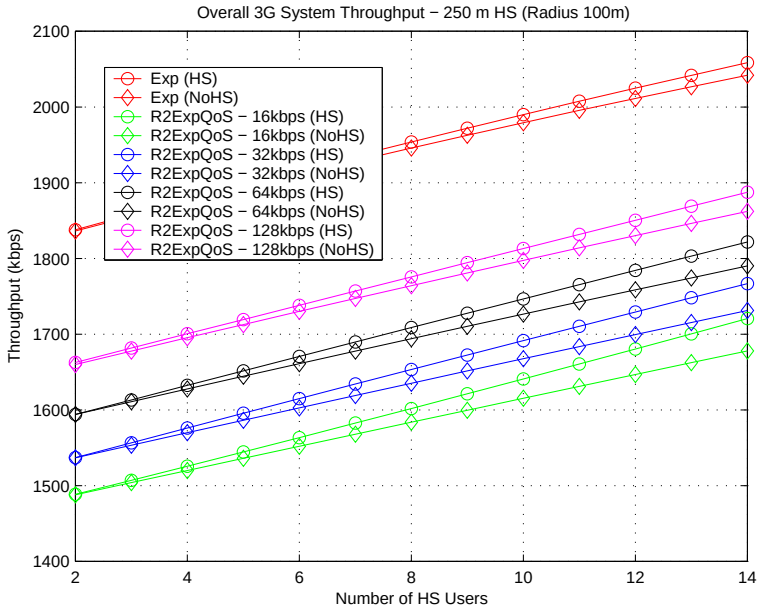

Figure 6.35: Overall 3G System Throughput - HS at 250m (100m HS radius)

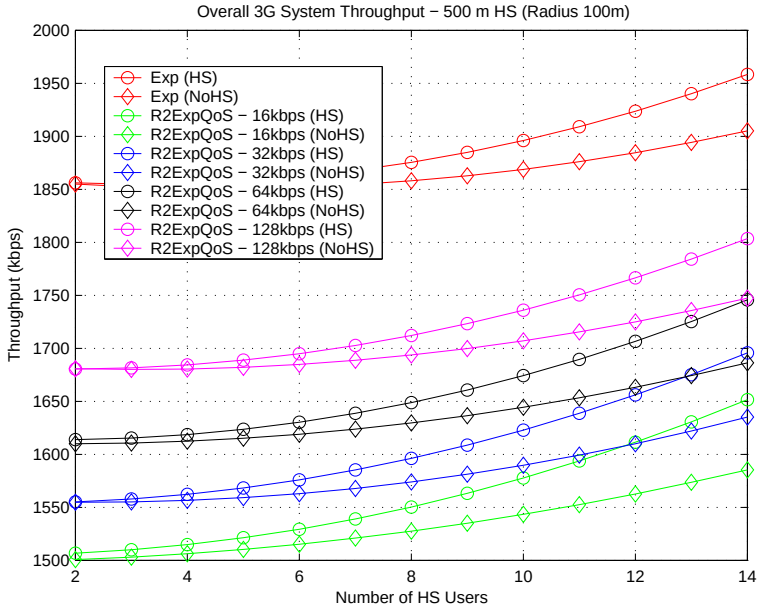

Figure 6.36: Overall 3G System Throughput - HS at 500m (100m HS radius)

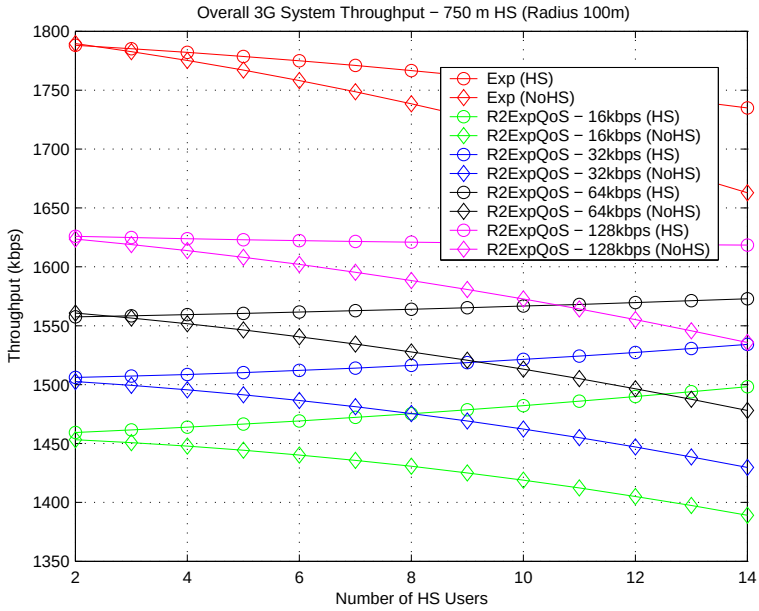

Figure 6.37: Overall 3G System Throughput - HS at 750m (100m HS radius)

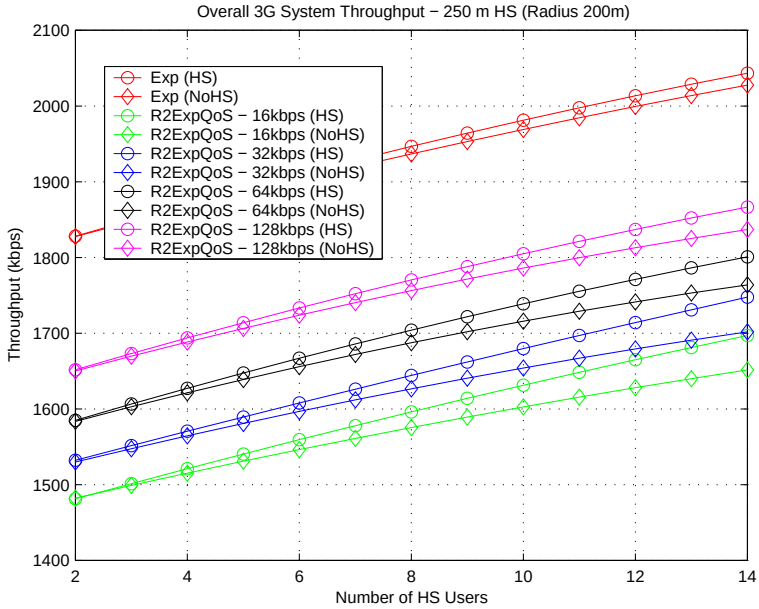

Figure 6.38: Overall 3G System Throughput - HS at 250m (200m HS radius)

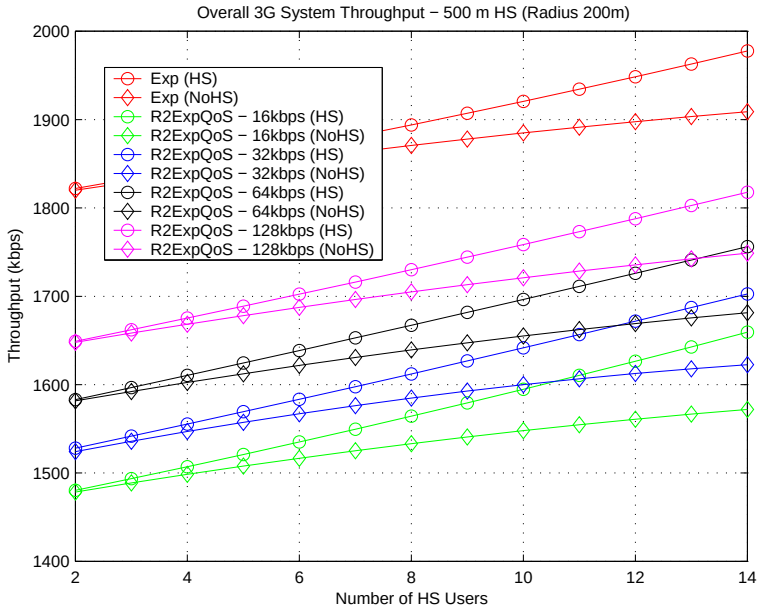

Figure 6.39: Overall 3G System Throughput - HS at 500m (200m HS radius)

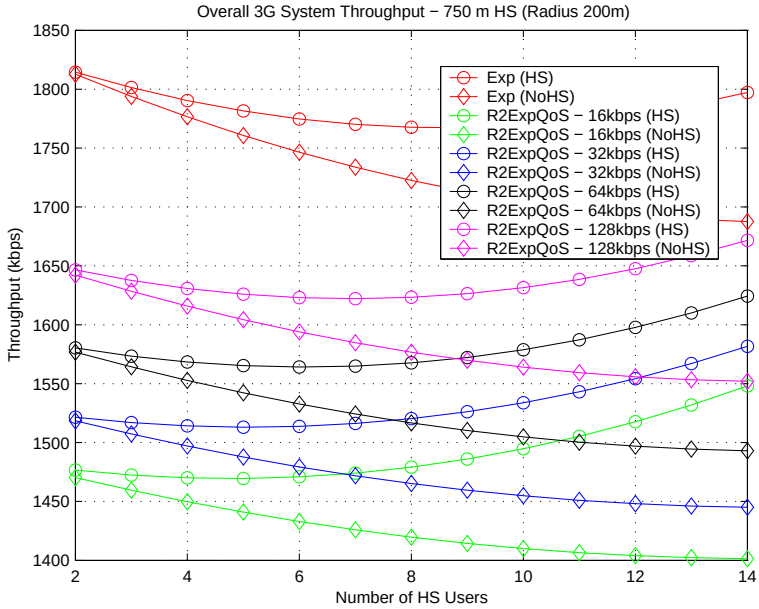

Figure 6.40: Overall 3G System Throughput - HS at 750m (200m HS radius)

Chapter 7

CONCLUSIONS

7.1 Conclusion

The advances in the world of wireless communications are taking place at a great pace. It has now become a reality to reach anyone, anywhere and anytime via the seamless interconnection of wireless systems.

Still, wireless systems have a long way to go in terms of overall system performance and service guarantees. With proper channel knowledge and adaptive coding strategies, the performance of the systems can be advanced at great amounts.

Besides the physical layer improvements, a wireless system should also be designed to satisfy the requirements of the upper layers, such as the application layer. Tomorrow's high data rate wireless systems will feature streaming audio/video applications. However both audio and video data have certain requirements in order to be received at an acceptable quality level at the receiving side. In order to transport streaming type content, a wireless system should be aware of the delay and/or data rate constraints imposed on the content. At this point a certain QoS level should be implemented in the system. QoS levels are determined by the type of traffic that is intended to be carried over the network. A novel wireless system design should accommodate both non-real-time data and real-time/streaming data users in a soft manner. The softness here implies the adaptivity of the system with respect to the non-real-time/real-time load at any time.

In thesis the major part of the research has been the statistical QoS mechanism implemented on the recently standardized 1xEV-DO system. Instead of a strict assurance of data rate for the mobile users, a statistical assurance has been provided via the proposed scheduling algorithms. The advantage of the statistical assurance is that it compromises between the best effort and strictly guaranteed service. It tries to combine the best of both worlds. Without sacrificing the overall system performance, the users are served data rates at statistical levels. For instance for 12 active users with a desired data rate of 256 kbps

(in the 3x MC case) for each user, the system guarantees the data rate (256 kbps) for 97 % of the time meaning in 27 seconds out of 30 seconds every user will be served with at least 256 kbps.

The other part of the research work carried out during the course of this thesis has been on the efficient integration of the 3G and WLAN systems. This integration procedure takes two important aspects of the design into consideration: enhancement of 3G system capacity and fair user treatment in terms of energy consumption. The framework we have introduced in this thesis tries to enhance the overall 3G system performance but at the same time employs battery efficient routing within the WLAN in order to treat the nodes in the system as fairly as possible in terms of battery usage. From the simulation results we can see that the WLAN assisted 3G system performs better than the one without assistance. Besides, the battery consumption results show that the routing procedure within the WLAN treats intermediate nodes quite fairly.

In QoS aware scheduling, the users are served in such a way to fairly allocate system resources to each user. In best effort schedulers, one user may be favored over the others, but in our case each user is treated equally by setting the QoS parameter the same for each user.

In WLAN routing, employing the similar methodology, users are treated in an equal way so as to keep battery levels the same.

As a summary for the outcome of the thesis, it can be said that the statistical assurance framework presented in this thesis can be an attractive alternative to strict assurance services since at some point, trying to provide strict assurances in the wireless channel will degrade the overall system performance which is not desired by the service providers. The concern in building wireless networks is to accommodate as many users as possible but at the same time satisfy the user requirements without much degradation on the system resources. In a way it turns out that the system should “fairly” treat every user in the network. Our study follows exactly the same motivation in both QoS aware scheduling and 3G/WLAN integration.

7.2 Suggestion for Future Directions

- QoS levels have been assumed the same for all of the users in the system. They can be defined uniquely for each user. The simulation system can be easily modified to achieve the results.

- More accurate mathematical models/emprical models can be used to model the wireless channel to obtain more realistic results for a better system design

- Omni-directional antennas have been used in the study. By employing directional antennas and by employing space diversity better resource allocation strategies can be found. A joint optimization between time, frequency, code and antenna selection may be employed.

- Other upper layers can be included in the design process like the network and transport layer. Information from the network as well as application layer and the wireless channel can be combined to come up with more accurate system designs.

Appendix A

GENERATION OF RAYLEIGH FADING ENVELOPES USING FILTERED GAUSSIAN NOISE

Let $g_{I,k} \equiv g_I(kT)$ and $g_{Q,k} \equiv g_Q(kT)$ represent the real and imaginary parts of the complex envelope at k^{th} sampling instant. $g_{I,k}$ and $g_{Q,k}$ are Gaussian random variables with the state equation:

$$(g_{I,k+1}, g_{Q,k+1}) = a(g_{I,k}, g_{Q,k}) + (1-a)(w_{1,k}, w_{2,k}) \tag{A.1}$$

where $w_{1,k}$ and $w_{2,k}$ are zero-mean independent Gaussian random variables and a is the parameter controlling the correlation between the envelope samples and will be presented below. The envelope $|g_k|$ is Rayleigh distributed. It can be shown that the discrete auto-correlation functions of $g_{I,k}$ and $g_{Q,k}$ is

$$\phi_{g_Q g_Q}(n) = \phi_{g_I g_I}(n) = E[g_{I,k} g_{I,k+n}] = \frac{1-a}{1+a}\sigma^2 a^{|n|} \tag{A.2}$$

From Clarke's 2-D isotropic scattering model [64], the desired autocorrelation is

$$\phi_{g_I g_I}(n) = \frac{\Omega_p}{2} J_o(2\pi f_m n T) \tag{A.3}$$

where Ω_p is the total envelope power, f_m is the maximum Doppler shift and J_o is the zero order Bessel function of the first kind. Taking the discrete time Fourier transform of (A.2), the PSD is obtained as

$$S_{g_I g_I}(f) = \frac{(1-a^2)\sigma^2}{1+a^2-2a cos(2\pi f T)} \tag{A.4}$$

When the 3dB point of $S_{g_I g_I}(f)$ is set f_m / 4 the value of a is obtained as

$$a = 2 - cos(2\pi f_m T) - \sqrt{(2-cos(2\pi f_m T))^2 - 1} \tag{A.5}$$

In order to normalize the mean square envelope to Ω_p, the value of σ^2 is chosen as

$$\sigma^2 = \frac{1+a}{1-a}\frac{\Omega_p}{2} \tag{A.6}$$

Appendix B

GENERATION OF CORRELATED RAYLEIGH FADING ENVELOPES

In order to generate N Rayleigh envelopes $(r_1, r_2, \cdots, r_N)$ we make use of the normalized covariance matrix

$$K_r = \begin{pmatrix} 1 & \rho_{r1,2} & \rho_{r1,3} & \cdots & \rho_{r1,N} \\ \rho_{r2,1} & 1 & \rho_{r2,3} & \cdots & \rho_{r2,N} \\ \vdots & & \ddots & & \\ \rho_{rN,1} & \rho_{rN,2} & \rho_{rN,3} & \cdots & 1 \end{pmatrix} \tag{B.1}$$

The idea is to generate N complex Gaussian random variables $(v_1, v_2, \cdots, v_N)$ with the corresponding normalized covariance matrix

$$K_g = \begin{pmatrix} 1 & \rho_{g1,2} & \rho_{g1,3} & \cdots & \rho_{g1,N} \\ \rho_{g2,1} & 1 & \rho_{g2,3} & \cdots & \rho_{g2,N} \\ \vdots & & \ddots & & \\ \rho_{gN,1} & \rho_{gN,2} & \rho_{gN,3} & \cdots & 1 \end{pmatrix} \tag{B.2}$$

$$r_i = |v_i| = \sqrt{x_i^2 + y_i^2} \tag{B.3}$$

The relationship between $\rho_{ri,j}$ and $\rho_{gi,j}$ is given in Table B.1 as presented in [44]. Figure B.1 shows the graphical dependance between $\rho_{ri,j}$ and $\rho_{gi,j}$.

The algorithm for generating N correlated Rayleigh envelopes is as follows:

1. Generate K_r.

2. Obtain K_g from K_r using the correspondence table and linear interpolation.

3. Generate N uncorrelated complex Gaussian samples $V = (v_1, v_2, \cdots, v_N)$ each with variance σ_g^2 then determine the coloring matrix L corresponding to K_g. L is obtained

Table B.1: The Relationship between $\rho_{ri,j}$ and $\rho_{gi,j}$

$\rho_{gi,j}$	$\rho_{ri,j}$	$\rho_{gi,j}$	$\rho_{ri,j}$
0.00	0.0000	0.50	0.2227
0.05	0.0047	0.55	0.2752
0.10	0.0056	0.60	0.3327
0.15	0.0243	0.65	0.4133
0.20	0.0337	0.70	0.4562
0.25	0.0559	0.75	0.5410
0.30	0.0737	0.80	0.6073
0.35	0.0965	0.85	0.6974
0.40	0.1494	0.90	0.7913
0.45	0.1836	0.95	0.9005

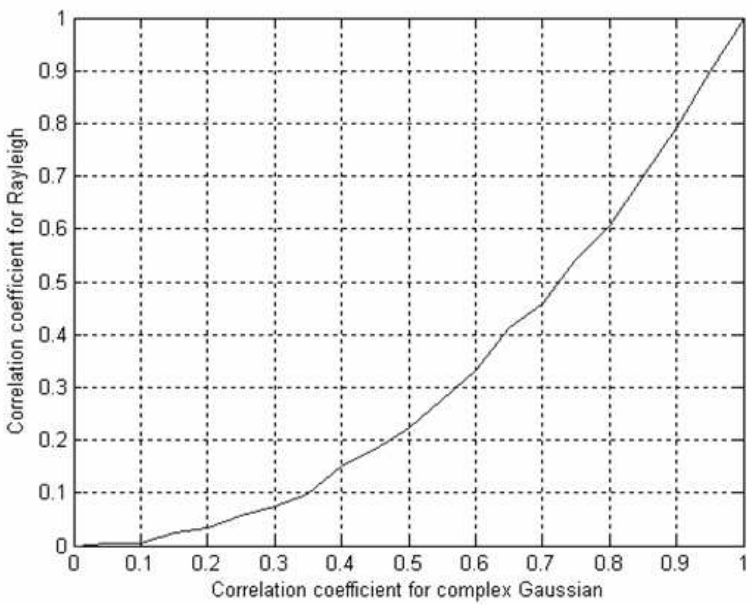

Figure B.1: $\rho_{ri,j}$ vs $\rho_{gi,j}$

from the Cholesky decomposition of K_g, i.e $LL^T = K_g$.

4. Generate correlated complex Gaussian samples using $W = LV$.

5. The N envelopes of the Gaussian samples in W correspond to Rayleigh random envelopes.

6. These Rayleigh envelopes are then normalized with respect to their rms values.

Appendix C

ANALYSIS OF THE GAIN OF RATE CONTROL OVER POWER CONTROL

The analysis given below is based on perfect knowledge of channel state and is carried out under the constraint of equal average effective data rate and following the derivations in [14].

Let the achievable data rate R be a linear function of the $SINR$ as

$$R = K\frac{Pg}{I} = K.SINR \tag{C.1}$$

where P is the BS transmit power, g is the fading constant, I is the interference and K is a constant determined by the bandwidth and the receiver. For a rate controlled system, with the fixed transmit power P_0, the average data rate will be

$$\overline{R} = K.E(SINR) \tag{C.2}$$

On the other hand for a power controlled system average power needed to maintain the same average data rate $\overline{R}$ can be expressed as

$$\overline{P} = \frac{\overline{R}}{K}E\left(\frac{I}{g}\right) \tag{C.3}$$

Dividing (C.3) by P_0 we get

$$\frac{\overline{P}}{P_0} = \frac{\overline{R}}{K}E\left(\frac{I}{P_0 g}\right) = E(SINR)E\left(\frac{1}{SINR}\right) \tag{C.4}$$

The fading constant g is a Rayleigh distributed random variable and the $SINR$ is characterized by the central chi-square distribution [65] which corresponds to the square of the Rayleigh distribution. So $SINR$ can be expressed as X^2 where X is the Rayleigh random variable corresponding to g. Likewise $1/SINR$ can be expressed as Y^2.

The Schwarz' Inequality states that [66, 67]

$$[E(XY)]^2 \leq E(X^2)E(Y^2) \tag{C.5}$$

Substituting X and Y in (C.5) we get

$$[E(\sqrt{SINR}\frac{1}{\sqrt{SINR}})]^2 = 1 \leq E(SINR)E\left(\frac{1}{SINR}\right) = \frac{\overline{P}}{P_0} \tag{C.6}$$

From (C.6) we can conclude that in a power controlled system the average power $\overline{P}$, will be greater than or equal to P_0 under the constraint of equal average data rate .

Appendix D

HOTSPOT HOP PERCENTAGE TABLES

50m radius HS												
HS at 100m			HS at 250m			HS at 500m			HS at 750m			
Number of Users	Hop Counts	% Occurrence	Number of Users	Hop Counts	% Occurrence	Number of Users	Hop Counts	% Occurrence	Number of Users	Hop Counts	% Occurrence	
	NoHS	93.511		**NoHS**	94.128		**NoHS**	93.794		**NoHS**	93.872	
	0	3.2278		**0**	3.0167		**0**	3.2889		**0**	3.0444	
	1	3.2611		**1**	2.8556		**1**	2.9167		**1**	3.0833	
	2	0		**2**	0		**2**	0		**2**	0	
2	**3**	0	**2**	**3**	0	**2**	**3**	0	**2**	**3**	0	
	NoHS	91.417		**NoHS**	91.339		**NoHS**	91.572		**NoHS**	90.2	
	0	2.9444		**0**	2.7222		**0**	2.6667		**0**	3.6167	
	1	4.4056		**1**	4.1722		**1**	4.1611		**1**	4.5778	
	2	1.2333		**2**	1.7667		**2**	1.6		**2**	1.6056	
3	**3**	0	**3**	**3**	0	**3**	**3**	0	**3**	**3**	0	
	NoHS	89.044		**NoHS**	89.361		**NoHS**	88.689		**NoHS**	86.844	
	0	2.6167		**0**	2.4333		**0**	2.6222		**0**	2.8944	
	1	4.4833		**1**	5.5667		**1**	5.9556		**1**	7.2333	
	2	2.5111		**2**	1.2333		**2**	1.9444		**2**	1.7889	
4	**3**	1.3444	**4**	**3**	1.4056	**4**	**3**	0.7889	**4**	**3**	1.2389	
	NoHS	86.939		**NoHS**	86.383		**NoHS**	86.428		**NoHS**	83.917	
	0	2.5056		**0**	2.4889		**0**	2.6222		**0**	3.1111	
	1	6.85		**1**	7.0833		**1**	7.3889		**1**	8.8222	
	2	2.4556		**2**	2.6167		**2**	2.6278		**2**	2.0556	
5	**3**	1.25	**5**	**3**	1.4278	**5**	**3**	0.9333	**5**	**3**	2.0944	
	NoHS	85.306		**NoHS**	85.206		**NoHS**	84.656		**NoHS**	80.9	
	0	2.1556		**0**	2.1722		**0**	2.2056		**0**	3.4	
	1	7.7389		**1**	7.9778		**1**	8.8389		**1**	9.6778	
	2	3.3833		**2**	3.2389		**2**	3.5889		**2**	4.3556	
6	**3**	1.4167	**6**	**3**	1.4056	**6**	**3**	0.7111	**6**	**3**	1.6667	
	NoHS	82.661		**NoHS**	82.467		**NoHS**	81.994		**NoHS**	78.383	
	0	2.1833		**0**	2.2389		**0**	2.1056		**0**	3.0222	
	1	10.528		**1**	9.6111		**1**	10.589		**1**	12.011	
	2	4.2611		**2**	4.8278		**2**	4.7111		**2**	4.8611	
7	**3**	0.3667	**7**	**3**	0.8556	**7**	**3**	0.6	**7**	**3**	1.7222	

Figure D.1: Hop percentage table for RR scheduling and HS with 50m radius - Part 1

	NoHS	79.722		NoHS	80.2		NoHS	79.606		NoHS	75.9
	0	2.0833		0	2.3056		0	2.5		0	2.8222
	1	12.217		1	10.356		1	12.072		1	14.078
	2	5.2722		2	5.8278		2	4.9056		2	6.25
8	3	0.7056	8	3	1.3111	8	3	0.9167	8	3	0.95
	NoHS	77.139		NoHS	77.489		NoHS	77.228		NoHS	72.55
	0	2.2556		0	2.2222		0	2.4444		0	2.8056
	1	13.139		1	13.783		1	13.45		1	16.5
	2	6.8611		2	5.8167		2	6.0111		2	6.5444
9	3	0.6056	9	3	0.6889	9	3	0.8667	9	3	1.6
	NoHS	75.333		NoHS	74.85		NoHS	74.717		NoHS	70.806
	0	2.2778		0	2.2333		0	2.2833		0	3.05
	1	14.039		1	14.756		1	15.017		1	17.194
	2	7.2444		2	7.3889		2	7.3944		2	7.8389
10	3	1.1056	10	3	0.7722	10	3	0.5889	10	3	1.1111
	NoHS	73.039		NoHS	73.067		NoHS	73.428		NoHS	68.539
	0	2.2111		0	2.1889		0	2.2		0	2.7
	1	15.811		1	15.578		1	17.328		1	19.917
	2	8.2278		2	8.2944		2	6.9056		2	8.4278
11	3	0.7111	11	3	0.8722	11	3	0.1389	11	3	0.4167
	NoHS	69.761		NoHS	69.094		NoHS	70.061		NoHS	65.667
	0	2.2444		0	2.1444		0	2.3111		0	2.6778
	1	17.511		1	18.706		1	18.028		1	21.728
	2	9.8056		2	8.9056		2	9.1722		2	9.2722
12	3	0.6778	12	3	1.15	12	3	0.4278	12	3	0.6556
	NoHS	67.606		NoHS	67.456		NoHS	67.294		NoHS	63.5
	0	2.2056		0	2.35		0	2.3167		0	2.6111
	1	20.328		1	19.75		1	20.994		1	21.094
	2	9.5111		2	10.006		2	9.0611		2	12.522
13	3	0.35	13	3	0.4389	13	3	0.3333	13	3	0.2722
	NoHS	63.867		NoHS	64.883		NoHS	64.039		NoHS	61.294
	0	2.5944		0	2.2278		0	2.2667		0	2.4333
	1	21.633		1	21.122		1	21.717		1	23.328
	2	11.311		2	11.156		2	11.289		2	12.517
14	3	0.5944	14	3	0.6111	14	3	0.6889	14	3	0.4278
	NoHS	63.022		NoHS	61.567		NoHS	61.689		NoHS	58.311
	0	2.3611		0	2.3278		0	2.5389		0	2.3778
	1	21.767		1	24.261		1	23.378		1	26.733
	2	12.333		2	11.556		2	11.678		2	12.461
15	3	0.5167	15	3	0.2889	15	3	0.7167	15	3	0.1167
	NoHS	58.872		NoHS	58.556		NoHS	58.778		NoHS	55.422
	0	2.3333		0	2.5056		0	2.5611		0	2.85
	1	24.383		1	25.144		1	26.094		1	28.022
	2	14.05		2	13.356		2	12.217		2	13.456
16	3	0.3611	16	3	0.4389	16	3	0.35	16	3	0.25

Figure D.2: Hop percentage table for RR scheduling and HS with 50m radius - Part 2

100m radius HS												
HS at 100m			HS at 250m			HS at 500m			HS at 750m			
Number of Users	Hop Counts	% Occurrence	Number of Users	Hop Counts	% Occurrence	Number of Users	Hop Counts	% Occurrence	Number of Users	Hop Counts	% Occurrence	
	NoHS	93.839		**NoHS**	93.706		**NoHS**	94.028		**NoHS**	93.817	
	0	3.1778		**0**	3.2722		**0**	2.9778		**0**	3.3667	
	1	2.9833		**1**	3.0222		**1**	2.9944		**1**	2.8167	
	2	0		**2**	0		**2**	0		**2**	0	
2	**3**	0	**2**	**3**	0	**2**	**3**	0	**2**	**3**	0	
	NoHS	91.356		**NoHS**	91.328		**NoHS**	90.8		**NoHS**	90.078	
	0	2.7778		**0**	3.0944		**0**	2.8722		**0**	3.2944	
	1	5.5222		**1**	4.9944		**1**	5.5278		**1**	6.55	
	2	0.3444		**2**	0.5833		**2**	0.8		**2**	0.0778	
3	**3**	0	**3**	**3**	0	**3**	**3**	0	**3**	**3**	0	
	NoHS	89.05		**NoHS**	89.172		**NoHS**	88.217		**NoHS**	86.828	
	0	2.7722		**0**	2.6389		**0**	2.9889		**0**	3.4389	
	1	7.8944		**1**	7.4722		**1**	8.2444		**1**	9.5333	
	2	0.2833		**2**	0.7167		**2**	0.4444		**2**	0.1333	
4	**3**	0	**4**	**3**	0	**4**	**3**	0.1056	**4**	**3**	0.0667	
	NoHS	86.656		**NoHS**	87.394		**NoHS**	86.967		**NoHS**	84.133	
	0	2.5944		**0**	2.2778		**0**	2.4667		**0**	3.1	
	1	10.167		**1**	9.9611		**1**	10.011		**1**	11.856	
	2	0.5833		**2**	0.3667		**2**	0.5556		**2**	0.9111	
5	**3**	0	**5**	**3**	0	**5**	**3**	0	**5**	**3**	0	
	NoHS	84.061		**NoHS**	84.606		**NoHS**	84.917		**NoHS**	81.622	
	0	2.5889		**0**	2.3444		**0**	2.5		**0**	3.0444	
	1	12.817		**1**	12.328		**1**	11.767		**1**	14.094	
	2	0.5333		**2**	0.7222		**2**	0.8167		**2**	1.2389	
6	**3**	0	**6**	**3**	0	**6**	**3**	0	**6**	**3**	0	
	NoHS	82.172		**NoHS**	82.428		**NoHS**	82.378		**NoHS**	78.622	
	0	2.4		**0**	2.5778		**0**	2.4778		**0**	3.0278	
	1	15.006		**1**	13.956		**1**	14.3		**1**	17.306	
	2	0.4222		**2**	1.0389		**2**	0.8444		**2**	1.0444	
7	**3**	0	**7**	**3**	0	**7**	**3**	0	**7**	**3**	0	

Figure D.3: Hop percentage table for RR scheduling and HS with 100m radius - Part 1

	NoHS	80.033		NoHS	80.111		NoHS	79.794		NoHS	77.089
	0	2.25		0	2.3111		0	2.2056		0	2.8444
	1	16.622		1	16.6		1	16.889		1	19.156
	2	1.0944		2	0.9778		2	1.1111		2	0.9111
8	3	0	8	3	0	8	3	0	8	3	0
	NoHS	78.022		NoHS	77.106		NoHS	77.667		NoHS	73.872
	0	2.0111		0	2.3833		0	2.6278		0	2.9556
	1	18.928		1	19.194		1	18.556		1	22.028
	2	1.0389		2	1.3167		2	1.15		2	1.1444
9	3	0	9	3	0	9	3	0	9	3	0
	NoHS	75.811		NoHS	75.494		NoHS	75.267		NoHS	71.15
	0	2.3167		0	2.2278		0	2.4722		0	2.8167
	1	20.778		1	20.65		1	20.878		1	24.856
	2	1.0944		2	1.6278		2	1.3833		2	1.1778
10	3	0	10	3	0	10	3	0	10	3	0
	NoHS	73.111		NoHS	73.511		NoHS	73.089		NoHS	69.006
	0	2.5667		0	2.3		0	2.3556		0	2.4667
	1	23.278		1	22.683		1	23.378		1	27.339
	2	1.0444		2	1.5056		2	1.1778		2	1.1889
11	3	0	11	3	0	11	3	0	11	3	0
	NoHS	69.978		NoHS	69.95		NoHS	69.878		NoHS	65.411
	0	2.5833		0	2.3167		0	2.3111		0	2.6944
	1	26.039		1	26.567		1	26.306		1	29.961
	2	1.4		2	1.1667		2	1.5056		2	1.9333
12	3	0	12	3	0	12	3	0	12	3	0
	NoHS	68.533		NoHS	67.494		NoHS	67.583		NoHS	64.578
	0	2.1667		0	2.3222		0	2.3944		0	2.7056
	1	28.144		1	28.483		1	28.344		1	30.789
	2	1.1556		2	1.7		2	1.6778		2	1.9278
13	3	0	13	3	0	13	3	0	13	3	0
	NoHS	64.75		NoHS	64.694		NoHS	64.539		NoHS	61.456
	0	2.6		0	2.4222		0	2.4167		0	2.6333
	1	31.294		1	31.072		1	31		1	34.033
	2	1.3556		2	1.8111		2	2.0444		2	1.8778
14	3	0	14	3	0	14	3	0	14	3	0
	NoHS	61.639		NoHS	62.056		NoHS	61.294		NoHS	58.206
	0	2.7278		0	2.8056		0	2.6889		0	2.7
	1	33.7		1	33.261		1	34.1		1	36.861
	2	1.9333		2	1.8778		2	1.9167		2	2.2333
15	3	0	15	3	0	15	3	0	15	3	0
	NoHS	59.139		NoHS	59.322		NoHS	59.278		NoHS	56.267
	0	2.8667		0	2.5833		0	2.5444		0	2.6944
	1	36.078		1	35.972		1	36.306		1	38.539
	2	1.9167		2	2.1222		2	1.8722		2	2.5
16	3	0	16	3	0	16	3	0	16	3	0

Figure D.4: Hop percentage table for RR scheduling and HS with 100m radius - Part 2

200m radius HS								
HS at 250m			HS at 500m			HS at 750m		
Number of Users	Hop Counts	% Occurrence	Number of Users	Hop Counts	% Occurrence	Number of Users	Hop Counts	% Occurrence
	NoHS	93.917		**NoHS**	93.694		**NoHS**	93.422
	0	3.1278		**0**	3.1722		**0**	3.3111
	1	2.9556		**1**	3.1333		**1**	3.2667
	2	0		**2**	0		**2**	0
2	**3**	0	**2**	**3**	0	**2**	**3**	0
	NoHS	91.139		**NoHS**	91.456		**NoHS**	89.906
	0	3.0167		**0**	2.9389		**0**	3.4333
	1	3.0556		**1**	2.4667		**1**	3.6278
	2	2.7889		**2**	3.1389		**2**	3.0333
3	**3**	0	**3**	**3**	0	**3**	**3**	0
	NoHS	88.956		**NoHS**	89.05		**NoHS**	87.683
	0	2.6333		**0**	2.7333		**0**	2.9389
	1	4.0167		**1**	3.7		**1**	4.4333
	2	2.8667		**2**	2.7944		**2**	2.6944
4	**3**	1.5278	**4**	**3**	1.7222	**4**	**3**	2.25
	NoHS	87.233		**NoHS**	87.183		**NoHS**	84.528
	0	2.3944		**0**	2.3944		**0**	3.4111
	1	5.4111		**1**	4.2222		**1**	4.8889
	2	2.0278		**2**	2.4444		**2**	1.9667
5	**3**	2.9333	**5**	**3**	3.7556	**5**	**3**	5.2056
	NoHS	84.7		**NoHS**	84.583		**NoHS**	82.906
	0	2.5056		**0**	2.4222		**0**	2.7389
	1	5.1667		**1**	5.25		**1**	5.0389
	2	2.9333		**2**	2.6056		**2**	3.4056
6	**3**	4.6944	**6**	**3**	5.1389	**6**	**3**	5.9111
	NoHS	82.611		**NoHS**	82.167		**NoHS**	79.383
	0	2.2778		**0**	2.1278		**0**	2.6667
	1	7.2667		**1**	6.0222		**1**	7.0833
	2	3.1444		**2**	3.2833		**2**	4.2833
7	**3**	4.7	**7**	**3**	6.4	**7**	**3**	6.5833
	NoHS	79.989		**NoHS**	79.6		**NoHS**	77.089
	0	2.3667		**0**	2.35		**0**	2.4444
	1	7.5667		**1**	7.4611		**1**	7.85
	2	4.6278		**2**	4.4944		**2**	5.2389
8	**3**	5.45	**8**	**3**	6.0944	**8**	**3**	7.3778

Figure D.5: Hop percentage table for RR scheduling and HS with 200m radius - Part 1

	NoHS	77.739		NoHS	77.5		NoHS	74.594
	0	2.3833		0	2.3167		0	2.4833
	1	8.7278		1	8.1944		1	10.05
	2	6.2444		2	5.75		2	6.9833
9	3	4.9056	9	3	6.2389	9	3	5.8889
	NoHS	76.25		NoHS	75.022		NoHS	72.661
	0	2.0667		0	2.3		0	2.5556
	1	8.6167		1	9.9556		1	9.2
	2	7		2	7.1389		2	6.2722
10	3	6.0667	10	3	5.5833	10	3	9.3111
	NoHS	72.394		NoHS	72.278		NoHS	70.161
	0	2.2611		0	2.3111		0	2.4333
	1	10.772		1	11.111		1	11.706
	2	7.9944		2	6.7167		2	9.1167
11	3	6.5778	11	3	7.5833	11	3	6.5833
	NoHS	70.289		NoHS	70.05		NoHS	66.583
	0	2.1111		0	2.3389		0	2.4833
	1	11.789		1	9.6778		1	11.817
	2	8.75		2	7.7944		2	10.267
12	3	7.0611	12	3	10.139	12	3	8.85
	NoHS	67.894		NoHS	68.222		NoHS	64.944
	0	2.0833		0	2.1944		0	2.3444
	1	12.167		1	12.228		1	12.911
	2	9.7		2	9.6056		2	10.933
13	3	8.1556	13	3	7.75	13	3	8.8667
	NoHS	65.339		NoHS	64.183		NoHS	62.339
	0	2.0833		0	2.3278		0	2.7111
	1	12.622		1	13.106		1	12.772
	2	11.75		2	12.05		2	12.267
14	3	8.2056	14	3	8.3333	14	3	9.9111
	NoHS	61.706		NoHS	62.789		NoHS	59.422
	0	2.1111		0	2.25		0	2.4111
	1	16.067		1	15.167		1	15.144
	2	13.094		2	11.767		2	14
15	3	7.0222	15	3	8.0278	15	3	9.0222
	NoHS	58.967		NoHS	58.711		NoHS	56.656
	0	2.3444		0	2.6389		0	2.5278
	1	16.522		1	16.561		1	16.1
	2	13.2		2	13.639		2	15.328
16	3	8.9667	16	3	8.45	16	3	9.3889

Figure D.6: Hop percentage table for RR scheduling and HS with 200m radius - Part 2

50m radius HS												
HS at 100m			HS at 250m			HS at 500m			HS at 750m			
Number of Users	Hop Counts	% Occurrence	Number of Users	Hop Counts	% Occurrence	Number of Users	Hop Counts	% Occurrence	Number of Users	Hop Counts	% Occurrence	
	NoHS	93.078		**NoHS**	92.989		**NoHS**	93.256		**NoHS**	93.844	
	0	5.5444		**0**	5.6167		**0**	5.6667		**0**	5.4278	
	1	1.3778		**1**	1.3944		**1**	1.0778		**1**	0.7278	
	2	0		**2**	0		**2**	0		**2**	0	
2	**3**	0	**2**	**3**	0	**2**	**3**	0	**2**	**3**	0	
	NoHS	89.733		**NoHS**	89.639		**NoHS**	89.95		**NoHS**	90.65	
	0	7.1889		**0**	7.35		**0**	7.4167		**0**	7.5833	
	1	2.5		**1**	2.2167		**1**	1.8944		**1**	1.3778	
	2	0.5778		**2**	0.7944		**2**	0.7389		**2**	0.3889	
3	**3**	0	**3**	**3**	0	**3**	**3**	0	**3**	**3**	0	
	NoHS	86.267		**NoHS**	86.256		**NoHS**	86.822		**NoHS**	87.572	
	0	8.1		**0**	8.5444		**0**	8.3944		**0**	9.4333	
	1	3.0833		**1**	3.5667		**1**	3.3167		**1**	2.1444	
	2	1.6556		**2**	0.7444		**2**	0.9778		**2**	0.4167	
4	**3**	0.8944	**4**	**3**	0.8889	**4**	**3**	0.4889	**4**	**3**	0.4333	
	NoHS	82.739		**NoHS**	83.094		**NoHS**	83.617		**NoHS**	84.683	
	0	9.2611		**0**	9.5556		**0**	10.289		**0**	10.8	
	1	5.25		**1**	5.0722		**1**	4.1944		**1**	2.9778	
	2	1.8722		**2**	1.5722		**2**	1.3833		**2**	0.7944	
5	**3**	0.8778	**5**	**3**	0.7056	**5**	**3**	0.5167	**5**	**3**	0.7444	
	NoHS	79.694		**NoHS**	79.9		**NoHS**	80.439		**NoHS**	81.772	
	0	9.6222		**0**	10.017		**0**	11.733		**0**	12.45	
	1	6.8333		**1**	6.4222		**1**	5.2667		**1**	3.5833	
	2	2.7611		**2**	2.6056		**2**	2.1389		**2**	1.5444	
6	**3**	1.0889	**6**	**3**	1.0556	**6**	**3**	0.4222	**6**	**3**	0.65	
	NoHS	76.45		**NoHS**	76.694		**NoHS**	77.272		**NoHS**	78.444	
	0	10.139		**0**	10.639		**0**	12.606		**0**	14.189	
	1	9.3222		**1**	8.0333		**1**	6.6889		**1**	4.7444	
	2	3.7111		**2**	3.9389		**2**	3		**2**	2.0222	
7	**3**	0.3778	**7**	**3**	0.6944	**7**	**3**	0.4333	**7**	**3**	0.6	

Figure D.7: Hop percentage table for EXP scheduling and HS with 50m radius - Part 1

	NoHS	73.072		NoHS	73.211		NoHS	74.456		NoHS	75.644
	0	11.072		0	11.1		0	13.789		0	15.594
	1	10.506		1	9.5556		1	8.0056		1	5.9778
	2	4.7778		2	5.0167		2	3.15		2	2.55
8	3	0.5722	8	3	1.1167	8	3	0.6	8	3	0.2333
	NoHS	69.628		NoHS	70.261		NoHS	71.222		NoHS	72.728
	0	11.867		0	12.111		0	15.383		0	17.211
	1	11.572		1	11.689		1	9.0667		1	6.9944
	2	6.4667		2	5.3056		2	3.7667		2	2.5056
9	3	0.4667	9	3	0.6333	9	3	0.5611	9	3	0.5611
	NoHS	67.061		NoHS	67.122		NoHS	68.278		NoHS	69.572
	0	12.161		0	12.889		0	16.233		0	18.8
	1	13.383		1	13.261		1	10.072		1	7.95
	2	6.3722		2	6.1111		2	5.0222		2	3.3
10	3	1.0222	10	3	0.6167	10	3	0.3944	10	3	0.3778
	NoHS	63.472		NoHS	63.717		NoHS	64.956		NoHS	66.922
	0	13.044		0	13.55		0	18.317		0	19.522
	1	15.289		1	14.461		1	12.05		1	9.6389
	2	7.5278		2	7.3889		2	4.5889		2	3.8056
11	3	0.6667	11	3	0.8833	11	3	0.0889	11	3	0.1111
	NoHS	60.572		NoHS	60.65		NoHS	61.789		NoHS	63.65
	0	13.911		0	14.628		0	18.844		0	20.844
	1	16.75		1	16.256		1	13.222		1	10.828
	2	8.1278		2	7.6833		2	5.8944		2	4.2611
12	3	0.6389	12	3	0.7833	12	3	0.25	12	3	0.4167
	NoHS	57.389		NoHS	57.5		NoHS	58.789		NoHS	60.706
	0	14.856		0	15.133		0	20.261		0	22.35
	1	19.217		1	18.306		1	14.106		1	11.028
	2	8.2889		2	8.7111		2	6.4444		2	5.7833
13	3	0.25	13	3	0.35	13	3	0.4	13	3	0.1333
	NoHS	54.65		NoHS	54.539		NoHS	56.094		NoHS	57.689
	0	14.894		0	15.394		0	21.011		0	23.456
	1	20.244		1	19.444		1	14.933		1	12.006
	2	9.7889		2	9.9944		2	7.5056		2	6.6778
14	3	0.4222	14	3	0.6278	14	3	0.4556	14	3	0.1722
	NoHS	50.822		NoHS	51.378		NoHS	53.178		NoHS	54.467
	0	16.206		0	16.05		0	21.833		0	25.139
	1	21.128		1	21.694		1	16.372		1	14.194
	2	11.394		2	10.589		2	7.9389		2	6.15
15	3	0.45	15	3	0.2889	15	3	0.6778	15	3	0.05
	NoHS	48.283		NoHS	48.661		NoHS	49.939		NoHS	51.683
	0	16.694		0	16.928		0	23.289		0	25.333
	1	22.278		1	22.578		1	18.189		1	15.2
	2	12.5		2	11.433		2	8.3556		2	7.6833
16	3	0.2444	16	3	0.4	16	3	0.2278	16	3	0.1

Figure D.8: Hop percentage table for EXP scheduling and HS with 50m radius - Part 2

100m radius HS												
HS at 100m			HS at 250m			HS at 500m			HS at 750m			
Number of Users	Hop Counts	% Occurrence	Number of Users	Hop Counts	% Occurrence	Number of Users	Hop Counts	% Occurrence	Number of Users	Hop Counts	% Occurrence	
	NoHS	92.961		**NoHS**	93.128		**NoHS**	93.422		**NoHS**	93.689	
	0	5.8778		**0**	5.8389		**0**	5.5667		**0**	5.7611	
	1	1.1611		**1**	1.0333		**1**	1.0111		**1**	0.55	
	2	0		**2**	0		**2**	0		**2**	0	
2	**3**	0	**2**	**3**	0	**2**	**3**	0	**2**	**3**	0	
	NoHS	89.561		**NoHS**	89.833		**NoHS**	90.15		**NoHS**	90.6	
	0	7.4667		**0**	7.2056		**0**	7.0778		**0**	7.7944	
	1	2.1667		**1**	1.9889		**1**	1.8222		**1**	0.9944	
	2	0.8056		**2**	0.9722		**2**	0.95		**2**	0.6111	
3	**3**	0	**3**	**3**	0	**3**	**3**	0	**3**	**3**	0	
	NoHS	86.211		**NoHS**	86.272		**NoHS**	86.772		**NoHS**	87.711	
	0	8.2056		**0**	8.8056		**0**	8.5444		**0**	9.1889	
	1	2.9333		**1**	3.1889		**1**	2.7278		**1**	1.2611	
	2	2.1444		**2**	1.4667		**2**	1.5		**2**	1.3	
4	**3**	0.5056	**4**	**3**	0.2667	**4**	**3**	0.4556	**4**	**3**	0.5389	
	NoHS	82.911		**NoHS**	82.861		**NoHS**	83.817		**NoHS**	84.578	
	0	9.4167		**0**	9.7056		**0**	9.8611		**0**	10.728	
	1	3.1778		**1**	3		**1**	2.2444		**1**	1.4889	
	2	2.8167		**2**	2.9556		**2**	2.0111		**2**	1.85	
5	**3**	1.6778	**5**	**3**	1.4778	**5**	**3**	2.0667	**5**	**3**	1.3556	
	NoHS	79.733		**NoHS**	79.828		**NoHS**	80.539		**NoHS**	81.694	
	0	9.1944		**0**	9.8056		**0**	10.756		**0**	12.689	
	1	3.7444		**1**	3.8778		**1**	2.6667		**1**	1.4722	
	2	3.4111		**2**	3.6833		**2**	2.8111		**2**	1.7667	
6	**3**	3.9167	**6**	**3**	2.8056	**6**	**3**	3.2278	**6**	**3**	2.3778	
	NoHS	76.55		**NoHS**	76.55		**NoHS**	77.311		**NoHS**	78.678	
	0	9.7889		**0**	10.722		**0**	12.033		**0**	13.317	
	1	4.1722		**1**	4.1111		**1**	2.7833		**1**	2.6556	
	2	3.8667		**2**	3.5056		**2**	2.6278		**2**	2.1333	
7	**3**	5.6222	**7**	**3**	5.1111	**7**	**3**	5.2444	**7**	**3**	3.2167	

Figure D.9: Hop percentage table for EXP scheduling and HS with 100m radius - Part 1

	NoHS	73.244		NoHS	73.306		NoHS	74.2		NoHS	75.567
	0	10.317		0	11.233		0	13.633		0	14.889
	1	4.7722		1	5.1056		1	3.3889		1	2.8056
	2	3.6611		2	4		2	3.1667		2	2.1889
8	3	8.0056	8	3	6.3556	8	3	5.6111	8	3	4.55
	NoHS	69.833		NoHS	70.328		NoHS	71.339		NoHS	72.85
	0	10.939		0	11.567		0	13.472		0	15.561
	1	5.0333		1	5.85		1	3.7		1	3.1
	2	4.6611		2	4.2556		2	3.3389		2	2.0667
9	3	9.5333	9	3	8	9	3	8.15	9	3	6.4222
	NoHS	66.817		NoHS	67.017		NoHS	68.311		NoHS	69.594
	0	11.144		0	11.267		0	15.144		0	16.978
	1	5.2611		1	5.5333		1	3.7278		1	3.4167
	2	5.35		2	4.9389		2	3.3056		2	2.4944
10	3	11.428	10	3	11.244	10	3	9.5111	10	3	7.5167
	NoHS	63.578		NoHS	63.628		NoHS	65.139		NoHS	66.894
	0	10.439		0	11.489		0	15.678		0	17.944
	1	7.3333		1	6.05		1	4.8111		1	4.2944
	2	5.6611		2	4.9611		2	4		2	2.7778
11	3	12.989	11	3	13.872	11	3	10.372	11	3	8.0889
	NoHS	60.467		NoHS	60.922		NoHS	62.211		NoHS	63.794
	0	11.206		0	12.006		0	16.717		0	18.617
	1	7.0722		1	7.1611		1	5.4722		1	3.9
	2	5.2833		2	5.7722		2	4.4444		2	3.1722
12	3	15.972	12	3	14.139	12	3	11.156	12	3	10.517
	NoHS	57.417		NoHS	57.767		NoHS	59.15		NoHS	60.844
	0	11.144		0	12.039		0	17.761		0	19.744
	1	8.3333		1	7.1167		1	5.05		1	4.6
	2	6.6556		2	6.5611		2	4.6		2	3.6333
13	3	16.45	13	3	16.517	13	3	13.439	13	3	11.178
	NoHS	54.506		NoHS	54.572		NoHS	56.111		NoHS	58.033
	0	11.589		0	12.25		0	18.083		0	20.25
	1	8.8389		1	8.7778		1	6.0222		1	5.0667
	2	7.6556		2	6.6389		2	5.1833		2	3.9389
14	3	17.411	14	3	17.761	14	3	14.6	14	3	12.711
	NoHS	51.206		NoHS	51.478		NoHS	53.083		NoHS	54.894
	0	11.944		0	12.183		0	18.994		0	21.433
	1	8.25		1	8.3		1	6.65		1	5.4944
	2	7.7333		2	7.6111		2	4.8889		2	4.5889
15	3	20.867	15	3	20.428	15	3	16.383	15	3	13.589
	NoHS	48.083		NoHS	48.578		NoHS	50.328		NoHS	51.661
	0	12.494		0	12.561		0	19.606		0	21.494
	1	9.4833		1	8.6		1	7.2778		1	6.2722
	2	7.9111		2	8.2556		2	7.1222		2	5.2722
16	3	22.028	16	3	22.006	16	3	15.667	16	3	15.3

Figure D.10: Hop percentage table for EXP scheduling and HS with 100m radius - Part 2

200m radius HS								
HS at 250m			HS at 500m			HS at 750m		
Number of Users	Hop Counts	% Occurrence	Number of Users	Hop Counts	% Occurrence	Number of Users	Hop Counts	% Occurrence
	NoHS	93.028		**NoHS**	93.411		**NoHS**	93.872
	0	6.0056		**0**	5.6056		**0**	5.4
	1	0.9667		**1**	0.9833		**1**	0.7278
	2	0		**2**	0		**2**	0
2	**3**	0	**2**	**3**	0	**2**	**3**	0
	NoHS	89.728		**NoHS**	90.25		**NoHS**	90.844
	0	7.5222		**0**	6.8667		**0**	7.25
	1	1.6889		**1**	1.4222		**1**	0.9278
	2	1.0611		**2**	1.4611		**2**	0.9778
3	**3**	0	**3**	**3**	0	**3**	**3**	0
	NoHS	86.389		**NoHS**	86.928		**NoHS**	87.794
	0	8.5722		**0**	8.2833		**0**	8.3944
	1	2.4833		**1**	2.2944		**1**	1.5278
	2	1.7111		**2**	1.4		**2**	1.4889
4	**3**	0.8444	**4**	**3**	1.0944	**4**	**3**	0.7944
	NoHS	83.178		**NoHS**	83.7		**NoHS**	85.056
	0	9.7556		**0**	9.5333		**0**	9.6833
	1	3.8667		**1**	2.4389		**1**	1.95
	2	1.4833		**2**	1.6611		**2**	1.0444
5	**3**	1.7167	**5**	**3**	2.6667	**5**	**3**	2.2667
	NoHS	79.861		**NoHS**	80.756		**NoHS**	81.844
	0	10.183		**0**	10.55		**0**	10.589
	1	4.1556		**1**	3.4778		**1**	2.8889
	2	2.1167		**2**	1.85		**2**	1.7333
6	**3**	3.6833	**6**	**3**	3.3667	**6**	**3**	2.9444
	NoHS	76.911		**NoHS**	77.489		**NoHS**	78.728
	0	10.483		**0**	11.517		**0**	11.806
	1	5.7667		**1**	4.2167		**1**	3.8333
	2	2.8611		**2**	2.4778		**2**	2.4722
7	**3**	3.9778	**7**	**3**	4.3	**7**	**3**	3.1611
	NoHS	73.4		**NoHS**	74.483		**NoHS**	75.9
	0	11.389		**0**	12.683		**0**	13.111
	1	6.6444		**1**	5.8167		**1**	4.4278
	2	3.5611		**2**	2.8278		**2**	2.7056
8	**3**	5.0056	**8**	**3**	4.1889	**8**	**3**	3.8556

Figure D.11: Hop percentage table for EXP scheduling and HS with 200m radius - Part 1

	NoHS	70.061		NoHS	71.589		NoHS	73.228
	0	12.017		0	13.322		0	14.228
	1	8.0611		1	6.4		1	5.3667
	2	5.4667		2	4.3111		2	3.7222
9	3	4.3944	9	3	4.3778	9	3	3.4556
	NoHS	67.139		NoHS	68.433		NoHS	70.378
	0	11.933		0	14.172		0	14.622
	1	8.5222		1	7.5333		1	5.5389
	2	6.7278		2	5.4722		2	3.9833
10	3	5.6778	10	3	4.3889	10	3	5.4778
	NoHS	64.017		NoHS	65.4		NoHS	67.028
	0	12.8		0	14.928		0	15.378
	1	9.4389		1	8.45		1	8.0111
	2	7.6333		2	5.3278		2	5.3389
11	3	6.1111	11	3	5.8944	11	3	4.2444
	NoHS	61.133		NoHS	62.317		NoHS	64.061
	0	12.506		0	15.3		0	16.383
	1	10.939		1	7.9667		1	8.55
	2	8.5111		2	6.35		2	6.0389
12	3	6.9111	12	3	8.0667	12	3	4.9667
	NoHS	57.5		NoHS	59.6		NoHS	61.283
	0	13.533		0	16.578		0	16.861
	1	11.756		1	10.117		1	9.0389
	2	9.1611		2	7.4333		2	7.4778
13	3	8.05	13	3	6.2722	13	3	5.3389
	NoHS	54.389		NoHS	56.556		NoHS	58.428
	0	13.939		0	17.083		0	17.633
	1	13.356		1	10.178		1	9.4444
	2	11.078		2	9.7333		2	8.4222
14	3	7.2389	14	3	6.45	14	3	6.0722
	NoHS	51.472		NoHS	53.633		NoHS	54.933
	0	15.433		0	18.083		0	17.628
	1	15.217		1	12.778		1	12.183
	2	11.75		2	9.1889		2	9.2333
15	3	6.1278	15	3	6.3167	15	3	6.0222
	NoHS	48.55		NoHS	50.389		NoHS	52.022
	0	14.272		0	18.328		0	18.172
	1	15.711		1	13.95		1	13.306
	2	13.017		2	10.739		2	11.089
16	3	8.45	16	3	6.5944	16	3	5.4111

Figure D.12: Hop percentage table for EXP scheduling and HS with 200m radius - Part 2

50m radius HS												
HS at 100m			HS at 250m			HS at 500m			HS at 750m			
Number of Users	Hop Counts	% Occurrence	Number of Users	Hop Counts	% Occurrence	Number of Users	Hop Counts	% Occurrence	Number of Users	Hop Counts	% Occurrence	
	NoHS	38.0444		NoHS	42.75		NoHS	70.8944		NoHS	97.1167	
2	0	61.9556	2	0	57.25	2	0	29.1056	2	0	2.8833	
	NoHS	24.0611		NoHS	28.1722		NoHS	67.0111		NoHS	94.9778	
3	0	75.9389	3	0	71.8278	3	0	32.9889	3	0	5.0222	
	NoHS	15.3111		NoHS	21.7222		NoHS	60.8944		NoHS	95.0333	
4	0	84.6889	4	0	78.2778	4	0	39.1056	4	0	4.9667	
	NoHS	11.1111		NoHS	15.6778		NoHS	59.3111		NoHS	93.8333	
5	0	88.8889	5	0	84.3222	5	0	40.6889	5	0	6.1667	
	NoHS	8.4833		NoHS	11.1222		NoHS	55.3278		NoHS	90.6167	
6	0	91.5167	6	0	88.8778	6	0	44.6722	6	0	9.3833	
	NoHS	7.0667		NoHS	7.5833		NoHS	52.6944		NoHS	88.4056	
7	0	92.9333	7	0	92.4167	7	0	47.3056	7	0	11.5944	
	NoHS	5.5167		NoHS	8.3722		NoHS	46.7111		NoHS	87.0944	
8	0	94.4833	8	0	91.6278	8	0	53.2889	8	0	12.9056	
	NoHS	3.8389		NoHS	4.95		NoHS	45.95		NoHS	88.5222	
9	0	96.1611	9	0	95.05	9	0	54.05	9	0	11.4778	
	NoHS	3.4389		NoHS	4.8167		NoHS	40.7833		NoHS	80.7389	
10	0	96.5611	10	0	95.1833	10	0	59.2167	10	0	19.2611	
	NoHS	2.8056		NoHS	2.7111		NoHS	35.4111		NoHS	80.9667	
11	0	97.1944	11	0	97.2889	11	0	64.5889	11	0	19.0333	
	NoHS	2.0444		NoHS	2.3889		NoHS	29.65		NoHS	81.5333	
12	0	97.9556	12	0	97.6111	12	0	70.35	12	0	18.4667	
	NoHS	2.2222		NoHS	1.9778		NoHS	32.9222		NoHS	72.0944	
13	0	97.7778	13	0	98.0222	13	0	67.0778	13	0	27.9056	
	NoHS	1.7444		NoHS	2.6833		NoHS	30.8667		NoHS	72.3278	
14	0	98.2556	14	0	97.3167	14	0	69.1333	14	0	27.6722	
	NoHS	1.4556		NoHS	2.0722		NoHS	25.35		NoHS	67.6	
15	0	98.5444	15	0	97.9278	15	0	74.65	15	0	32.4	
	NoHS	1.3667		NoHS	1.1667		NoHS	23.0611		NoHS	66.4556	
16	0	98.6333	16	0	98.8333	16	0	76.9389	16	0	33.5444	

Figure D.13: Hop percentage table for MaxR scheduling and HS with 50m radius

100m radius HS												
HS at 100m			HS at 250m			HS at 500m			HS at 750m			
Number of Users	Hop Counts	% Occurrence	Number of Users	Hop Counts	% Occurrence	Number of Users	Hop Counts	% Occurrence	Number of Users	Hop Counts	% Occurrence	
	NoHS	37.2056		NoHS	43.0056		NoHS	77.3833		NoHS	95.4	
2	0	62.7944	2	0	56.9944	2	0	22.6167	2	0	4.6	
	NoHS	25.95		NoHS	27.6111		NoHS	68.7611		NoHS	94.6944	
3	0	74.05	3	0	72.3889	3	0	31.2389	3	0	5.3056	
	NoHS	19.3278		NoHS	22.6833		NoHS	64.7278		NoHS	92.6111	
4	0	80.6722	4	0	77.3167	4	0	35.2722	4	0	7.3889	
	NoHS	12.1056		NoHS	13.6333		NoHS	60.9944		NoHS	93.3167	
5	0	87.8944	5	0	86.3667	5	0	39.0056	5	0	6.6833	
	NoHS	9.4		NoHS	11.2278		NoHS	53.6278		NoHS	87.6778	
6	0	90.6	6	0	88.7722	6	0	46.3722	6	0	12.3222	
	NoHS	6.5333		NoHS	8.7889		NoHS	41.6556		NoHS	87.6056	
7	0	93.4667	7	0	91.2111	7	0	58.3444	7	0	12.3944	
	NoHS	5.3944		NoHS	8.2333		NoHS	47.5722		NoHS	86.1667	
8	0	94.6056	8	0	91.7667	8	0	52.4278	8	0	13.8333	
	NoHS	3.55		NoHS	5.1444		NoHS	44.5111		NoHS	86.0833	
9	0	96.45	9	0	94.8556	9	0	55.4889	9	0	13.9167	
	NoHS	3.7556		NoHS	5.1944		NoHS	40.0722		NoHS	78.3278	
10	0	96.2444	10	0	94.8056	10	0	59.9278	10	0	21.6722	
	NoHS	2.8		NoHS	2.8556		NoHS	34.9611		NoHS	78.8444	
11	0	97.2	11	0	97.1444	11	0	65.0389	11	0	21.1556	
	NoHS	1.9611		NoHS	2.9222		NoHS	25.7833		NoHS	78.5722	
12	0	98.0389	12	0	97.0778	12	0	74.2167	12	0	21.4278	
	NoHS	2.3111		NoHS	2.3		NoHS	31.1056		NoHS	72.0278	
13	0	97.6889	13	0	97.7	13	0	68.8944	13	0	27.9722	
	NoHS	1.6611		NoHS	2.4778		NoHS	24.8444		NoHS	71.9778	
14	0	98.3389	14	0	97.5222	14	0	75.1556	14	0	28.0222	
	NoHS	1.65		NoHS	1.8611		NoHS	26.2556		NoHS	72.6944	
15	0	98.35	15	0	98.1389	15	0	73.7444	15	0	27.3056	
	NoHS	1.2278		NoHS	1.2611		NoHS	19.2722		NoHS	68.8167	
16	0	98.7722	16	0	98.7389	16	0	80.7278	16	0	31.1833	

Figure D.14: Hop percentage table for MaxR scheduling and HS with 100m radius

200m radius HS								
HS at 250m			HS at 500m			HS at 750m		
Number of Users	Hop Counts	% Occurrence	Number of Users	Hop Counts	% Occurrence	Number of Users	Hop Counts	% Occurrence
	NoHS	45.872		NoHS	74.7056		NoHS	96.7667
2	0	54.128	2	0	25.2944	2	0	3.2333
	NoHS	34.583		NoHS	64.8667		NoHS	93.8222
3	0	65.417	3	0	35.1333	3	0	6.1778
	NoHS	24.339		NoHS	62.0833		NoHS	91.7167
4	0	75.661	4	0	37.9167	4	0	8.2833
	NoHS	16.989		NoHS	45.7222		NoHS	89.7889
5	0	83.011	5	0	54.2778	5	0	10.2111
	NoHS	13.9		NoHS	44.3389		NoHS	86.0167
6	0	86.1	6	0	55.6611	6	0	13.9833
	NoHS	9.7722		NoHS	44.1222		NoHS	79.7556
7	0	90.228	7	0	55.8778	7	0	20.2444
	NoHS	8.6167		NoHS	43.25		NoHS	83.55
8	0	91.383	8	0	56.75	8	0	16.45
	NoHS	6.5944		NoHS	34.3333		NoHS	79.55
9	0	93.406	9	0	65.6667	9	0	20.45
	NoHS	4.4611		NoHS	38.6556		NoHS	75.3
10	0	95.539	10	0	61.3444	10	0	24.7
	NoHS	4.5278		NoHS	32.8556		NoHS	74.4222
11	0	95.472	11	0	67.1444	11	0	25.5778
	NoHS	3.9944		NoHS	29.3944		NoHS	75.2833
12	0	96.006	12	0	70.6056	12	0	24.7167
	NoHS	3.2833		NoHS	21.7944		NoHS	72.2833
13	0	96.717	13	0	78.2056	13	0	27.7167
	NoHS	3.1389		NoHS	26.35		NoHS	71.7444
14	0	96.861	14	0	73.65	14	0	28.2556
	NoHS	2.6833		NoHS	20.5333		NoHS	63.0222
15	0	97.317	15	0	79.4667	15	0	36.9778
	NoHS	2.55		NoHS	17.8833		NoHS	62.4167
16	0	97.45	16	0	82.1167	16	0	37.5833

Figure D.15: Hop percentage table for MaxR scheduling and HS with 200m radius

BIBLIOGRAPHY

[1] H. R. Hertz, *Untersuchungen Ueber Die Ausbreitung Der Elektrischen Kraft*, 1st ed. Johann Abrosius Barth, 1892.

[2] J. C. Maxwell, *A Treatise on Electricity and Magnetism*, 3rd ed. New York: Dover, 1991, vol. 1.

[3] ——, *A Treatise on Electricity and Magnetism*, 3rd ed. New York: Dover, 1991, vol. 2.

[4] C. E. Shannon, "A mathematical theory of communication," *Bell System Technical Journal*, 1948.

[5] D. H. Ring, "The cellular concept," 1947, unpublished.

[6] W. R. Young, "Amps: Introduction, background and objectives," *The Bell System Technical Journal*, pp. 1–14, January 1979.

[7] V. H. MacDonald, "Amps: The cellular concept," *The Bell System Technical Journal*, pp. 15–43, January 1979.

[8] D. E. Comer, *Computer Networks and Internets*, 4th ed. Prentice Hall, 2000, no. ISBN 0-13-018380-6.

[9] *IS-856-2 cdma2000 High Rate Packet Data Air Interface Specification*, TIA Std., Rev. 2, October 2002.

[10] R. Knopp and P. Humblet, "Information capacity and power control in single cell multi-user communications," in *IEEE ICC*, Seattle, WA, USA, 1995.

[11] A. J. Goldsmith and P. P. Varaiya, "Capacity of fading channels with channel side information," *IEEE Transactions on Information Theory*, vol. 43, no. 6, pp. 1986–1992, 1997.

[12] *IS-95-B Mobile Station-Base Station Compatibility Standard for Dual-Mode Wideband Spread Spectrum Cellular System*, Std., 1999.

[13] *IS-856-A cdma2000 High Rate Packet Data Air Interface Specification*, TIA Std., Rev. A, April 2004.

[14] J. Wang and T.-S. Ng, Eds., *Advances in 3G Enhanced Technologies for Wireless Communications*, March 2002, ch. 4.

[15] [Online]. Available: http://mathworld.wolfram.com/WalshFunction.html

[16] [Online]. Available: http://mathworld.wolfram.com/HadamardMatrix.html

[17] J. G. Proakis, *Digital Communications*, 4th ed. McGraw Hill, 2001.

[18] M. Yavuz, D. Paranchych, G. Wu, G. Li, and W. A. Krzymien, "Performance improvement of the hdr system due to hybrid arq," in *IEEE 2001 Semi-Annual Vehicular Technology Conference (VTC2001-Fall)*, Atlantic City, New Jersey, USA.

[19] C. Berrou, A. Glavieux, and P. Thitimajshima, "Near shannon limit error-correcting coding and decoding: Turbo-codes," in *International Conference on Communications*, vol. 2, Geneva, Switzerland, May 1993, pp. 1064–1070.

[20] J. Briffa, "Interleavers for turbo codes," Master's thesis, University of Malta, Malta, October 1999.

[21] P. Bender, P. Black, M. Grob, R. Padovani, N. Sindhushayana, and A. Viterbi, "Cdma/hdr: A bandwidth efficient high-speed wireless data service for nomadic users," *IEEE Communications Magazine*, vol. 38, no. 7, pp. 70–77, July 2000.

[22] [Online]. Available: http://www.umtsworld.com/technology/wcdma.htm

[23] A. V. Arunachalam, "Quality of service (qos) classes for bwa," IEEE 802.16sc-99/28, Tech. Rep., July 1999.

[24] S. Blake, D. Black, M. Carlson, E. Davies, Z. Wang, and W. Weiss, "An architecture for differentiated services," RFC 2475, December 1998.

[25] F. Baker, J. Heinanen, W. Weiss, and W. Wroclowski, "Assured forwarding phb group," RFC 2597, June 1999.

[26] K. Nichols, V. Jacobson, and K. Poduri, "An expedited forwarding phb group," RFC 2598, June 1999.

[27] F. O. Akgul and M. O. Sunay, "Efficient resource allocation for statistical qos assurances in hdr based wireless packet data," in *IEEE PIMRC Conference*, Barcelona, Spain, September 2004.

[28] *Physical Layer Standard for cdma2000 Spread Spectrum Systems Release D*, 3GPP2 Document No. C.S0002-D V1.0, Rev. D, February 2003. [Online]. Available: http://www.3gpp2.org/Public_html/specs/C.S0002-D_v1.0_021704.pdf

[29] [Online]. Available: http://www.iec.org/online/tutorials/gsm/

[30] M. G. H. Katevenis, "Fast switching and fair control of congested flow in broadband networks," *IEEE Journal on Selected Areas in Communications*, vol. SAC-5, no. 8, pp. 1315–1326, October 1987.

[31] A. Jalali, R. Padovani, and R. Pankaj, "Data throughput of cdma-hdr: A high efficiency high data rate personal communcations system," in *IEEE 51st Vehicular Technology Conference*, Tokyo, Japan, May 2000.

[32] S. Shakkottai and A. Stolyar, "Scheduling algorithms for a mixture of real-time and non-real-time data in hdr," Bell Laboratories, Tech. Rep., 2000.

[33] X. Liu, E. Chong, and N. Shroff, "Opportunistic transmission scheduling with resource-sharing constraints in wireless networks," *IEEE Journal on Selected Areas in Communications*, vol. 19, pp. 776–785, October 2001.

[34] R. Elliott and W. Krzymien, "Scheduling algorithms for the cdma2000 packet data evolution," in *Proc. 2002 IEEE Semi-Annual Vehicular Technology Conference (VTC2002-Fall)*, Vancouver, BC, Canada, September 2002.

[35] X. Liu, E. K. P. Chong, and N. Shroff, "Transmission scheduling for efficient wireless resource utilization with minimum-performance guarantees," *Infocom*, pp. 776–785, 2001.

[36] X. Liu, E. K. P. Chong, and N. B. Shroff, "Opportunistic scheduling for efficient wireless network utilization with qos constraints," 2000. [Online]. Available: http://shay.ecn.purdue.edu/x̃inliu/papers.html

[37] M. Gudmundson, "Correlation model for shadow fading in mobile radio systems," *Electronic Letters*, vol. 27, pp. 2145–2146, November 1991.

[38] Y. Okumura, E. Ohmori, T. Kawano, and K. Fukuda, "Field strength and its variability in vhf and uhf land-mobile service," *Review of the Electrical Communication Laboratory*, vol. 16, no. 9-10, pp. 825–873, 1968.

[39] W. C. Y. Lee, *Mobile Communications Design Fundamentals.* John Wiley, 1993.

[40] E. Damosso, Ed., *Digital mobile radio towards future generation systems*, 1999, cOST 231 Final Report. [Online]. Available: http://www.lx.it.pt/cost231/

[41] ITU, "Recommendation itu-r m.1225, guidelines for evaluation of radio transmission technologies for imt-2000," ITU, Tech. Rep.

[42] R. Knopp and P. A. Humblet, "Multiple accessing over frequency selective fading channels," in *Proc. IEEE PIMRC 1995*, Toronto, Canada, October 1995.

[43] W. C. Y. Lee, *Mobile Communications Engineering.* McGraw-Hill, 1982.

[44] B. Natarajan, C. R. Nassar, and V. Chandrasekhar, "Generation of correlated rayleigh fading envelopes for spread spectrum applications," *IEEE Communications Letters*, vol. 4, January 2000.

[45] M. Gurelli and P. Black, "Capacity simulation of cdma2000 1xev wireless internet access system," in *IEEE MWCN*, 2001.

[46] G. L. Stuber, *Principles of Mobile Communications*, 2nd ed. Kluwer Academic Publishers, 2001.

[47] [Online]. Available: http://grouper.ieee.org/groups/802/11/

[48] *802.11 Wireless LAN Medium Access Control (MAC) and Physical Layer (PHY) Specifications*, IEEE Std 802.11-1999, 1999.

[49] *802.11 Wireless LAN Medium Access Control (MAC) and Physical Layer (PHY) Specifications - High Speed Physical Layer in the 5 GHz Band*, IEEE Std 802.11a-1999, 1999.

[50] *802.11 Wireless LAN Medium Access Control (MAC) and Physical Layer (PHY) Specifications*, IEEE Std 802.11b-1999, 1999.

[51] *802.11 Wireless LAN Medium Access Control (MAC) and Physical Layer (PHY) Specifications*, IEEE Std 802.11g-2003, 2003.

[52] [Online]. Available: ISM Bands as defined in ITU-T S5.138, http://www.itu.int/ITU-R/terrestrial/pub-reg/faq/index.html#g013

[53] R. W. Chang, "Synthesis of band-limited orthogonal signals for multi-channel data transmission," *Bell Systems Technical Journal*, pp. 1775–1796, 1966.

[54] [Online]. Available: http://wi-fiplanet.webopedia.com/TERM/C/CCK.html

[55] H.-Y. Wei and R. D. Gitlin, "Wwan/wlan two-hop-relay architecture for capacity enhancement," in *IEEE Wireless Communications and Networking Conference (WCNC 04)*, Atlanta, Georgia, USA, March 2004.

[56] M. M. Buddhikot, G. Chandranmenon, S. Han, Y.-W. Lee, S. Miller, and L. Salgarelli, "Design and implementation of a wlan/cdma2000 interworking architecture," *IEEE Communications Magazine*, vol. 41, no. 11, pp. 90–100, November 2003.

[57] M. Buddhikot, G. Chandranmenon, S. Han, Y. W. Lee, S. Miller, and J. . L. Salgarelli, "Integration of 802.11 and third-generation wireless data networks."

[58] C.-K. Toh, "Maximum battery life routing to support ubiquitous mobile computing in wireless ad hoc networks," *IEEE Communications Magazine*, vol. 39, no. 6, pp. 138–147, June 2001.

[59] S. Singh and C. S. Raghavendra, "Pamas-power aware multi-access protocol with signaling for ad hoc networks," *ACM Commun. Rev*, vol. 28, no. 3, pp. 5–26, July 1998.

[60] E. W. Dijkstra, "A note on two problems in connexion with graphs," *Numerische Mathematik*, vol. 1, pp. 269–271, 1959.

[61] K. Scott and N. Bambos, "Routing and channel assignment for low power transmission in pcs," in *Proc. ICUPC 96*, vol. 2, Cambridge, MA, USA, October 1996, pp. 498–502.

[62] S. Singh, M. Woo, and C. S. Raghavendra, "Power-aware routing in mobile ad hoc networks," in *Proc. MobiCom 98*, Dallas, Texas, USA, October 1998.

[63] "Preliminary product brief - wavelan(tm) 802.11b chip set for standard form factors," Agere Systems, December 2002.

[64] R. Clarke, "A statistical theory of mobile radio reception," *Bell System Technical Journal*, vol. 47, pp. 957–1000, 1968.

[65] E. W. Weisstein, "Chi-squared distribution," from MathWorld–A Wolfram Web Resource. [Online]. Available: http://mathworld.wolfram.com/SchwarzsInequality.html

[66] A. Papoulis, *Probability, Random Variables and Stochastic Processes*, 3rd ed., McGraw-Hill International Editions, 1991.

[67] [Online]. Available: http://mathworld.wolfram.com/SchwarzsInequality.html

VITA

Ferit Ozan Akgül was born in Ankara, Türkiye on January 14th, 1980. There he attended TED Ankara College High School. He received his BS degree from the Middle East Technical University (METU), Ankara in 2002. He worked as a summer intern at HAVELSAN and ASELSAN in Ankara where he got acquainted with the industry. From October 2002 till June 2004, he worked as a teaching and research assistant at Koc University, Istanbul where he also has pursued his MS studies. During his MS studies he worked on the project: *"Adaptive Resource Allocation for Spectrally Efficient Wideband Communication Systems"* funded by *Nokia Mobile Phones*. Within this project he investigated QoS performances of 3G wireless cellular systems (both single and multi-carrier) and 3G/WLAN integration methodologies on a comprehensive simulation platform. He has presented a conference paper in the PIMRC2004 (Barcelona, Spain) on "Statistical QoS Assurance" with travel award from TUBITAK. There are also 2 journals that are in preparation.

PUBLICATIONS

- Ferit O. Akgul and M. Oguz Sunay, "Efficient Resource Allocation for Statistical QoS Assurances in HDR Based Wireless Packet Data," Proceedings of the IEEE PIMRC Conference, Barcelona, Spain, September 5-8, 2004.

- Ferit O. Akgul and M. Oguz Sunay, "Enhancing 3G High Speed Wireless Data Performance through Utilization of 3G-WLAN System Integration: A Cross-Network, Cross-Layer Approach," in preparation.

- Ferit O. Akgul and M. Oguz Sunay, "Efficient Resource Allocation for Statistical QoS Assurances vs. Assured and Best Effort Service in 1x and 3x MC HDR Type Packet Data", in preparation.